Gajanthini Vamathevan

Norwegian Day-ahead Electricity Price Forecasting using AI Models

Master's thesis in Energy and Environmental Engineering
Supervisor: Ümit Cali
Co-supervisor: Marthe Fogstad Dynge

June 2022

Master's thesis

NTNU
Norwegian University of Science and Technology
Faculty of Information Technology and Electrical Engineering
Department of Electric Power Engineering

Institute of Energy for South-East Europe (IENE)

NTNU
Norwegian University of
Science and Technology

Gajanthini Vamathevan

Norwegian Day-ahead Electricity Price Forecasting using AI Models

NTNU
Norwegian University of
Science and Technology

Acknowledgement

18/06/2022, Trondheim

Gajanthini Vamathevan

Abstract

The transformation from the regulated, local monopoly power markets in Norway to the liberalization in the electricity trading due to the Energy Act in 1991, has caused competitiveness among the market participants. In addition comes the recent awareness of the need of climate stabilisation that has produced arrangements such as the Paris Agreement and the Climate Law that focus on the global need of decarbonization that may be solved with renewable energy resources. Hence, a magnifying amount of these sources have been arising over time and is expected to further increase in order to reach the climate goals. Thus, the growing number of such insecure resources such as wind, solar and hydropower production depending on non-dispatchable weather conditional elements is leading to the elevated unforeseeable volatility in the electricity price that suppliers and consumers are competing against. Well-performing forecasting models would be beneficial for relevant market participants to predict the most favorable choices in power market auctions such that the economical benefits are maximized. Deep learning (DL) models basing on artificial intelligence (AI) have received much attention lately for its great-performing forecasting and hybrid fusion of DL, AI or other traditional models have in recent time been detected to enhance the forecasting accuracy even further. Thus, the quality of AI forecasting models should be investigated in details.

This thesis evaluates the performance of two vastly differentiating deep learning (DL) models, namely the artificial neural network (ANN) and the long short-term memory (LSTM) models with the needful pre- and postprocessing respectively before and after running the forecasting models, along with the latter step of visualising the outcome for interpretation and analysis of the forecasting results. Hybrid solution of such DL models and machine learning (ML) based k-means clustering is conducted in regards of forecasting as well, with the quality of the data grouping methodology to be compared to manual clustering accordingly to the type of day. Supplementary modifications to the DL models such as adding a hidden layer or a dropout layer will be implemented to testify any amelioration of the results. Additionally, the significance and influence of certain input parameters, e.g. the temperature, precipitation and CO_2-price data that have on the forecasting accuracy are investigated.

The day-ahead electricity price of 2021 in each of the five bidding zones of Norway is chosen to be predicted. Results indicate a resemblance in the results among the so-called stable zones comprising of NO3 and NO4 with stable and relatively low electricity prices in 2021, revealing to perform at its best with ANN. However, the remaining bidding areas, NO1, NO2 and NO5, categorized as the unstable zones due to the immensely oscillating price behaviour detected in 2021, excel the most precise forecasting through the LSTM model. Neither clustering nor does additional model modifications contribute to enhancing the prediction. Another discovery is how the stable zones in fact gain improved prediction when input data such as weather condition elements and CO_2-prices are neglected, while the unstable zones seem to be relied on these data types. The LSTM model is also observed to have a slower rate of reaction when abrupt changes are faced in the electricity prices, in contradiction to the rapid ANN model.

Sammendrag

Omleggingen fra de regulerte, lokale monopolkraftmarkedene i Norge til liberaliseringen av krafthandelen som følge av energiloven i 1991, har skapt konkurransekraft blant markedsaktørene. I tillegg kommer den nylige bevisstheten om behovet for klimastabilisering som har gitt ordninger som Parisavtalen og klimaloven som fokuserer på det globale behovet for avkarbonisering som kan løses med fornybare energiressurser. Derfor har en økende mengde av disse kildene oppstått over tid og forventes å øke ytterligere for å nå klimamålene. Den økende mengden av vind-, sol- og vannkraftproduksjon som er avhengig av det uforutsigbare værforholdet, bidrar derfor til volatiliteten i strømprisen som leverandører og forbrukere konkurrerer mot. Godt fungerende prognosemodeller vil være fordelaktig for relevante markedsdeltakere å forutsi de mest gunstige valgene i kraftmarkedsauksjoner slik at de økonomiske fordelene maksimeres. Dyplæringsmodeller (DL) basert på kunstig intelligens (AI) har fått mye oppmerksomhet i det siste for sine gode prognoser og hybridfusjon av DL, AI eller andre tradisjonelle modeller har i nyere tid blitt oppdaget i å forbedre prognosenøyaktigheten ytterligere. Derfor bør kvaliteten på AI-prognosemodeller undersøkes i detalj.

Denne oppgaven evaluerer ytelsen til to vidt differensierende dyplæringsmodeller (DL), nemlig artificial neural network (ANN) og long short-term memory (LSTM) modellene med nødvendig for- og etterbehandling henholdsvis før og etter kjøring av prognosemodellene , sammen med det siste trinnet med å visualisere resultatet for tolkning og analyse av prognoseresultatene. Hybridløsning av slike DL-modeller og maskinlæringsbasert (ML) k-means clustering (datagruppering) utføres også med hensyn til prognoser, med kvaliteten på datagrupperingsmetodikken som skal sammenlignes med manuell gruppering i henhold til typen dag. Supplerende modifikasjoner til DL-modellene som å legge til et skjult lag eller et dropout-lag vil bli implementert for å vitne om enhver forbedring av resultatene. I tillegg kan betydningen og påvirkningen av visse input sparametere, f.eks. temperatur, nedbør og CO_2-prisdata som har på prognosenøyaktigheten undersøkes.

Day-ahead strømprisen for 2021 i hver av de fem budsonene i Norge skal predikeres. Resultatene indikerer en likhet i resultatene blant de såkalte stabile sonene som består av NO3 og NO4 med stabile og relativt lave strømpriser i 2021, noe som viser å prestere på sitt beste med ANN. De gjenværende budområdene, NO1, NO2 og NO5, kategorisert som de ustabile sonene på grunn av den uhyre oscillerende prisatferden oppdaget i 2021, utmerker seg imidlertid den mest presise prognosen gjennom LSTM-modellen. Verken datagruppering eller ytterligere modellmodifikasjoner bidrar til å forbedre prediksjonen. En annen oppdagelse er hvordan de stabile sonene faktisk får forbedret prediksjon når input data som værforholdselementer og CO_2-priser blir neglisjert, mens de ustabile sonene ser ut til å være avhengig av disse datatypene. LSTM-modellen er også observert å ha en langsommere reaksjonshastighet når det oppleves brå endringer i strømprisene, i motsetning til den raske ANN-modellen.

Contents

List of Figures

List of Tables

Acronyms

EEX	European Energy Exchange.
EPEX SPOT	European Power Exchange.
PXE	Power Exchange Central Europe.
TSO	Transmission System Operator.
MAR	Minimum Acceptance Ratio.
HVDC	High-Voltage Direct Current.
AI	Artificial Intelligence.
DL	Deep Learning.
ML	Machine Learning.
AR	AutoRegression.
MA	Moving Average.
I	Integration.
X	Additional input to AR.
F	Fractional.
ESM	Exponential Smoothing Method.
ARIMA	AutoRegressive Integrated Moving Average.
ARX	Autoregressive models with exogenous inputs.
ARMA	AutoRegressive Moving Average.
ARFIMA	Autoregressive Fractionally Integrated Moving Average.
GARCH	Generalized AutoRegressive Conditional Heteroskedasticity.
DWT	Discrete Wavelet Transform.
ANN	Artificial Neural Network.
FNN	Feed-Forward Neural Network.
RNN	Recurrent (feedback) Neural Network.
SVM	Support Vector Machine.

SCR	Support Vector Regression.
LSTM	Long Short-Term Memory.
AdaGrad	Adaptive Gradient Algorithm
RMSProp	Root Mean Square Propagation
BS	Batch size
TS	Timesteps
MAE	Mean Absolute Error
MSE	Mean Squared Error
RMSE	Root-Mean-Squared Error
MAPE	Mean Absolute Percentage Error
GMRAE	Geometric mean relative absolute erro
MRAE	Mean relative absolute erro

Chapter 1

Introduction

1.1 Background and Motivation

The original structure of the Norwegian power market could be described as comprising of local monopoly-driven market places that produced greater economical incentives among the producers and an inefficient system of power supply [3]. As a consequence of the adoption of the Energy Act in 1991 in Norway - a concept that soon was spreading to the rest of Europe - the wholesale electricity market had to undergo radical changes in order to fulfill the new requirements. The power exchange, Nord Pool was formed and trading platforms were established, each with a different functional contribution to the wholesale market. The Norwegian power market got to be more well-integrated with the Nordic and later the rest of the European market, and deregulation was introduced [14]. Liberalization of the electricity market has caused competition among the supplier, consumers and brokers as the electricity price now would depend on the bids and offers processed in a trading. Thus, it is vital for these market participants to make the most optimal decisions in the light of minimizing economic losses in the auction and exploiting forecasting tools may provide with the answer.

However, predicting the electricity price has revealed to be a great challenge as it follows a tremendously fluctuating behaviour over time caused by factors such as the generation amount, bidding strategies, transmission congestions and outages. Additionally, weather conditional elements such as the temperature and the precipitation excels an essential role regarding the market price as a cause of the decarbonizing obligations such as the Paris Agreement and the European Climate Law that lead to the growing amount of non-dispatchable renewable energy resources [15][16]. Hence, a major difficulty may be encountered in Norway with most of its production originating from hydropower, e.g. when the Norwegian average electricity price elevated to four times the normal range in the last quarter of 2021, all due to mainly the lack of precipitation, hence, reduction in the hydropower production [17]. This again, led to introducing other affecting elements to the Norwegian electricity price, such as gas, coal and CO_2-price due to the escalated reliability on Central-European power production in which its price normally would depend on these factors. Therefore, forecasting the electricity price is a complex problem that may always be enhanced through discovering new influential parameters, and not to mention, through refining forecasting models.

Machine learning (ML) models encompassing artificial intelligence (AI) has received much attention the past time for its great performance in forecasting [18]. Especially the deep learning (DL) models such as the artificial neural networks (ANN) and long short-term memory (LSTM), are frequently used in regards of predicting the electricity price due to its simplicity in implementing the forecasting models, its high robustness and the

excellent outcome of predicting accuracy compared to the conventional statistical models [19][20]. Additional preprocessing methods, input parameters adjustments, and the eminently popular choice of hybrid solutions of ML, DL, statistical models or a combination of these methods may be applied to the forecasting models in order to achieve a more boosted model and improved results.

Although several papers underline the importance of including e.g. the gas, fuel and the CO_2-price as input parameters to ameliorate the prediction, such data is often not included in the actual forecasting due to the lack of data access [21][22]. The hybrid solution of the ML k-means clustering method or the manual clustering comprising of grouping the input data accordingly to the type of day and/or hour, all in combination with a forecasting model have been employed frequently in papers [23][24][25]. However, none of them aim to compare the performance of the clustering methods. This thesis will therefore provide a detailed study concerning the forecasting of the Norwegian electricity price, investigating DL forecasting models, hybrid solutions and sensitivity analysis of certain input parameters.

1.1.1 Problem Description

This master thesis has its goal of contributing to the following:

- Forecasting the NO1-NO5 area electricity prices with the simple artificial neural network (ANN) and the long short-term memory (LSTM) model for comparing the results of two differently functioning deep learning (DL) methods.

- Investigation of the hybrid combination of a DL model with k-means clustering and manual clustering accordingly to the type of day and analyse the grouping mechanism behind the clustering methodologies.

- Evaluation of potential improvement in the DL models through parametrization.

- An analysis of the sensitiveness in forecasting accuracy in terms of neglecting input parameters such as weather conditional and CO_2-price data.

1.2 Approach

The day-ahead electricity price in 2021 of the five bidding zones in Norway is to be forecasted. Essential input data will be assembled from various entities, appropriate preprocessing actions such as feature extraction, restructuring and cleansing of data, normalization and clustering may be incorporated to the input data. These will further be injected to the two disparate DL models, ANN and LSTM, implemented in Python, and necessary postprocessing techniques like de-normalization and de-clustering may be applied before inserting the results into model output statistics (MOS) for visualisation and analysis of the performance of the various models through evaluation metrics.

1.3 Structure of the Thesis

Chapter 1 - *Introduction*: Gives an insight of the background, motivation and the goal of this thesis.

Chapter 2 - *The Nordic Wholesale Electricity Market*: Provides an overview regarding the structure of the Nordic power market, with a deeper elaboration of the day-ahead

market function and mechanism.

Chapter 3 - *Methodologies for Electricity Price Forecasting*: Presents a literature review of the most common electricity price forecasting models with a narrowed focus on the working process of the ANN and LSTM models.

Chapter 4 - *Methodology*: Explains the approach of establishing the DL models.

Chapter 5 - *Input Data*: Illustrates the input data involved in the forecasting models that are relevant for the analysis and discussion of the results.

Chapter 6 - *Results*: Presents the forecasting results of various model types and cases.

Chapter 7 - *Discussion*: Elaborates and examines the outcome of the results.

Chapter 8 - *Conclusion and Future Work*: Provides a brief summary of the thesis along with a conclusion of the revealed results and main points of the discussion, and lastly presents future recommended work on this field of study.

Chapter 2

The Norwegian Wholesale Electricity Market

In order to forecast the electricity price, knowledge about the power market structure and mechanism must be acquired. Thus, this chapter shall enlighten the general Norwegian power market structure and give the deeper insight into the functioning of the Day-ahead market. One should have in mind that the presented theory and sections in this chapter has mostly been previously covered in an earlier thesis written by the author, proposing a forecasting model that also required such a literature review [13].

2.1 A General Overview

Figure 2.1 illustrates the market division that is found in the Norwegian power trading. The electricity market may be segregated into the financial and the physical market that respectively involves future-based trading and the actual deliveries.
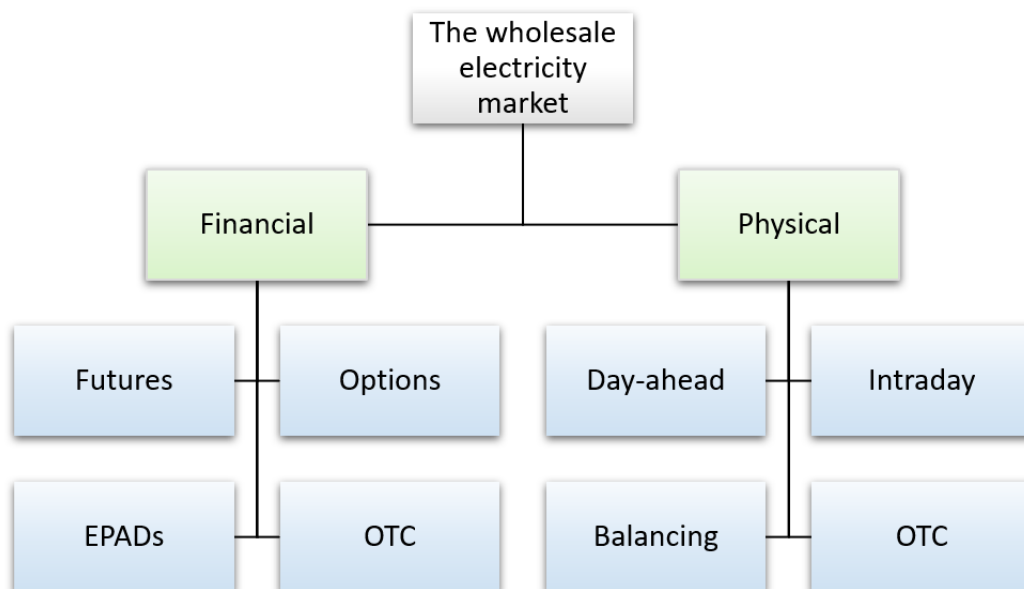
Figure 2.1: A model presenting the market divisions presented in this chapter.

Figure 2.2 is supplied as to easier visualise the order of the processing of each submarket types. Financial markets occur in the early stages of determining the electricity price, while the day-ahead market is the first physical market to enter the time line. This is

where most of the electricity is traded, hence, this thesis will be focusing on forecasting the Day-ahead electricity price, which will be elaborated further.
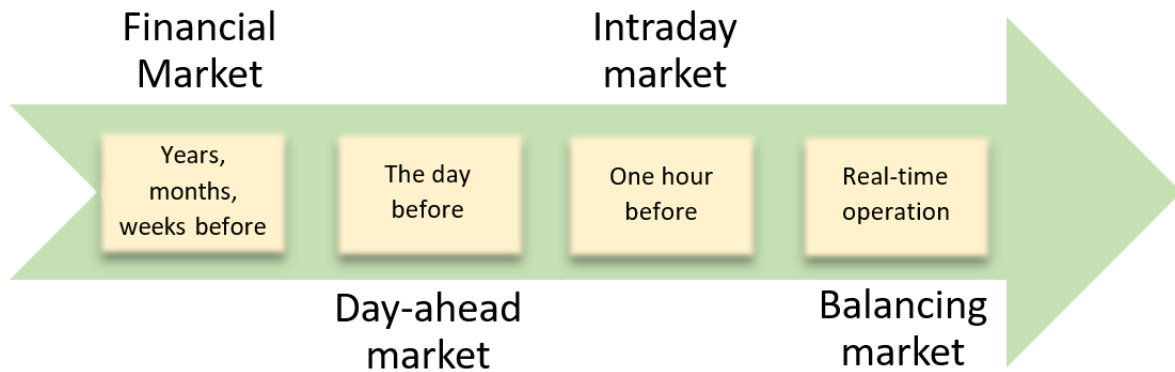
Figure 2.2: A timeline showing a simplification of the order of trading [1].

2.2 The Day-Ahead Market

Norway make use of the day-ahead market available at Nord Pool, called "Elspot", for trading. This market determines the spot price for the next 24 hours. The available capacities in the grid are published at 10:00 CET. Buyers and sellers have until 12:00 CET to decide their bid/offer based on the given information. This includes the price [EUR/MWh] and the given quantity of energy [MW] that the participant is willing to buy or sell in the day-ahead market. Since the market is hourly-based, each market participant has to submit bids/offers for each individual hour for a certain bidding zone for the upcoming next 24 hours, leading to 24 different closed auctions. Bidding zones are quite unique for the Norwegian power market, and Figure 2.3 illustrates the zone boundaries Nord Pool follows, all defined by the local transmission system operator (TSO). [26]

Figure 2.3: An overview of the Norwegian bidding zones [2].

Norway has five bidding areas as shown in Figure 2.3, and the bidding zones for the rest of the Nordic as well as the Baltic areas are also included. The goal of such area segregation is to avoid grid congestions. That is, avoiding exceeding the maximum transfer capacity on the transmission lines going across the areas, so to steer clear from bottlenecks in the power flows in the grid [27].

2.2.1 Electricity Price Calculation

Two types of price calculations are performed in the day-ahead market by Nord Pool; area price and system price calculation. The pricing mechanism presented in this section for both of the price types are equivalent to what is utilised by Nord Pool [3].

Area price

Nord Pool make the use of the bidding areas due to potential congestion between the zones, and the "market price" in each area is denoted as the area price. The maximum transmission capacity on the lines across the border of the zone are taken into account.

Surplus areas (low area price) and deficit areas (high area price) may occur when using area pricing due to including transmission flow limits, leading to other more expensive generators requiring to produce more, if needed, in order to fulfill the demand of all areas. However, if the power flow were to be well within the maximum capacity, the resulting area prices would be identical and equal to each other. The direction of the power flow is determined by the area price/nodal price. Power always flows from a lower nodal price to a higher nodal price. All participants in the Norwegian market have to follow the electricity area price regarding payment. The easiest way to explain the pricing method is by assuming two areas connected together with one transmission line, as shown in Figure 2.4.
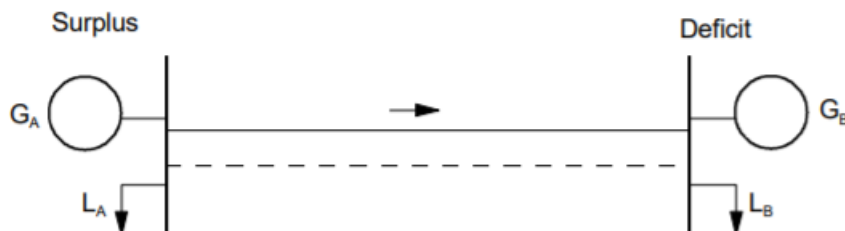
Figure 2.4: A two-area example with area A to the left and area B to the right [3].

In an un-congested state, the transmission line have no limiting capacity. Thus, as depicted in Figure 2.4, the power will flow from area A (surplus area) to area B (deficit area) with nodal prices similar to the system price. However, when transmission congestion occurs, a restriction in the power flow on the line is introduced, affecting the nodal prices as shown in Figure 2.5.

(a) Market equilibrium in area A.   (b) Market equilibrium in area B.
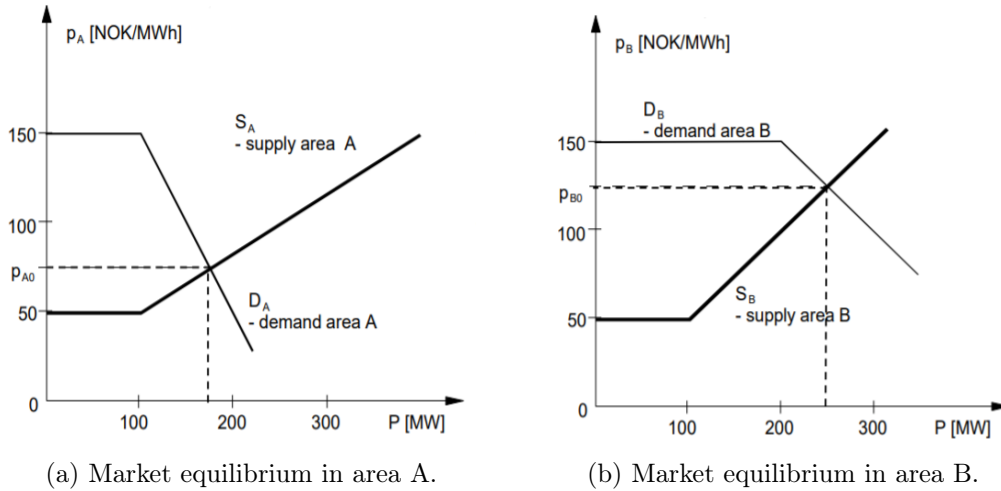
Figure 2.5: Market balance when congestion included [3].

Demand curves in Figure 2.5a and Figure 2.5b remains constant, but the change in the supply curves lead to different area prices. The congestion leads to generator A, G_A, reducing production, which in Figure 2.5a results in the supply curve moving to the left, depending on how much generation in area A is cut off compared to the un-congested situation. This again, leads to a lower area price in zone 1 as seen in Figure 2.5a. The area price in zone 2 increases compared to the original case, seen in Figure 2.5b. This, due to adding the power flow limit to the supply curve, forcing the supply curve to displace to the right (also depending on the value of the line capacity).

System price

The system price, or the marginal price/market-clearing price, is equivalent to the reference price in Norway and is calculated by Nord Pool as soon as the area prices are computed. For the system price calculations, it is assumed to be infinite amount of transmission capacity within the Norwegian bidding zones. Also, the calculated hourly flows from area pricing between Norway and other countries in Europe where Nord Pool operates, are utilised as price independent purchases and sales depending on the direction of flow.

Each hourly system price in the day-ahead market is computed by the use of the supply curve (marginal cost) and the demand curve (marginal willingness to pay), all based on the price and quantity in each hourly offer and bid given. The intersection point between the two curves is equal to the system price of a particular hour. Figure 2.6 illustrates the concept of system price, whereas the equilibrium point is equivalent to the system price. All bids and offers after this point, that is on the right side of the equilibrium point, are rejected.
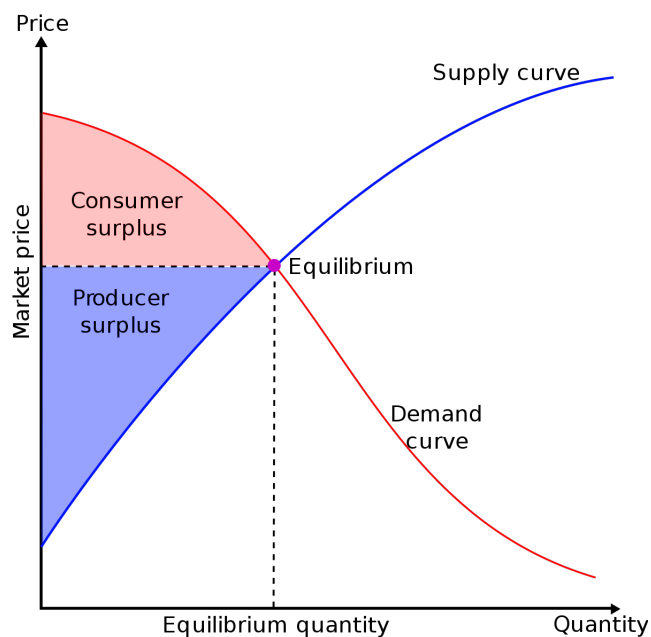
Figure 2.6: Market balance given no congestion [4].

The goal of this pricing mechanism is to maximize the social welfare, this by approximating to a perfect competition. If non-intersecting supply and demand curves where to occur, the system price would be defined as the average of the hourly area prices, and the trading quantity would be equal to the average hourly quantity in Nord Pool [28].

2.2.2 Order Types

The customers in Nord Pool may choose between the following orders in the day-ahead market: single hourly orders, block orders, exclusive groups and flexi orders, whereas the first two orders mentioned above is explained further as these are the most used order in the Nordic power market [29][30].

Single hourly orders

Single hourly order is when the participant denotes the buying and/or selling volume for each individual hour, and either choose between price dependent or a price independent order. In the price independent order the participant may specify the desired amount of volume that is wished to be bought or sold each hour for a total 24 hours, and receive the wished amount regardless of the price. The price dependent order, however, accepts bids/offers of different volume sizes, and the price may be decided by the participant to be at a preferred range for each of the hours. In that case, linear interpolation is utilised to combine all price-volume pairs for each hour in order to calculate the actual price. Both of the mentioned orders require a price limit between -500 EUR and 3000 EUR [29].

Block orders

Block bidding is also possible in Nord Pool, meaning that firms may link biddings consisting of prices and desired volumes together into a block. Nord Pool offers four types of block orders: regular, profiled, curtailable and linked block orders explained below [30].

The regular block orders are the most frequently used block order and follow the "all-or-nothing" property. That is, either the block order is fully accepted, or the block order is completely rejected. For a sales block, the block is accepted only if the order price

is lower or equal to the average day-ahead price, as this would be the most beneficial scenario. For a purchase block, the block order would rather be accepted if the order price would be higher or equal to the average day-ahead price. If the above mentioned criteria is not the case, the block order will be fully rejected.

In linked blocked order the different block orders are connected together. For instance, accepting one block order, may require the participant to accept another block order if the orders are linked together. One case of using such type of block order is when the producer has a high start and stop cost, and thus, would like to require a higher price in the beginning of the production time to cover the expenses. After the start-up of a generator, the cost for the producer would be based on the marginal cost, and hence, the price may be reduced. One way of solving this issue is by specifying a higher price for the first couple of hours in one block order, and if this order is accepted, then a new block order with a lower price for the next certain amount of hours has to be accepted.

Curtailable block orders are block orders that may be partially accepted depending on a user-defined Minimum Acceptance Ratio (MAR) [%], unlike the regular block order. Profile block orders requires a minimum duration of three hours where the volume may vary over the defined time span. The average price over this particular time span is further compared with the average day-ahead price with respect to the volume, and based on this, the profile block is accepted or rejected.

2.2.3 Ramping

If there is a large deviation in the power flow from one to another time unit, also called ramping, the frequency will be harder to control, and thus, risking instability in the power system that threatens the safety of the production. Therefore, Nord Pool introduce to ramping restrictions which defines net maximum allowed power flow variation on certain lines [31]. The three TSOs, Svenska Kraftnat, Energinet and Statnett have together listed the HVDC connections that need such a ramping restriction, which Nord Pool has decided to have an upper limit of 600 MW, and this is used both in the day-ahead and the intraday market.

Chapter 3

Methodologies for Electricity Price Forecasting

Several forecasting models are available today and may be utilised for predicting the electricity price. In this chapter, an overview following with a literature review of the most utilised forecasting models will be presented. As stated in the past chapter, the provided sections in this chapter were also mostly elaborated in the identical previous work performed by the author [13]. Exceptions are the slightly modified Section 3.3.1 and the novel Section 3.3.4 given in Section 3.3.

3.1   Available Forecasting Methodologies

Forecasting models may be categorized as done in Figure 3.1. Although Weron in his detailed state-of-the-art literature review [6] described electricity price forecasting models found in reviewed papers and studies to be divided into the categories; multi-agent, fundamental, reduced-form, statistical and computational intelligence models, a more recent state-of-the-art study [32] the focus is rather pulled over to particularly statistical and deep learning models.
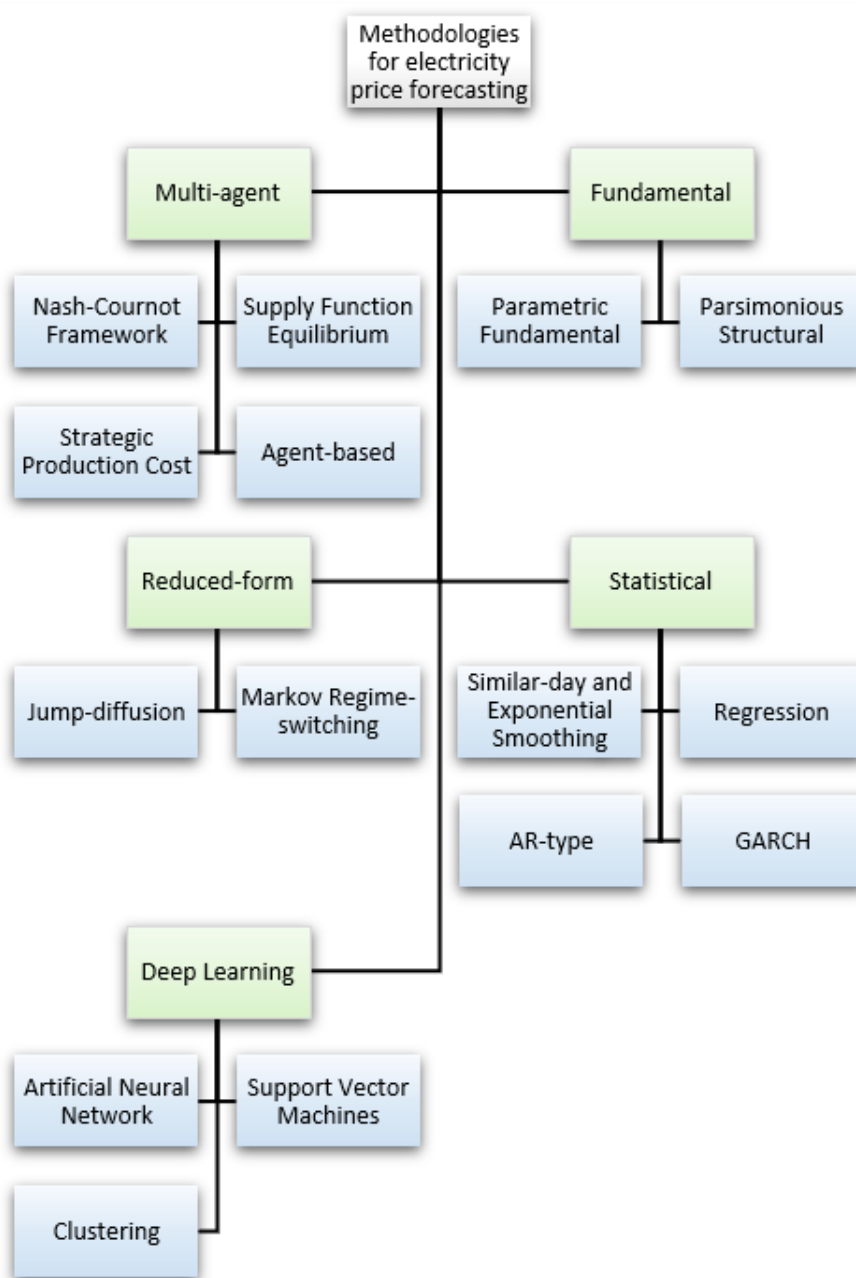
Figure 3.1: A categorization of the most used electricity price prediction techniques inspired by state-of-the-art papers [5][6][7].

3.2 Statistical Models

Statistical models use a mathematical approach, either additive by summing certain factors such as demand, generation and temperature, or multiplicative by taking the product of these factors. One drawback of these models are their incapability of handling non-linearity which is crucial in the non-regulated electricity market. Similar-day, exponential smoothing, regression, AR-types and generalized autoregressive conditional heteroskedastic models are common statistical models used for electricity price forecasting [6].

3.2.1 Similar-day and Exponential Smoothing Methods (ESM)

The similar-day method predicts the future electricity price by the use of historical data of electricity prices that have characteristics similar to the day that is wished to be predicted. These characteristics may be day of the week, consumption, generation, and more. The popular technique called the naïve-method, use the similar-day approach by predicting the electricity price on behalf of the average of other similar-day prices. The implementation of the method is simple, but has the drawback of giving low accuracy for large deviations in similar-day prices [33].

The exponential smoothing method (ESM) is a very popular method used for smoothing time series data values. Smoothing is a technique where noises in the data are removed in order to achieve a more coherent and elegant visualisation of the data set. Moving average, exponential, double exponential and triple exponential are the main smoothing techniques [34][35]. With the current smoothed statistic and the current observation denoted as respectively s_t and x_t, assuming that the observations starts at t = 0 with s_0 = x_0, using a smoothing factor, $\alpha \in \{0,1\}$, the formula for exponential smoothing may be defined as done in Equation (3.1) [33].

$$s_i = \alpha x_i + (1 - \alpha)s_{i\text{-}1} \tag{3.1}$$

The resulting smoothed statistic, s_i, is based on the current observation (x_i) and the smoothed statistic from the last round ($s_{i\text{-}1}$). Exponential smoothing is often used as one of many steps performed in a model. Double exponential smoothing has been utilised for predicting the hourly electricity price in the Spanish market [36], and results indicated a slightly improved performance compared to using ARIMA and the naïve method. However, all these techniques are outperformed by ARX and neural networks.

3.2.2 Regression Models

Regression models demand linearity and follow the sum of squares method to form a regression line based on data points. The most popular regression model is the linear regression [6]. Daily spot prices have been analysed with regression models in combination with ARIMA and GARCH in a study [37]. The authors noticed that for especially the electricity market in Nord Pool, a long-term memory based model should be utilised for predicting daily spot prices.

3.2.3 AR-types of Models

AR (autoregression)-type models illustrate the dynamic behaviour of the system through linear representation. These models have been formulated in different styles and notations. The following formulations are based on mix of resources [6][38][39]. AR stands for autoregression, MA is moving average, I is integration and X denotes extra input to AR. p is the order of AR, denoted as AR(p), q is the order of MA, defined as MA(q), and d is the order of integration. The AR(p) and MA(q) model are defined as done in respectively Equation (3.2) and Equation (3.3).

$$Y_t = a_0 + a_1 Y_{t-1} + a_2 Y_{t-2} + ... + a_p Y_{t-p} + \epsilon_t \tag{3.2}$$

$$Y_t = b_0 + b_1 \epsilon_{t-1} + b_2 \epsilon_{t-2} + ... + b_q \epsilon_{t-q} + \epsilon_t \tag{3.3}$$

ARMA(p,q) is formulated by combining Equation (3.2) and Equation (3.3) as done in Equation (3.4), and is only usable in cases of stationary data.

$$Y_t = a_0 + a_1 Y_{t-1} + \ldots + a_p Y_{t-p} + b_0 + b_1 \epsilon_{t-1} + \ldots + b_q \epsilon_{t-q} + \epsilon_t \qquad (3.4)$$

However, by differencing, the model can be useful for non-stationary cases. Such models are called ARIMA models. These act like a filter by separating the signal from the white noise, and then using the residual signal for forecasting.

AR has been utilised for forecasting the electricity prices in California [40]. One study designs a wavelet-ARIMA combined model for hourly electricity price forecasting by decomposing the price data using DWT (discrete wavelet transform) which then is forwarded to the ARIMA model for predicting the 24 hourly electricity prices of a future day [41]. The inclusion of the wavelet transform to the regular ARIMA model improved the results. Another, even more, relevant example is the use of seasonal ARFIMA (f for fractional) on area prices from Nord Pool for forecasting due to observations in the area prices from 2000 - 2003, indicating strong coupling between long memory and fractional integration, which is supported by the explanation of most of the generation produced from hydropower plants [42].

3.2.4 Generalized Autoregressive Conditional Heteroskedastic (GARCH) Models

GARCH models, unlike the ARIMA models, have the ability to take the error between the predicted and actual value, into consideration [43]. In other words, GARCH has the great value of measuring volatility in time series data, such as spikes in the electricity prices, leading to a more parsimonious model than ARIMA, also supported by a study performed in 2005 [43]. Historical price data from the Spanish power market has been decomposed with the help of wavelet transform, and forwarded to both an ARIMA-GARCH model and a GARCH model to predict future electricity prices [44]. As GARCH-type models have a greater focus on the smaller details in the input data, including weather forecasts to such a model gave more accurate day-ahead electricity price predictions in Scandinavia [45].

3.3 Deep Learning Models

Deep learning algorithms use neural networks to model the problem with a certain learning approach for training the network in order to produce a model that can be utilised for predictions [46]. Neural network-based models are found to be quite unique for its flexibility due to handling non-linear problems, unlike all other methodologies mentioned in this section. Of the learning approaches available, supervised and unsupervised are the ones mostly seen in the context of electricity price forecasting. Input and output data can be assumed to be given for the supervised learning-based model, in which the algorithm based on the data, maps the needed functions for producing a fitting model, such that the very same model can be used for predicting new outputs given a new set of input parameters. If the goal is to understand the input data and its structure, unsupervised approaching models should be utilised. Available deep learning-based methods are artificial neural networks, support vector machines, clustering and recurrent neural networks, presented in this chapter.

3.3.1 Artificial Neural Network (ANN)

The ANN model evaluated in this section is equivalent to the so-called feed-forward neural network (FNN). The general ANN structure is displayed in Figure 3.2 with one input and output layer, and one to multiple hidden layers decided by the user as well as the number of neurons in each layer.
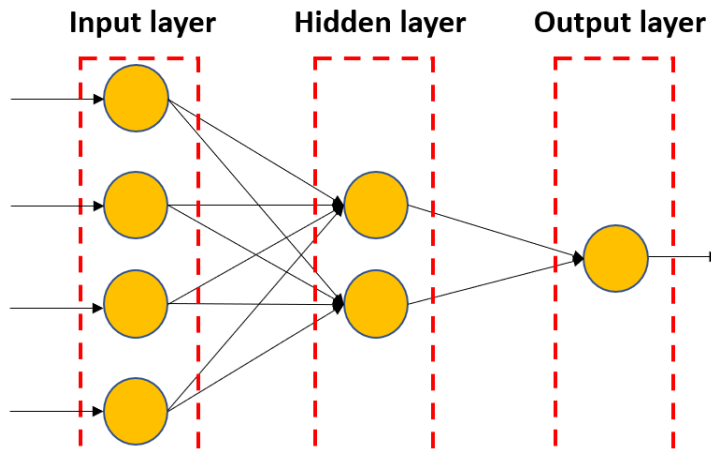

Figure 3.2: A representation of a simple neural network [8].

The more layers in the network, the greater amount of neurons can be used for training the model to find a better link between input and output, giving a higher output quality, but unfortunately also coming a long with high time complexity. The performance of ANN is dramatically reduced if few input parameters are injected to the model, and it is very difficult to get an understanding of what happens in the hidden layer(s) [46].

The transformation occurring between the layers are provided in Figure 3.3, with W_1, W_2, ..., W_n denoting the weight on each signal and X_1, X_2, ..., X_n representing the value of the neuron in the first layer. The output is acquired by the summation of each multiplied term of X and W as performed in Equation (3.5), which is further employed to an activation function, f as presented in Equation (3.6).
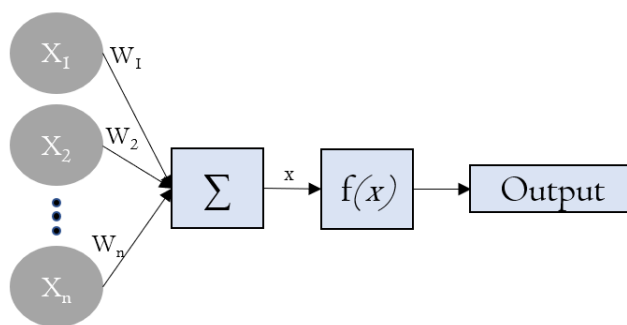

Figure 3.3: The transformation in between the layers.

$$x = W_1 X_1 + W_2 X_2 + ... + W_n X_n = \sum_{j=1}^{i} W_j \cdot X_j \quad (3.5)$$

$$output = f(x) \quad (3.6)$$

ANN requires a training algorithm that changes the model in each iteration in order to find the best approximated model fitting the injected data. The model is changed by

adjusting the weights each signal is assigned with. Back-propagation (gradient steepest descent method) and the Levenberg-Marquardt algorithm are popular training algorithms used in this case [6].

ANN has been utilised for predicting day-ahead electricity prices for the European Energy Exchange (EEX) market, discovering that the neural networks are almost insensitive to the length of the forecasting period [47]. Instead of using one neural network for forecasting, the data may be decomposed into smaller subgroups of data, each connected to its own neural network. Combining predictions from each network has found to be a challenge due to the mapping of each network being dependent on the individual input. A study proposes to use weighting coefficients denoting the probability that a network has reached the optimal model, to combine the predictions, which has proved to increase the forecasting quality [48].

3.3.2   Support Vector Machines (SVM)

SVM is a modified version of SVR (support vector regression), and is able to handle non-linear regressions. It is often used to predict a category or a class by plotting the data in an n-dimensional space such that each dimension regarding a data point represents a feature. A hyper-plane is used as a frontier to separate the data into classes in such way that the distance between the hyper-plane and the closest data point to the plane is maximized [46][49]. Prediction with SVM is defined as SVM training and forming a classifier based on parts of the input data, and further using the designed classifier to predict/classify the rest of the data set [50].

SVM is normally a part of a hybrid model, representing one of many stages for forecasting. One proposed hybrid model is the combination of ARFIMA and least-squares SVM used on data from Nord Pool [51]. Enhanced results are received compared to applying each individual model on the same data. Another model, the SVRARIMA, supposedly outperforms certain ANN and ARIMA models for price forecasting [52].

3.3.3   Clustering

While the other methodologies in this section follow the supervised learning approach, unsupervised-based techniques such as clustering can be a quite useful tool in regards of electricity price forecasting. Clustering is a centroid-based representation of the data and the k-means clustering algorithm is the simplest of all unsupervised learning forms. The purpose of this algorithm is to structure the data into smaller groups, called clusters, which then is forwarded to another model for forecasting.

Spikes in historical electricity prices can be clustered such that each cluster contains spikes in the same price range [53]. Another study clustered the load data into peak, normal and off-normal hours and in combination with an ANN-based model predicted the electricity price [54].

3.3.4   RNN

Unlike the case of ANN with feed-forward connections between the neurons, RNN models allow neurons to pass information to the next, previous or even the same layer and has the unique ability to memorize previous information and use this for current output computation. In other words, if input data of dependency is utilised, using very recent information for predicting current output would improve the accuracy even further compared to regular ANN models.

Figure 3.4 is illustrating how this deep learning technique is memory-based. The left figure is the unrolled version of RNN while the right figure is rolled out for understanding the process of maintaining the memory in the network. Let x_t denote the input information at current time, t, s_t and o_t be the output of the network according to the memory (state) of the current network, s_t. The weights, u, v and w of respectively input, output and internal connections in the hidden state are updated for each training simulation of the network. In the unrolled version of RNN each hidden state at each unit of time receives all previous memory knowledge of the network from the previous step. In other words, at time unit, t, the model will receive both the input information, x_t, and the knowledge about the hidden state of the previous time unit, s_{t-1}, which combined is contributing to predict a more precise output, o_t, while storing the current network information, s_t, in order to easily supply this to the next time unit [9].
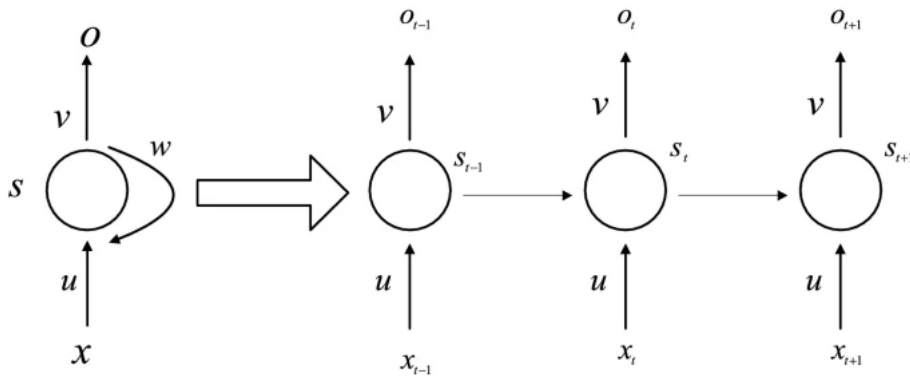

Figure 3.4: An unfolded RNN model [9].

LSTM

LSTM (long short-term memory), a type of RNN model that avoids problems such as gradient disappearance and gradient explosion due to its unique structure as seen in Figure 3.5, is designed for solving short- and long-term dependency problems [55][56]. LSTM differ from ANN and other RNNs by consisting of memory blocks rather than neurons and Figure 3.5b, shows the basic structure of such a cell with the three gates, input, output and forget gate.

The explanation of the computational processes in the memory cell are based on several papers [9][57][58].The following parameters, w_f, w_i, w_c and w_o are weight matrices, and b_f, b_i, b_c and b_o are bias vectors used in equations that are to be presented in this subsection.

The forget gate, f_t, decides whether previous information should be kept or thrown away through Equation (3.7), based on the previous hidden layer output state, h_{t-1}, and the current input information, x_t. The input gate, i_t, decides what values should be entering and updating the cell state through Equation (3.8) and Equation (3.9). The new memory cell value, C_t, is then computed as seen in Equation (3.10) based on the input gate i_t, $\tilde{C}_t$, the forget gate, f_t and the previous memory cell information, C_{t-1}. Lastly, the output gate, o_t, regulating the amount of data in the memory cell that should be allowed to flow any further, is calculated through Equation (3.11) in which the obtained results from this gate combined with the memory cell, C_t contributes in determining the overall hidden layer output of the LSTM memory cell, as seen in Equation (3.12). The weights in the equations presented above are to be adjusted for each round of training of the model in order to receive the most optimally predicted electricity price.

$$f_t = \sigma(w_f[h_{t-1}, x_t] + b_f) \tag{3.7}$$
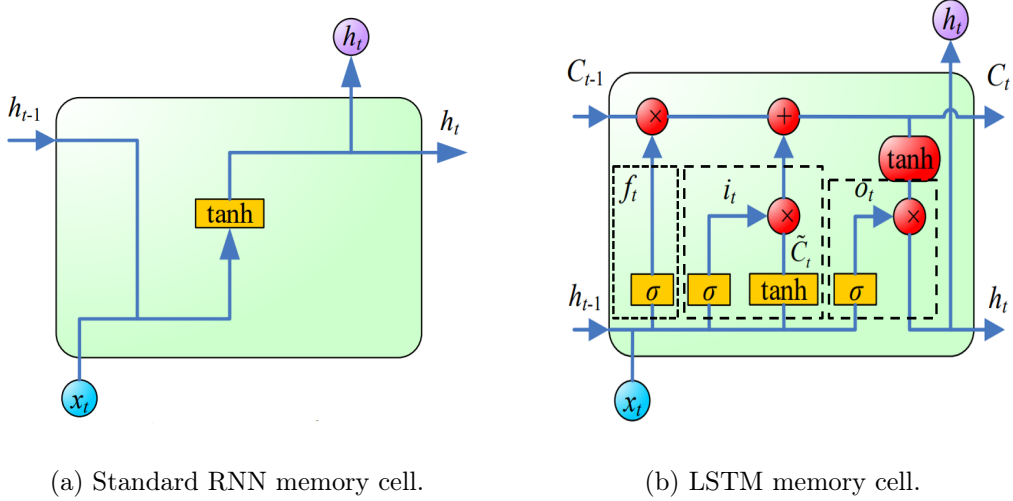
27

(a) Standard RNN memory cell. (b) LSTM memory cell.

Figure 3.5: Memory cells in a typical RNN model vs. a LSTM model illustrated in a paper [10].

$$i_t = \sigma(w_i[h_{t-1}, x_t] + b_i) \tag{3.8}$$

$$\tilde{C}_t = tanh(w_c[h_{t-1}, x_t] + b_c) \tag{3.9}$$

$$C_t = f_t \cdot C_{t-1} + i_t \cdot \tilde{C}_t \tag{3.10}$$

$$o_t = \sigma(w_o[h_{t-1}, x_t] + b_o) \tag{3.11}$$

$$h_t = o_t \cdot tanh(C_t) \tag{3.12}$$

The Adam-optimized LSTM model was proposed for forecasting the electricity price in New South Wales in Australia, revealing to performing far better than traditional models such as ANN and ARIMA [59]. Another paper exploit it in the forecasting of the day-ahead market in the Victoria region of Australia and Singapore, comparing the outcome hybrid methods of BP-ANN, WT-ANN, PSO-ANFIS and SARIMA, concluding the LSTM executing with the greatest improvement in the forecasting accuracy [60]. There are also studies exploring hybrid solutions of LSTM [61][62][63].

Chapter 4

Methodology

Figure 4.1 is illustrating the various stages of the proposed models. Figure 4.1a is showing how the basic AI-model forecasting will be conducted, while Figure 4.1b visualise how the hybrid method of clustering combined with an AI methodology would be working. The rest of the chapter describe each of the stages in the proposing AI-models.
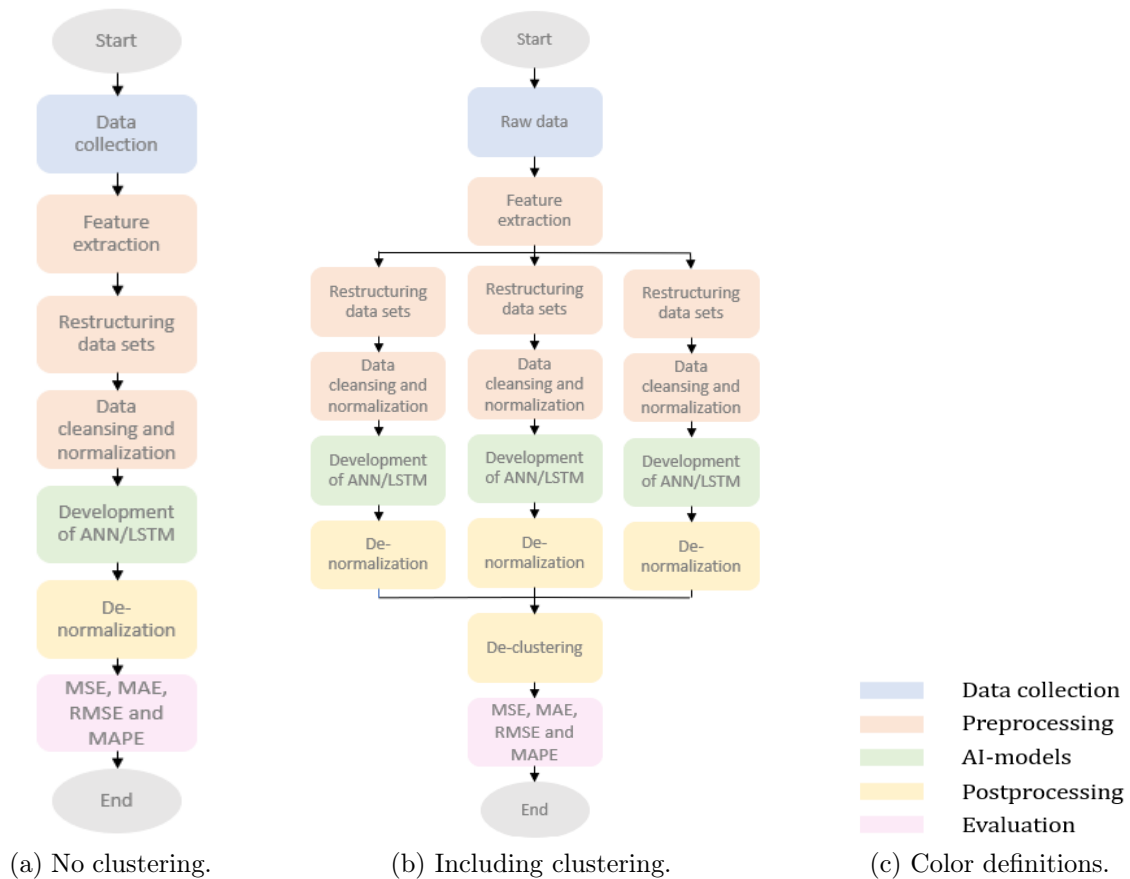

(a) No clustering.   (b) Including clustering.   (c) Color definitions.

Figure 4.1: A framework describing each stage of the electricity price forecasting model.

4.1 Data collection

Historical electricity prices, consumption, relevant power flows, temperature, precipitation and CO_2-price data spanning from 2013 to 2021 was collected. Data concerning gas and fuel price were not available, and thus is disregarded in this thesis. Information for each collected data type is presented in Table 4.1.

Table 4.1: Information regarding the collected data.

Data type	Hourly	Daily Average	Other	Source
Electricity price	✓			Nord Pool
Consumption	✓			Nord Pool
Power flow	✓			Nord Pool
Temperature		✓		Meteostat and Norsk Klimaservicesenter
Precipitation		✓		Meteostat
CO_2-price			✓	EPEX SPOT

Hourly historical electricity price and consumption for zones NO1-NO5 were available, and relevant hourly power flows from transmission lines between nodes NO1 - NO2, NO1 - SE3, NO4 - SE2, SE2 - NO3, NO2 - DK1, NO3 - NO4, NO4 - SE1, NO1 - NO3, NO1 - NO5, NO5 - NO2, NO3 - NO5, NO2 - NL and NO2 - DE were utilised in the process of training and predicting. Other cables pertinent for the Norwegian bidding zones with unfortunately lack of accessibility of data, are NO4 - FI and GB - NO2 with the first having observed low to zero power present in the transmission line, and the latter cable officially commencing in the last quarter of 2021 with a foreshortened capacity of maximum 700 MW and ramping of 300 MW due to a trial operation of safety and cable functionality being performed [64, 65]. Instead of directly injecting the power flow data to the AI model, the values are transferred into equalling zero representing no flow and one indicating a flow in attendance.

The CO_2-price data stems from the Emission Spot Primary Market, and the auctions subjected to the auction name, *EU*, undertaking the EU and EEA EFTA states such as Norway, seemed to be the most appropriate emission trading platform to settle on [66]. As the auctions are taking place Mondays, Tuesdays and Thursdays at 11:00 CET, CO_2-price is assumed to be constant for the next consecutive day(s) until the next auction is performed.

4.2   Preprocessing

The raw input data is further feature extracted, structured in a certain manner as well as being applied with preprocessing techniques such as data cleansing, normalization and clustering for the AI models to be functional for predicting future values and for increasing the forecasting accuracy. These measures are further explicated below.

Feature Extraction

Figure 4.2 displays the precise input parameters extracted from the raw data collection based on the conducted literature review in Chapter 2 and Chapter 3. The type of forecasting day, d, is highlighted as indices $\{0, 1, ..., 6\}$ accordingly to day types Monday, Tuesday, ..., Sunday, the predicting time of the day, t, is weighted as integers $\{0, 1, 2, ..., 23\}$ emphasising the commencing timestamp of the hourly electricity price and demand time span. The prior 24, 48, 168 and 672 hours representing the previous day, two days, one week and approximately one month of electricity price and demand are included in the input data. The power flows denoted as PF with exactly 24 hours from the predicting hour, t, and $i = \{1, ..., n\}$, indicating the number of cross-border flows of the area, where n depends on the predicting zone, are also injected to the model. As average values of

temperature and precipitation were obtained, as well as one specific CO_2-price applying throughout a day, constant values of these parameters from the foregoing day are applied for predicting all 24 hours of the next day.
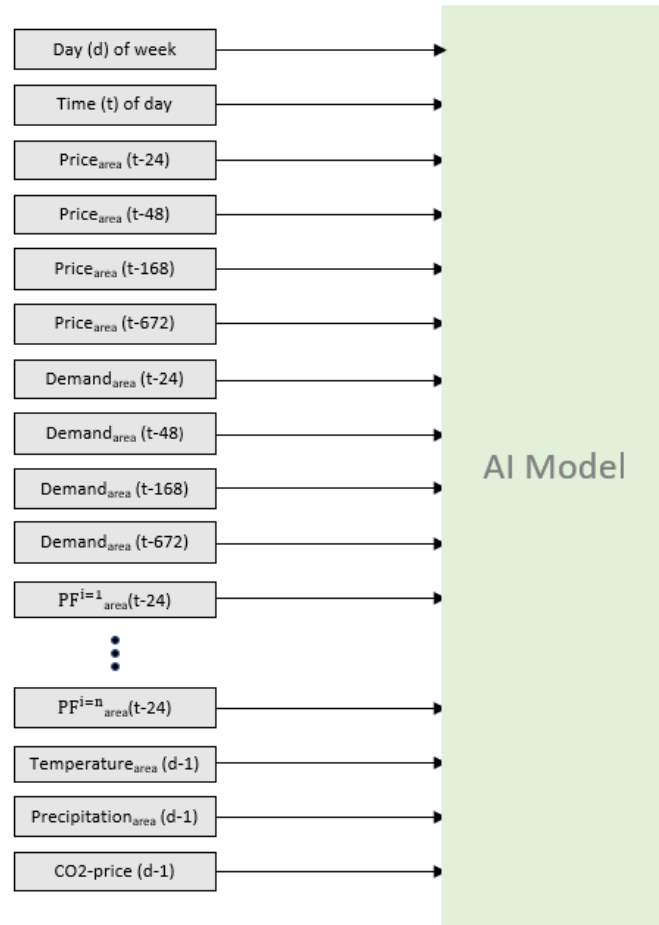

Figure 4.2: Overview of the input parameters the ML model is injected with.

Structuring the Data Sets

The ANN-based AI model requires a 2D-shaped input. Therefore, a 2D matrix is formed with each column containing information regarding each type of input parameter as depicted in Figure 4.2, and each row representing each time step and the last column being the actual electricity price of hour, t on day d, used for comparing with the predicted value. Figure 4.3a depicts the conventional way of structuring the ANN input. Even though ANN and LSTM both base on the concept of neural networks, the added memory-function lead to the necessity of restructuring from the classic ANN input arrangement as illustrated in Figure 4.3b.

(a) Typical ANN structure.   (b) Typical LSTM structure.
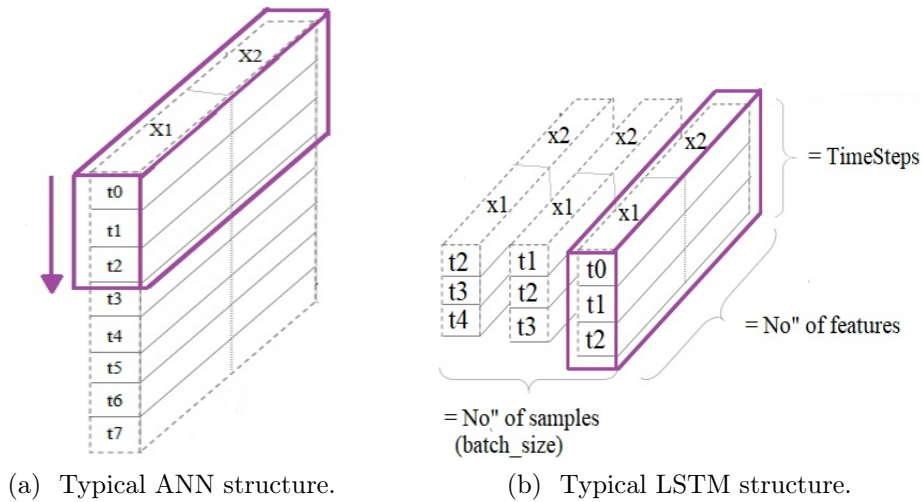
Figure 4.3: Restructuring of an ANN and an LSTM data set [11].

The LSTM model requires a 3D input shape of dimensions equal to (number of samples, time steps, features) and as shown in Figure 4.3b, it gives the effect of a sliding window that for each round with the exception of round one, excludes the first row and includes an additional time step of data. The memory function of the neural network is hence applied in the manner of including several recent time steps in one batch input, while the ANN would utilise only the last recent time step in order to predict for a certain hour of electricity price. The number of features is pre-determined from the feature extraction, the time step is chosen by the user and the number of samples will reveal its value when the bottom has reached in an iterative method of forming each batch of x time steps, in other words, when the window sliding terminates.

Three data sets, namely training, test and a validation set must be formed for each AI model based on the collected data ranging from 2013 to 2021. In this thesis, the test set is decided to comprise the necessary input data for forecasting hourly electricity prices of 2021 as this is set to be the goal. The remaining data is further sorted into training and test sets embodying a share of respectively 90% and 10%. The inclusion of a validation set is optional, but has its function of reducing any potential overfitting and guide the training model in a more proper direction. All these data sets must follow the recently described prerequisite structure in accordance with the type of ML model employed.

Data Cleansing and Normalization

In order for the input data to be compatible with the AI model, essential preprocessing techniques must be applied, which here is decided to be data cleansing and normalization. A plausibility analysis should be performed on all data sets for data cleansing and if missing or inconsistent values are discovered, appropriate actions should take place.

Some values are detected to be missing in the temperature and/or the precipitation data in NO2. This is compensated with replacing the missing values with data from another city within the same bidding zone. There is a tremendous lack of precipitation data from Meteostat on bidding area NO4, which is where Norsk Klimaservicesenter steps in, providing the missing data type of NO4.

The sklearn.preprocessing Python package offers preprocessing techniques, such as the MinMaxScaler, that may be effortlessly applied to a data set. Normalization was proceeded by transforming the raw input data to values ranging [0,1] through one common MinMaxScaler. This, by defining a scaling with the fit-function on the training and

validation set and further implementing the transform function on all three data sets, so to avoid data leakage.

Clustering

Optionally, clustering may be incorporated to the training, validation and test sets as a final preparation of the input data. The k-means clustering, as investigated, in Section 3.3.3, is one possible way of grouping the data in an unsupervised manner. Another method, exploited in certain papers, manually organize the input data based on the type of day and/or hour [54, 67]. This thesis is decided to investigate both the usage of k-means clustering and so-called *manual clustering*, with the latter approach segregating each of the three data sets into three clusters encompassing input parameters related to day types 1) Mondays to Fridays, 2) Saturdays and 3) Sundays. The k-means procedure of clustering is also determined to take upon three clusters as well with an unsupervised data grouping strategy as studies proclaim a choice of three and four clusters is effectively accumulating a more optimal forecasting accuracy [68, 69].

4.3 AI-models

Two AI methodologies will be evaluated in this master thesis, that is, the ANN and LSTM models with one hidden layer, as to see how the performance vary from a simple neural network in comparison with a memory-based network. The formation of the AI-models are dependent on the hyperparameters settings such as epochs, batch size, input dimension and timesteps.

Epochs are defined as the number of times the datasets are submitted to the model, and for each epoch, a certain amount of samples are injected before the weight of each signal is updated [70]. Utilisation of the trial-and-error method by observing what epochs and batch size values improve and aggravate the prediction, is the strategy that these AI models will follow. The LSTM model requisites an additional hyperparameter, namely the timesteps which may be adjusted and shall be given from restructuring the input data in the preprocessing.

The input, hidden and output dimensions may be circumscribed differently for each AI method and must be defined as a part of configuring the models. The ANN would in such case require an input dimension commensurating to the number of features in the input matrix, while the LSTM model demand a 2D input shape equivalent to (timesteps x features), denoted as input$_{size}$. The magnitude of the output layer size is fixed to be equal to one, the hourly predicted day-ahead electricity price, defined as output$_{size}$. The hidden layer is in this thesis decided follow Equation (4.1), based on the input and output dimensions.

$$hidden_{size} \approx \frac{2}{3} \cdot input_{size} + output_{size} \qquad (4.1)$$

An optimizer and a loss function must also be determined. An optimizer is an algorithm that adjusts the weights of each neuron connection such that the error is minimized. Available optimizers are SGD, RMSprop, Adam and Adagrad, among others [71]. The loss function is a formula that is exploited for computing the deviation between actual and predicted output as a goal to be minimized in the model, and alternatives for regression losses are the mean squared error, mean absolute error and mean absolute percentage error loss functions [72].

The selected optimizer for the forecasting models are the Adam stochastic optimizer, a more memory space efficient and robust method that bases on the best qualities of two other stochastic gradient descent extensions, the Adaptive Gradient Algorithm (Ada-Grad) and the Root Mean Square Propagation (RMSProp) [73][74]. In this thesis, the loss function is designated to be the classic mean squared error function as written in Equation (4.2), using the output of the function as the objective of minimizing in the training process.

$$loss = \sqrt{y_{act} - y_{pred}} \qquad (4.2)$$

Not to mention, activation functions are one of the core elements of the DL models. Of the available functions, the usage of the sigmoid and the hyperbolic tangent functions, as described in correspondingly Equation (4.4) and Equation (4.3), will be investigated when forecasting. In between each layer of the ANN an activation function must be appointed. The LSTM model, however, have several locations in one single memory cell where activation functions are utilised. Therefore, a *recurrent activation*, denoting the use of activation functions on input, forget and output gates, and an *activation*, characterizing the employment of activation functions in the cell and hidden layer output state, must be deciding on beforehand.

$$f(x) = \frac{e^x - e^{-x}}{e^x + e^{-x}} \qquad (4.3)$$

$$f(x) = \frac{1}{1 + e^{-x}} \qquad (4.4)$$

4.4   Postprocessing

Depending on the preprocessing techniques applied, the necessary postprocessing of the output of the AI models must be performed. As the output of the forecasting models are expected to be in the range {0,1} due to the normalization, readable values must be obtained by de-normalizing the output through e.g. the inverse_transform tool from sklearn.preprocessing package. If clustering is involved, de-clustering should be applied, connecting the three clusters of data together into one coherent and correctly ordered prediction output data set.

4.5   Evaluation

The results of the forecasting may be analysed by the exploitation of evaluation metrics that produce an indication of the overall accuracy of the model, and model output statistics (MOS) in which tools and programs such as the Matplotlib Python package are utilised for visualizing the prediction outcome. The following metrics values, that is, MAE, MSE, RMSE and MAPE presented in Equation (4.5), Equation (4.6), Equation (4.7) and Equation (4.8) in the identical order will be computed given the number of total samples, N, and the actual and predicted day-ahead hourly electricity price, P_t^{act} and P_t^{pred}. These will further be used for comparison between models with small adjustments and models with different machine learning algorithms.

$$MAE = \frac{1}{N} \sum_{t=1}^{N} |P_t^{act} - P_t^{pred}| \qquad (4.5)$$

$$MSE = \frac{1}{N} \sum_{t=1}^{N} |P_t^{act} - P_t^{pred}|^2 \tag{4.6}$$

$$RMSE = \sqrt{\frac{1}{N} \sum_{t=1}^{N} |P_t^{act} - P_t^{pred}|^2} \tag{4.7}$$

$$MAPE = \frac{1}{N} \sum_{t=1}^{N} \frac{|P_t^{act} - P_t^{pred}|}{P_t^{act}} \cdot 100 \tag{4.8}$$

A percentage error of 100% or more is evaluated as a model deviating exceedingly from the original values, while an error of 0% indicate a perfectly predicted solution. MAE often gives the overall impression of the forecasted results, while MSE and RMSE highlights outliers with the latter emphasizing it more powerfully as a cause of the inclusions of the square root in Equation (4.7). For mathematical reasons seen in the equations of MAE, MSE and RMSE regarding the sample size, N, RMSE is expected to obtain a value higher than MAE, which again is anticipated to be greater than MSE. MAPE may be well-functioning in load forecasting, but arise problems in electricity price forecasting [6]. In the reviews found on forecasting error measurements in general, MAPE had the tendency to favour predictions that were located beneath the actual values and produced high percentage errors when outliers are present, but yet, is one of the most popular error metrics [75][76].

Chapter 5

Input Data

Interesting phenomenons are observed in the input data. Not to mention, studying the past trends and patterns of the various input data may contribute in improving the results of the forecasting. Thus, electricity price and relevant power flow plots are provided in this chapter and remaining figures of the demand, rest of the power flows, temperature, precipitation and CO_2-price may be found in Appendix A.

5.1 Electricity prices

Looking at the electricity prices of previous years and including the 2021, a strong resemblance is seen among the zones of NO1, NO2 and NO5 depicted in Figure 5.1 and NO3 and NO4 as shown in Figure 5.2.

(a) NO1.

(b) NO2.

(c) NO5.
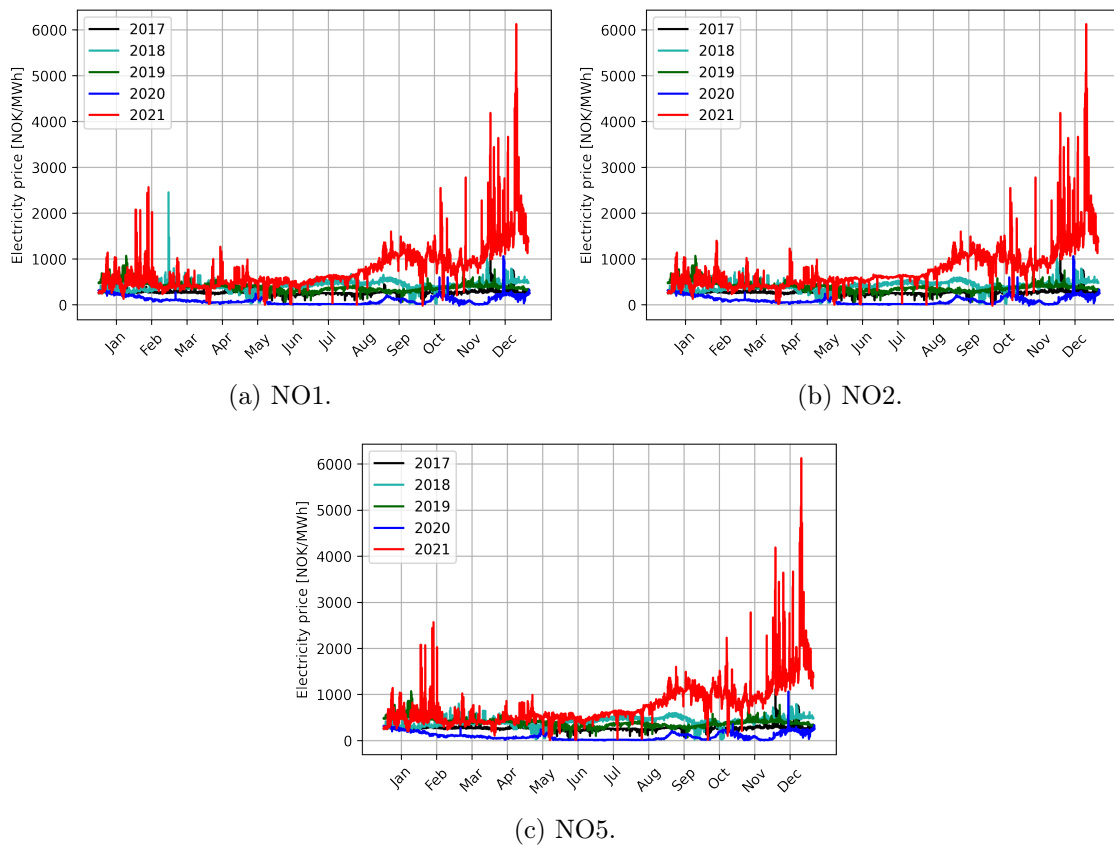
Figure 5.1: The hourly historical electricity prices in NO1, NO2 and NO5 from 2017-2021.

There are repeating peaks and troughs from year to year seemingly to be quite identical, in addition to the similar electricity prices that were the reasons for divided the figures in such way.

(a) NO3. (b) NO4.
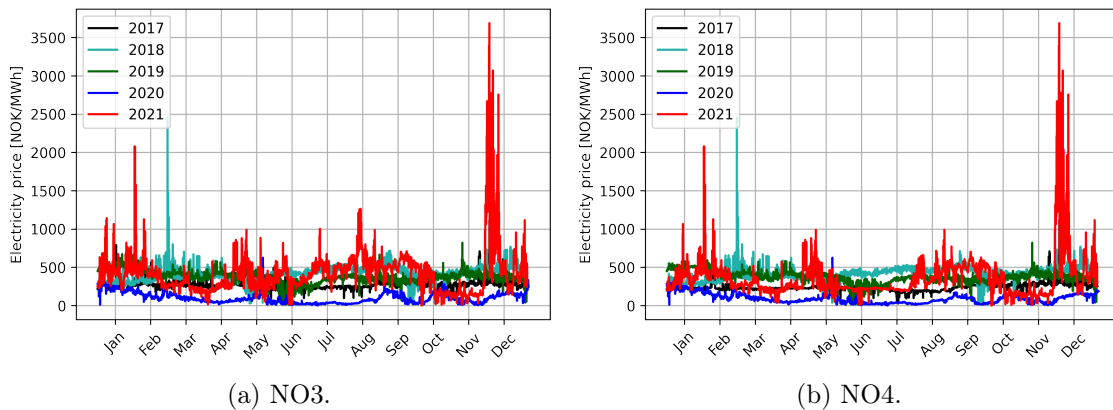
Figure 5.2: The hourly historical electricity prices in NO3 and NO4 from 2017-2021.

5.2 Power flows

Relevant power flows that may be of advantage to bring to the discussion, are presented in this section. Cable connections NO3-NO4, NO3-NO5, NO1-NO2, NO1-NO3, NO1-NO5, NO2- DE, NO1-SE3, NO4-SE2, SE2-NO3, NO4-SE1, and are illustrated accordingly in Figure 5.3,Figure 5.4 Figure 5.5, Figure 5.6, Figure 5.7, Figure 5.8, Figure 5.9, Figure 5.10, Figure 5.11 and Figure 5.12 showing flows in both directions. Moving average has been utilised as to increase the readability of the figures, thus, affecting the y-values of the figures due to calculating an average of a window size of 100. However, the actual values are not vital to know in this case as the goal of providing these plots are for the reader to get the sense of the power flow trends for the past years.

(a) NO3->NO4. (b) NO4->NO3.
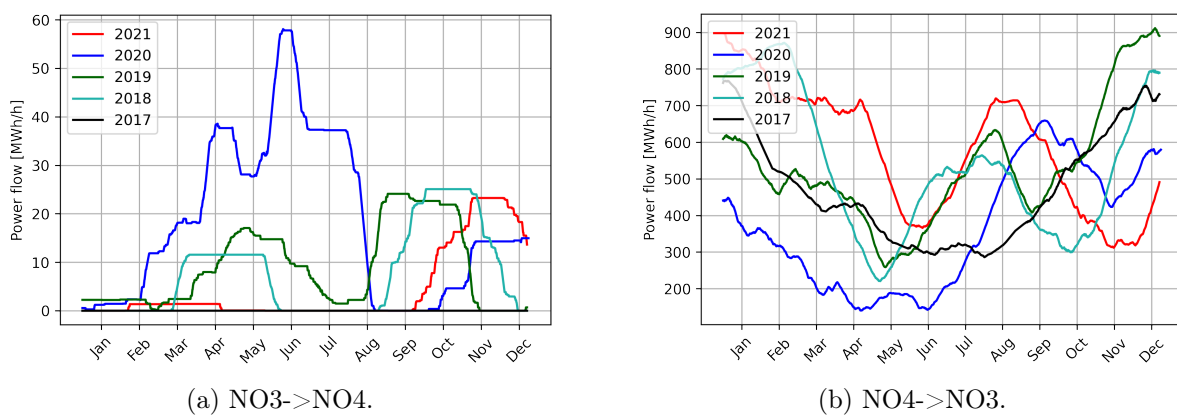
Figure 5.3: Power flow between nodes NO3 and NO4 in each direction.
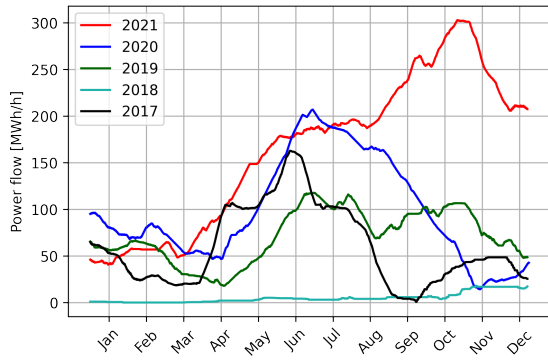
(a) NO3->NO5.
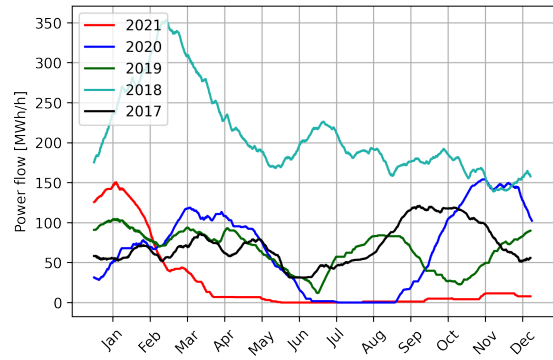
(b) NO5->NO3.

Figure 5.4: Power flow between nodes NO3 and NO5 in each direction.

NO1 and NO2 are the bidding zones with the most connections to other Norwegian bidding zones. The power flow plots of these NO1 cables are provided below.
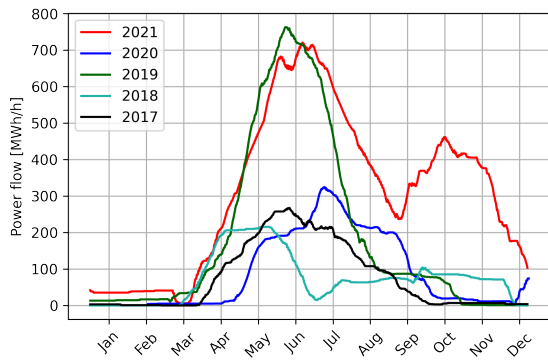
(a) NO1->NO2.
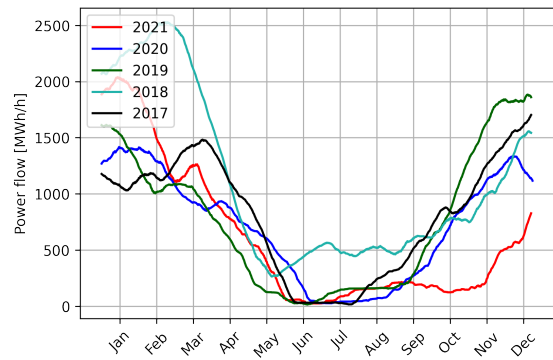
(b) NO2->NO1.

Figure 5.5: Power flow between nodes NO1 and NO2 in each direction.
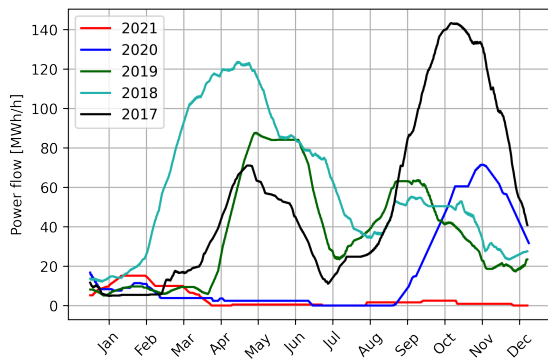
(a) NO1->NO3.
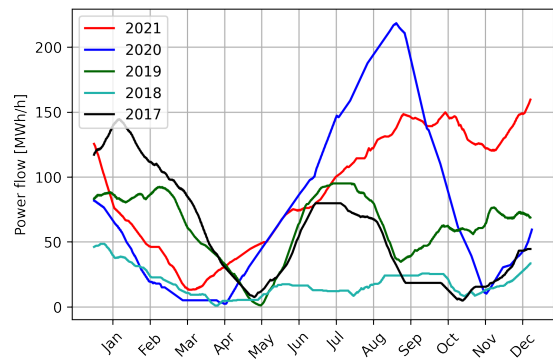
(b) NO3->NO1.

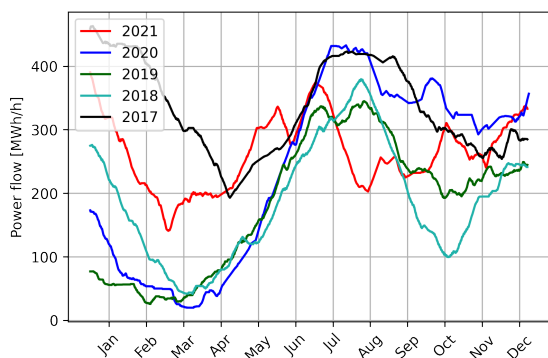Figure 5.6: Power flow between nodes NO1 and NO3 in each direction.
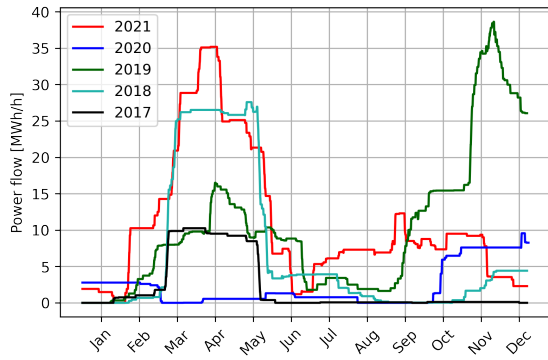
(a) NO1->NO5.
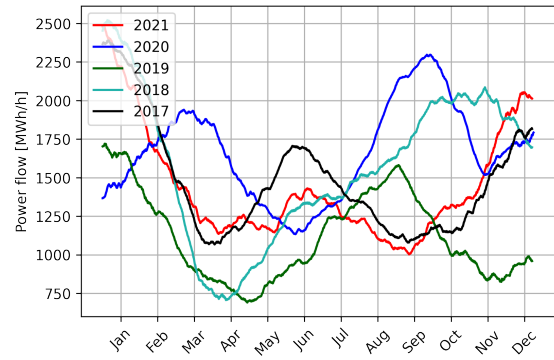
(b) NO5->NO1.

Figure 5.7: Power flow between nodes NO1 and NO5 in each direction.

NO2, on the other hand, has four outgoing cables to UK, Germany, Denmark and the Netherlands. The interconnection between Norway and Germany was quite recently established. Therefore, only data regarding the power flow in 2021 was available, as shown below.
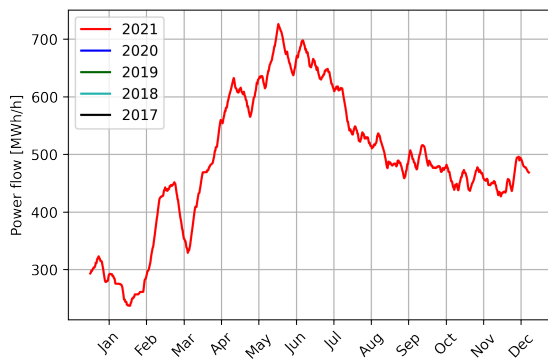
(a) NO2->DE.
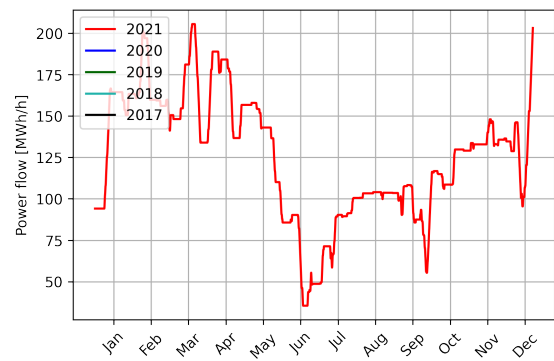
(b) DE->NO2.

Figure 5.8: Power flow between nodes NO2 and DE in each direction.

Norway has both internal connections, but also several linking cables to neighbouring countries, such as Sweden that play a vital role in determining the electricity price in Norway.
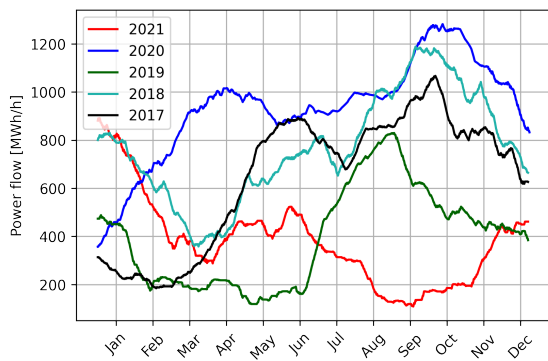
(a) NO1->SE3.
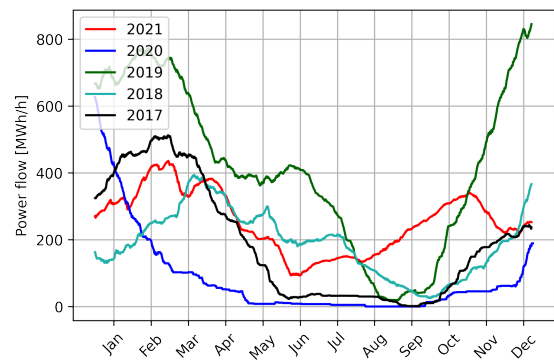
(b) SE3->NO1.

Figure 5.9: Power flow between nodes NO1 and SE3 in each direction.
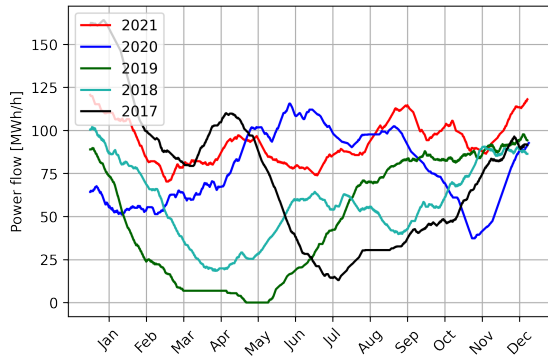
(a) NO4->SE2.
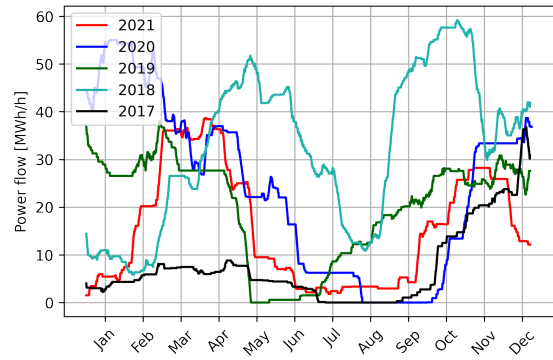
(b) SE2->NO4.

Figure 5.10: Power flow between nodes NO4 and SE2 in each direction.

Norway is interconnected with three of the four bidding zones in Sweden, namely SE1, SE2 and SE3.
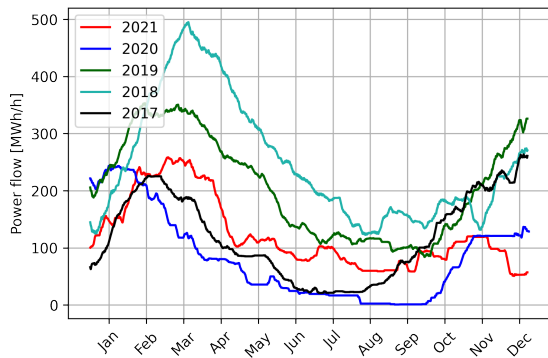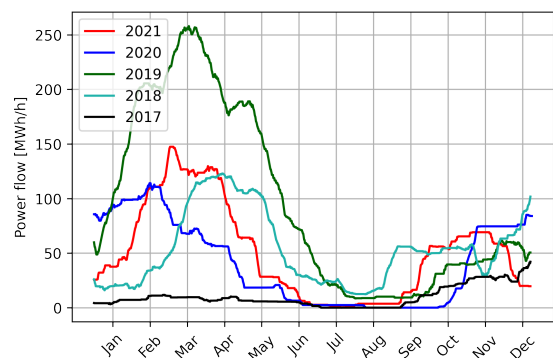

(a) SE2->NO3.
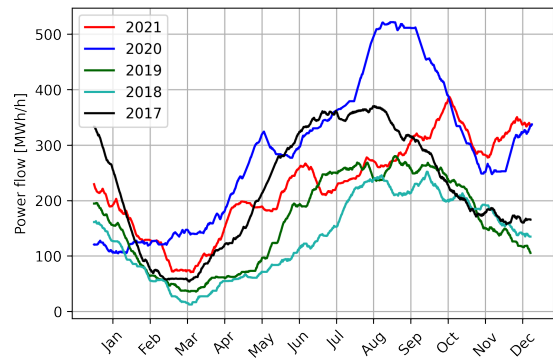
(b) NO3->SE2.

Figure 5.11: Power flow between nodes SE2 and NO3 in each direction.

(a) NO4->SE1.

(b) SE1->NO4.

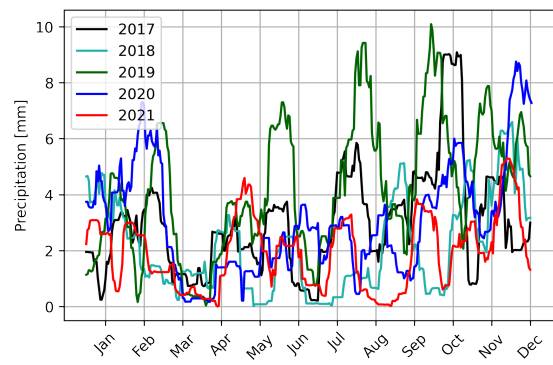Figure 5.12: Power flow between nodes NO4 and SE1 in each direction.

5.3 Precipitation

As most of the Norwegian generation is produced from hydropwer, the precipitation may be in relevance for the discussion. Thus, the precipitation in NO1, NO2 and NO5 for the
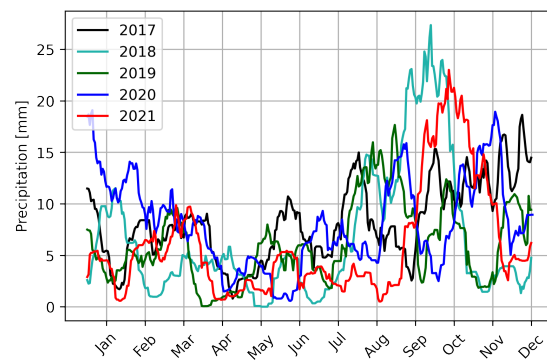
years 2017-2021 is depicted in Figure 5.13.
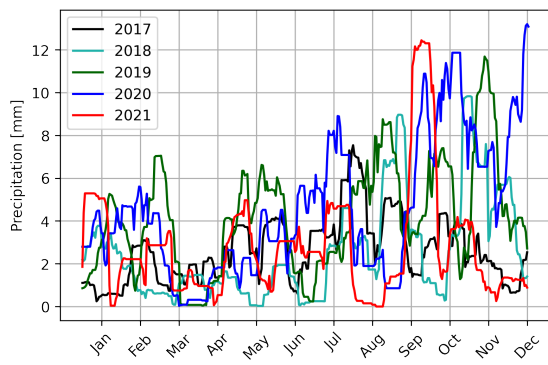
(a) NO1.

(b) NO2.

(c) NO5.

Figure 5.13: The precipitation in the unstable zones from 2017-2021.

Chapter 6

Results

On behalf of the methodology presented in Chapter 4, simulations were conducted with the basis of the two AI-models of ANN and LSTM methods. The ANN had the basic construction of one hidden layer and the LSTM comprised of one LSTM layer. Firstly, hyperparameters were adjusted to the most optimal state, further exploring the forecasting accuracy of the different models and for different cases of modifications, and lastly a sensitivity analysis on the input data was performed. The resulting outcome is presented in below and in Appendix C.

6.1 Hyperparameter Tuning

Hyperparameters such as the batch size, epochs, timesteps and activation functions were tuned manually. The number of epochs were optimized through the Early Stopping regularization in Python while the remaining parameters were varied in the following manner with BS shortened for batch size:

- ANN:

  - BS = {5, 10, 15}
  - Activation function between all layers = {Sigmoid, Tanh}

- LSTM:

  - BS = {5, 10, 15}
  - Timesteps = {5, 10, 15}
  - Recurrent activation = {Sigmoid, Tanh}
  - Activation = {Sigmoid, Tanh}

The outcome of adjusting the BS and activation function in the ANN model is depicted in Figure 6.1. A 3D-repesentation was selected, as to easier comprehend the results of the evaluation metrics. MSE, MAE and RMSE are denoted on the axis, while the MAPE is notified as the size of the plotted points. Colors are to indicate the batch size and cross- and circle-marked points are to emphasize the use of respectively tanh and sigmoid as activation function between input and hidden layer, and hidden and output layer of the ANN.
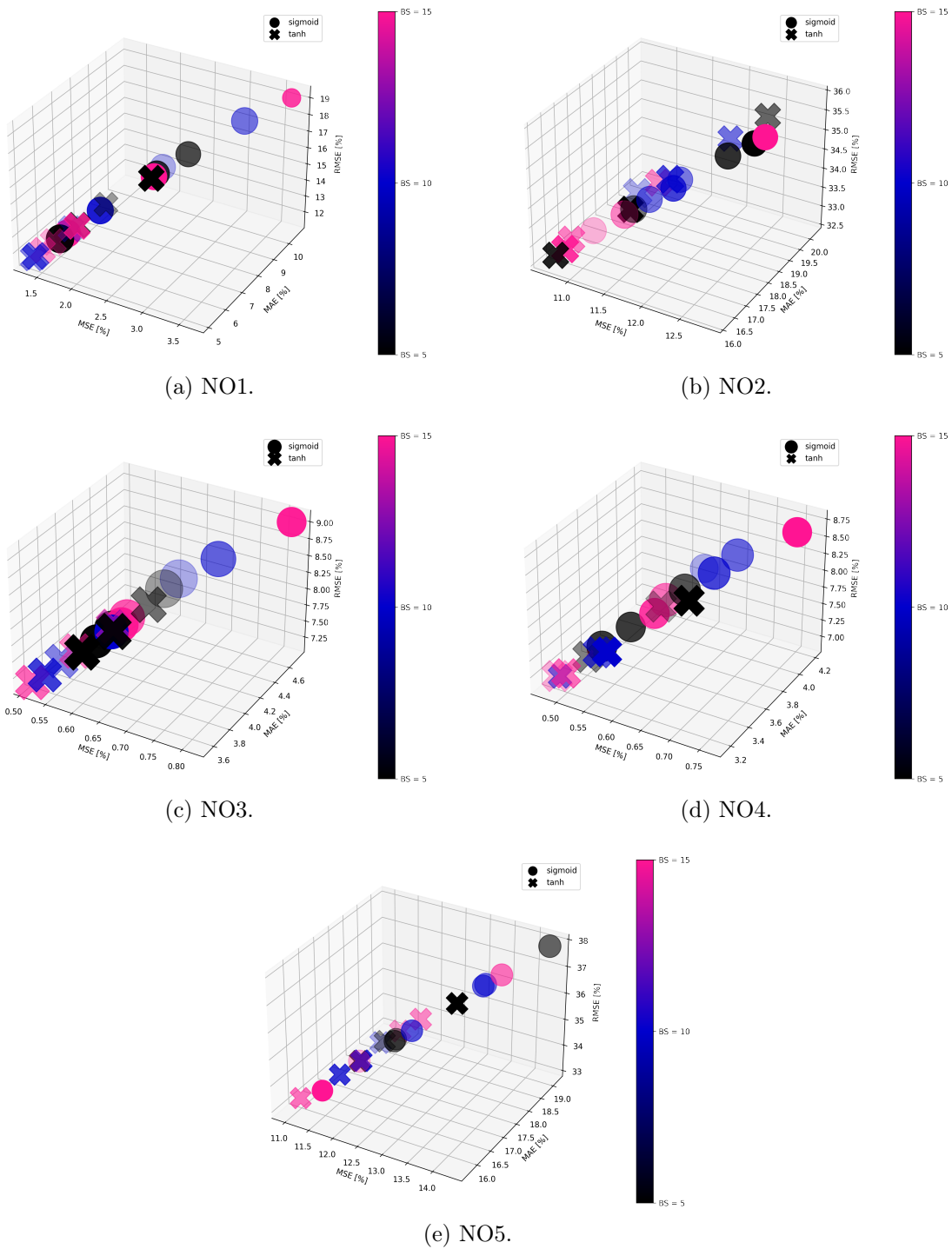
(a) NO1.

(b) NO2.

(c) NO3.

(d) NO4.

(e) NO5.

Figure 6.1: Hyperparameter tuning results of ANN.

As more parameters were required to be tuned in the LSTM model, the tuning was segregated into Part 1 comprising modification of the BS and timesteps, represented in Figure 6.2 in the equivalent means of style as in Figure 6.1. A constant defined recurrent activation and activation function as correspondingly sigmoid and tanh are assumed for all cases and the shape of the plotted points denotes the size of the timesteps.

(a) NO1.

(b) NO2.

(c) NO3.

(d) NO4.

(e) NO5.
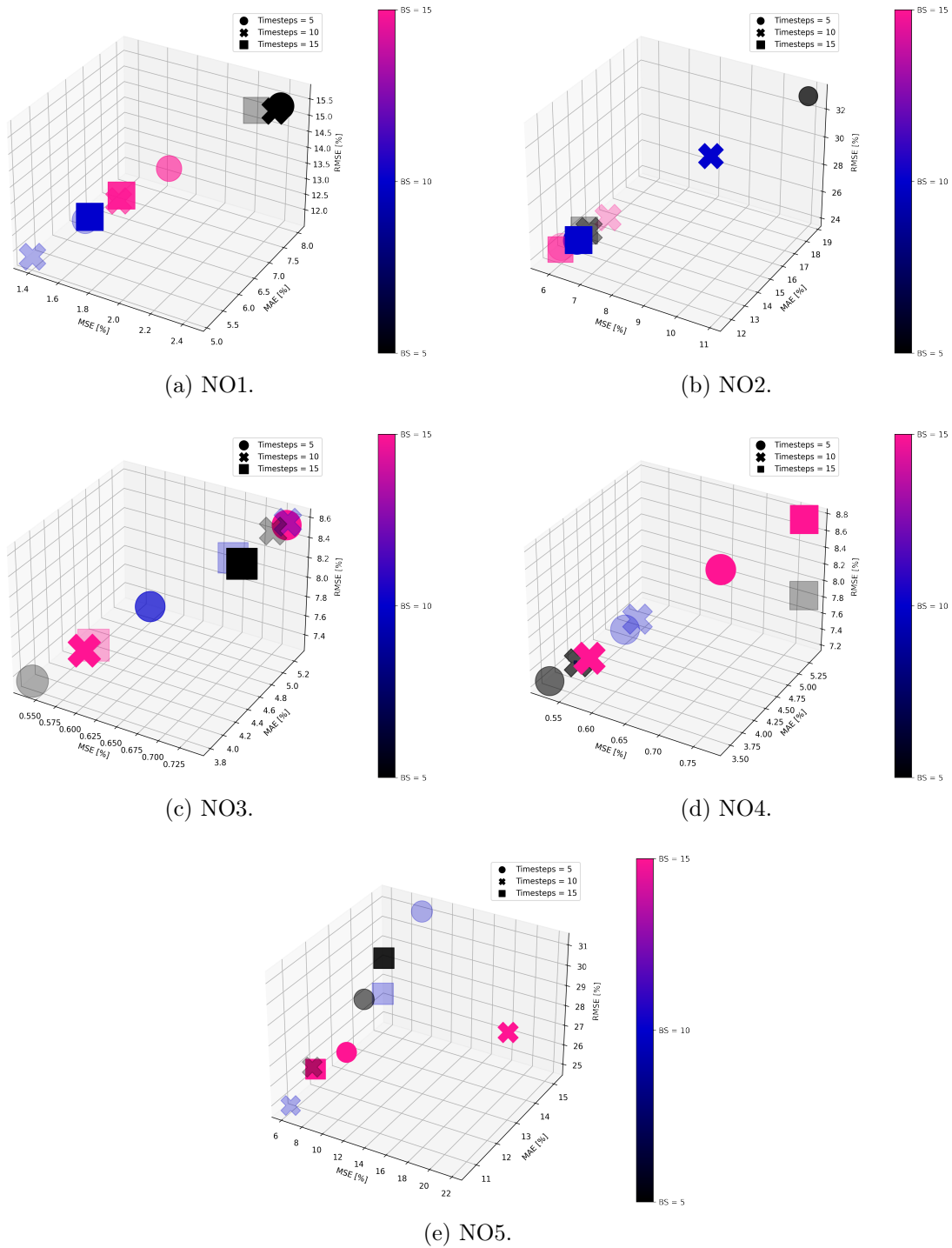
Figure 6.2: Hyperparameter tuning outcome of LSTM - Part 1.

The latter part, Part 2, of optimizing the recurrent activation and activation function were then performed based on the best scenario of BS and timesteps values that produced the overall lowest evaluation metrics from Part 1. The optimization results are illustrated Figure 6.3.
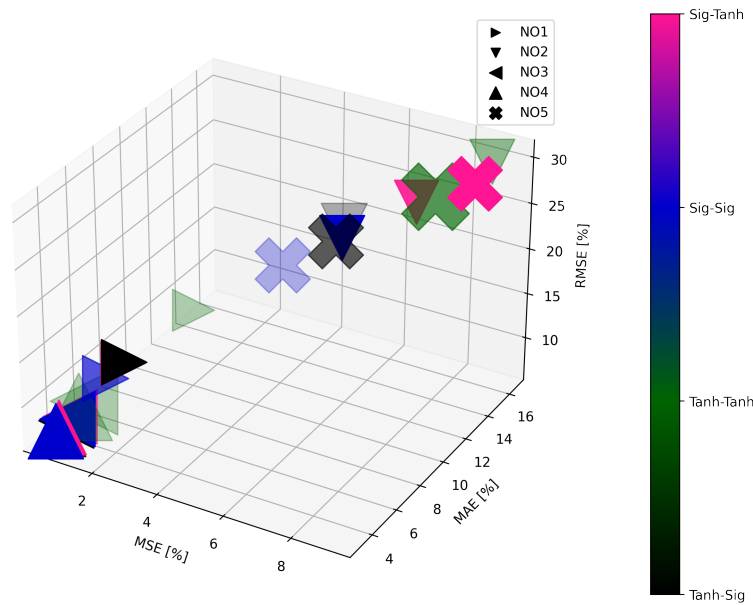
Figure 6.3: Hyperparameter tuning outcome of LSTM - Part 2.

The exact values of BS, timesteps and activation functions of the best cases regarding ANN and LSTM in each area is provided in details in Appendix C, and is from now on referred to as the base cases of each zone.

6.2 Forecasting results

The residual findings from forecasting and further analysis are presented in this section. Various model types and cases are investigated and these are further elaborated in the next subsections.

6.2.1 A Compact Overview of the Findings

A certain amount of simulation rounds of each type of model were performed, encompassing all from hyperparameter tuning, model modifications to sensitivity analysis on the input data. The model types may be defined as:

- Model A: ANN without clustering

- Model B: ANN with manual clustering

- Model C: ANN with unsupervised clustering

- Model D: LSTM

The last Model D also includes results from combining the AI-method with manual and unsupervised clustering. To encapsulate the general performance of each model type, evaluation metrics results of all simulation rounds associated with a particular model is summarized into one box of a box plot. Figure 6.4, Figure 6.5, Figure 6.6, Figure 6.7 and Figure 6.8 presents the results of each evaluation metrics, the range of the values that are covered and potential outliers in sequentially NO1, NO2, NO3, NO4 and NO5.
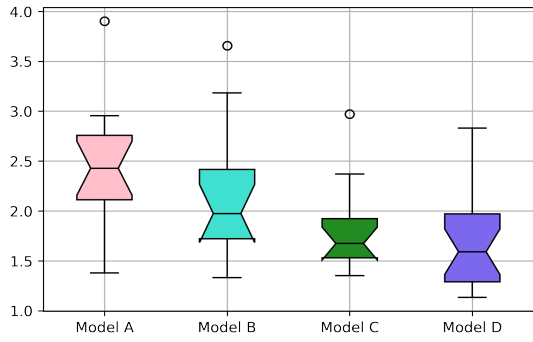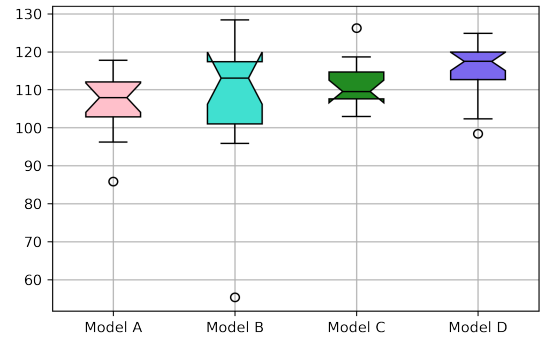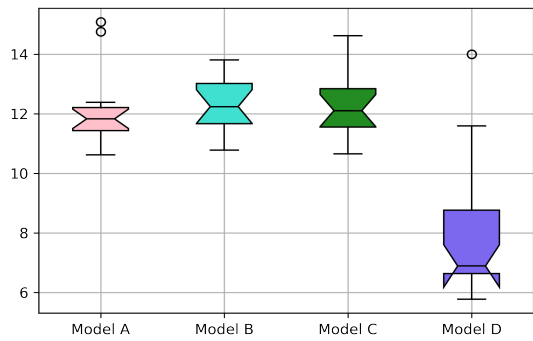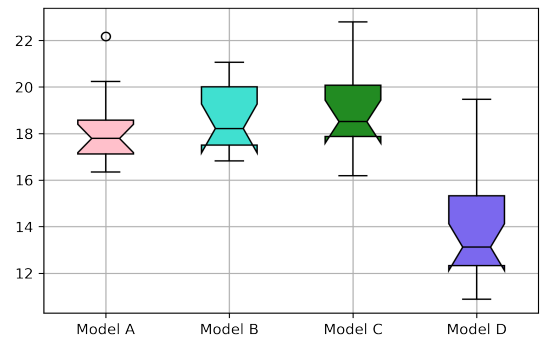
(a) MSE
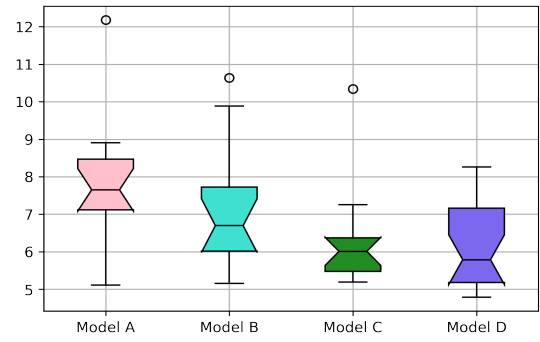
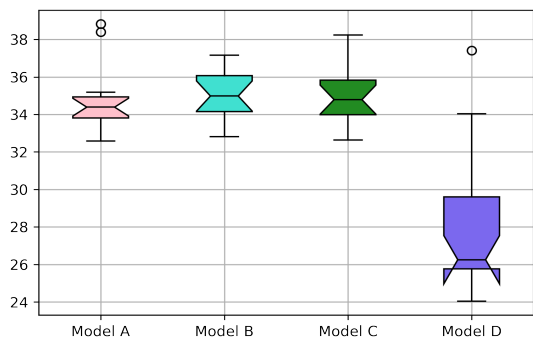(b) MAE
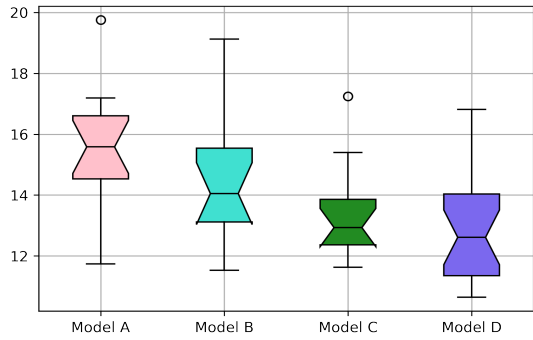
(c) RMSE

(d) MAPE

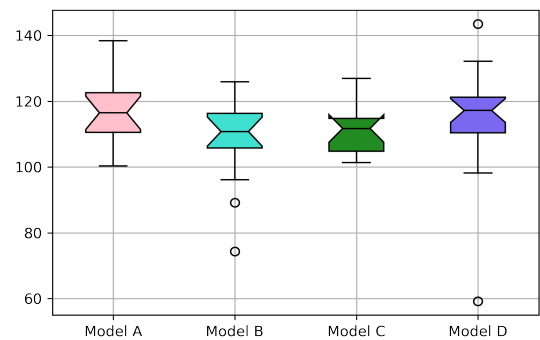Figure 6.4: The merging of all the evaluation measurement results of NO1.

(a) MSE

(b) MAE

(c) RMSE

(d) MAPE

Figure 6.5: The merging of all the evaluation measurement results of NO2.

(a) MSE

(b) MAE

(c) RMSE

(d) MAPE

Figure 6.6: The merging of all the evaluation measurement results of NO3.
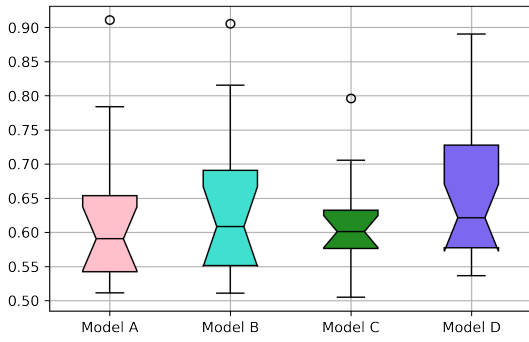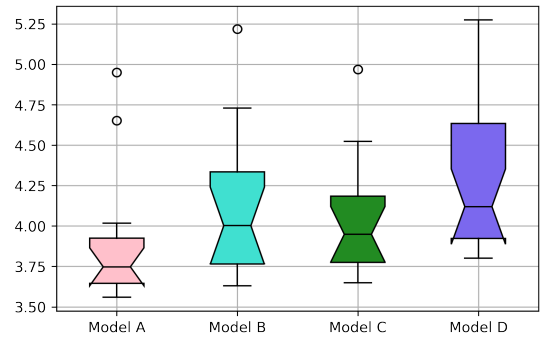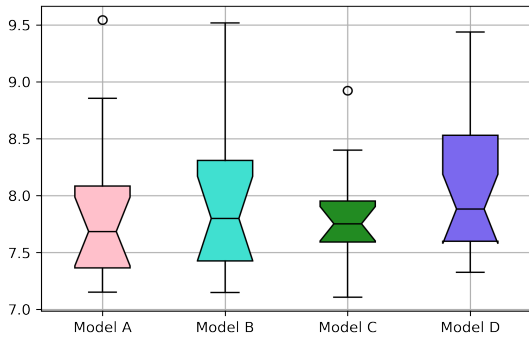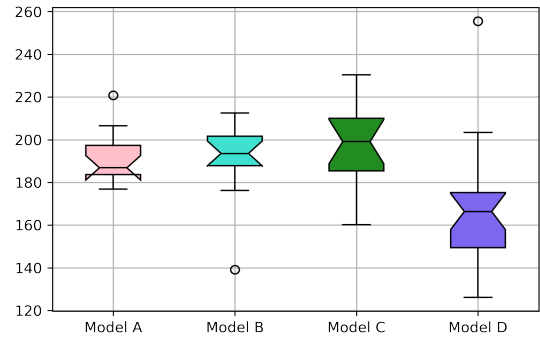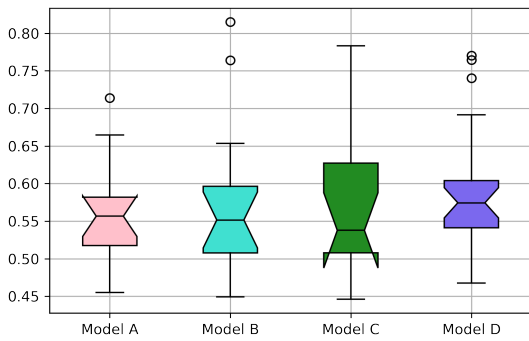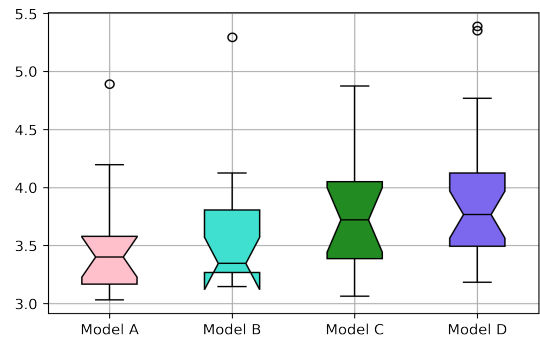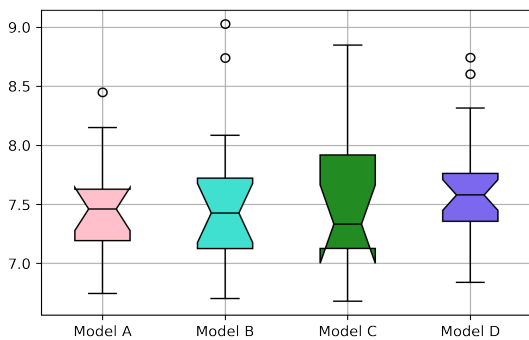

(a) MSE

(b) MAE

(c) RMSE
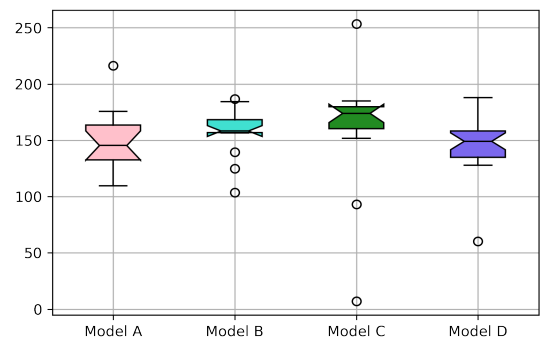
(d) MAPE

Figure 6.7: The merging of all the evaluation measurement results of NO4.
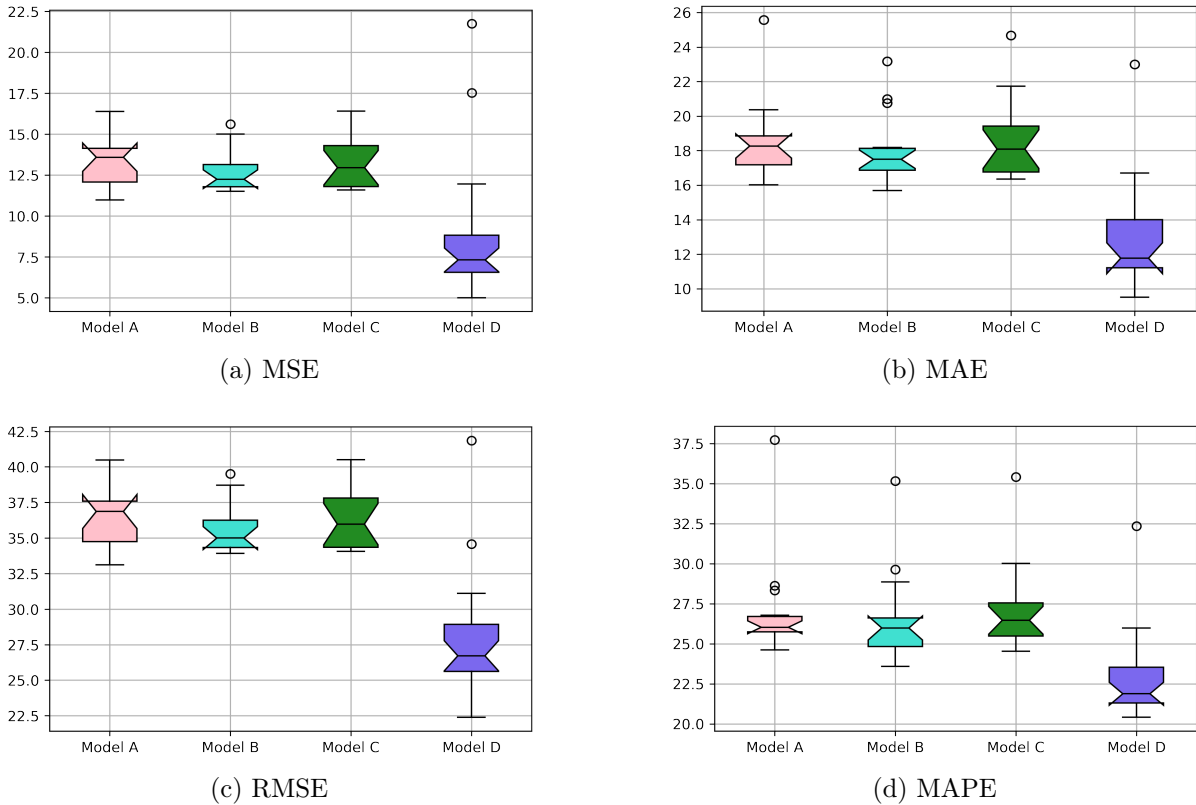
Figure 6.8: The merging of all the evaluation measurement results of NO5.

6.2.2   The Best Results of Each Model

The given results above in Section 6.2.1 are further narrowed down as to highlight the most significant findings. Therefore, the lowest obtained evaluation metric value of all cases are chosen for each of the four evaluation metrics and for each of the model types to be plotted as carried out in Figure 6.9. One remark to notice is that the Model D is now elaborated more in details, disparating the simulations with a clustering method from the simulations with the absence of clustering as presented below:

Model D: LSTM

- Model D.1: LSTM without clustering.

- Model D.2: LSTM with manual clustering.

- Model D.3: LSTM with unsupervised clustering.

The clustering method was an added feature to the Model D as part of a model modification, and not a default setting as in Model B and C. That is why LSTM with clustering is merged into the Model D rather than separated as done with the ANN models.

(a) MSE

(b) MAE

(c) RMSE

(d) MAPE

Figure 6.9: The best outcome in terms of evaluation metrics of each type of models.

6.2.3 A Closer Insight on Model Modifications

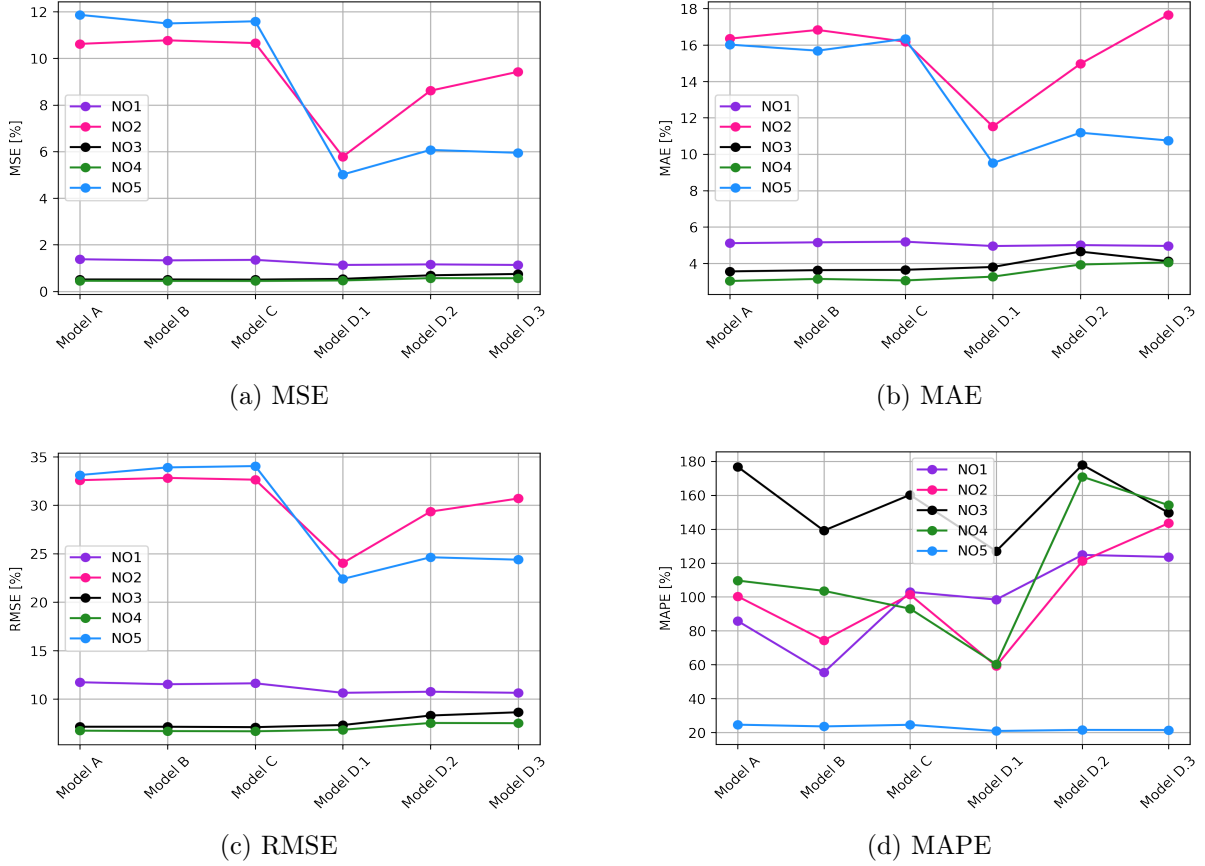The general overview of Figure 6.9 indicate NO1, NO2 and NO5 scoring the lowest evaluation metrics values overall when the ANN models are utilised, while the contradictory statement would apply on bidding zones NO3 and NO4, preferring model D.1. Hence, further exploring is performed by adjusting the best-performing model of each zone, given the base case as defined earlier in Section 6.1 through hyperparameter tuning.

The executed modifications are categorized into the cases 1-6, given that the size of the hidden layer is signified as $hidden_{\text{size}}$:

- Case 1: Base case of AI-model

- Case 2: Additional hidden layer of neurons = ($hidden_{\text{size}}$ - 2)

- Case 3: Additional hidden layer of neurons = ($hidden_{\text{size}}$ - 4)

- Case 4: Additional hidden layer of neurons = ($hidden_{\text{size}}$ - 6)

- Case 5: Additional dropout layer on the input layer

- Case 6: Additional dropout layer on the hidden layer

The dropout layer may be assumed to have a constant rate of 20%. Results from the remodeling accordingly to each case are illustrated in Figure 6.10 comprising of the usage of model D.1 on zones NO1, NO2 and NO5, and Figure 6.11 and Figure 6.12 for respectively NO3 and NO4 employing models A-C.
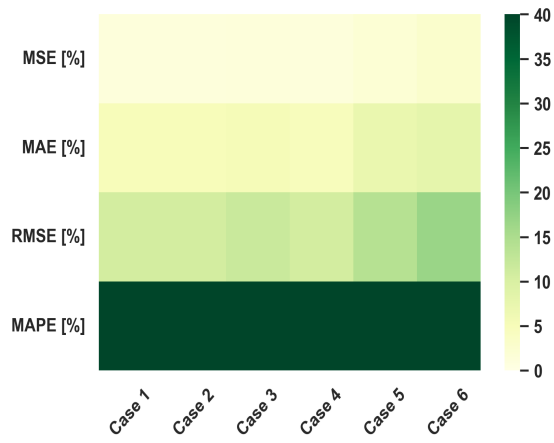
(a) NO1.
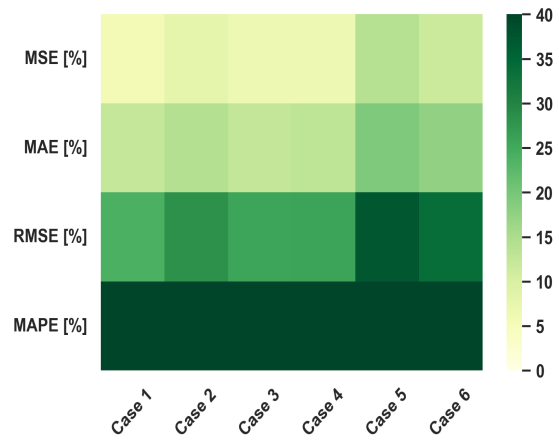
(b) NO2.
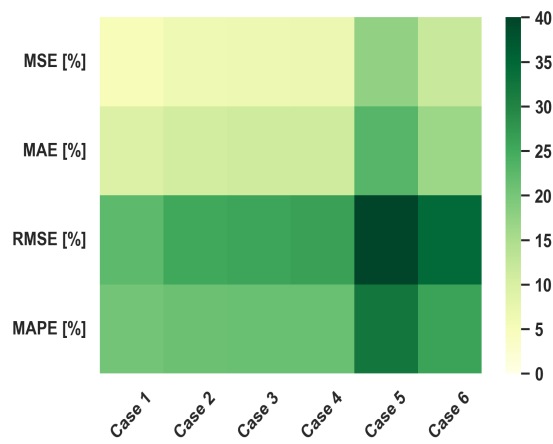
(c) NO5.

Figure 6.10: Model modification results of cases 1-6 of NO1, NO2 and NO5 using Model D.1.
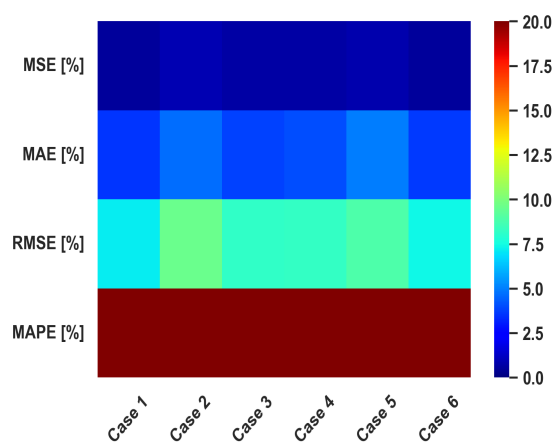
(a) Model A
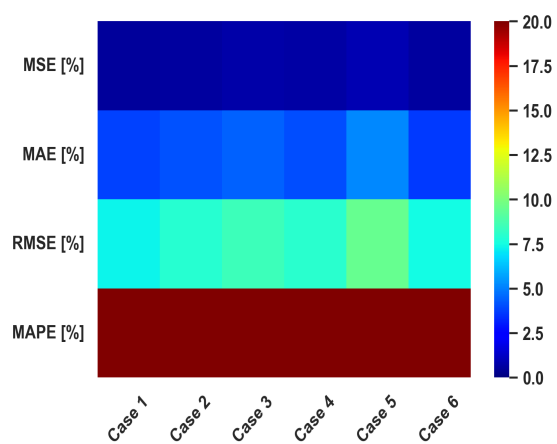
(b) Model B
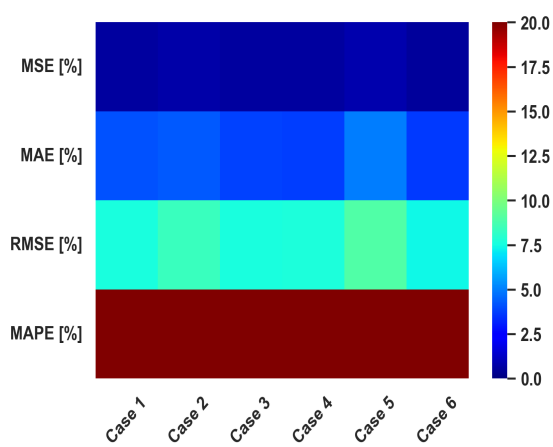
(c) Model C

Figure 6.11: Model modification results of cases 1-6 of NO3 using Model A-C.

(a) Model A

(b) Model B

(c) Model C
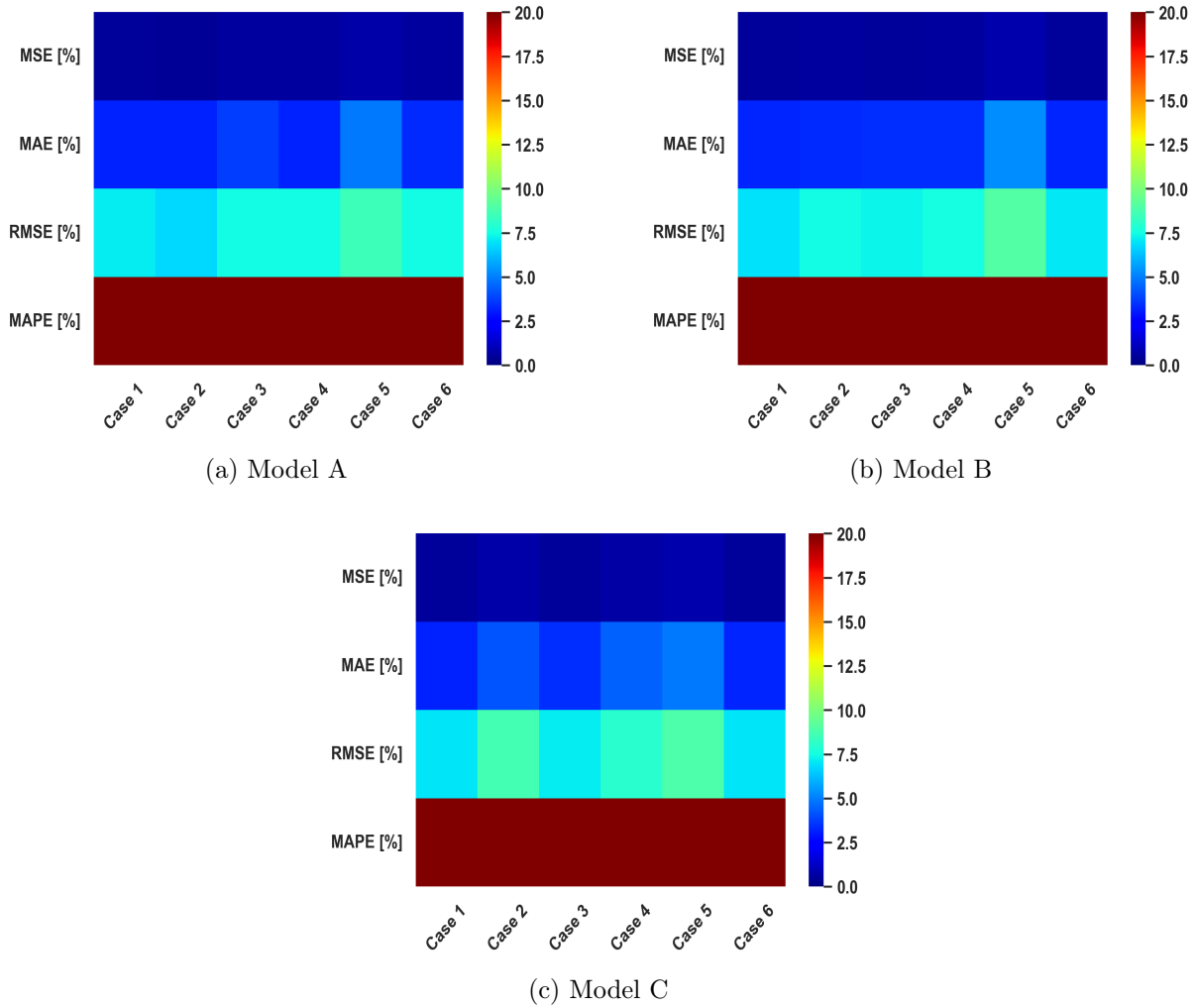
Figure 6.12: Model modification results of cases 1-6 of NO4 using Model A-C.

6.2.4 Sensitivity Analysis Regarding the Input Data

Aside from model modifications, another aspect to investigate may be the degree of dependency the forecasting accuracy has on the different input parameters for detecting which contributes the most. The temperature, precipitation and the CO_2-price data are captivated as the most appealing input parameters, and therefore selected to further sensitivity analysis. The examination is executed by removing each of the three data types separately, performed on the base case. Since ANN was established to produce excellent forecasting accuracy on NO1, NO2 and NO5, whilst LSTM was rather preferred in NO3 and NO4, the base cases of Model A and Model D are conducted with the data removal sensitivity analysis on the respectively groups of zones.
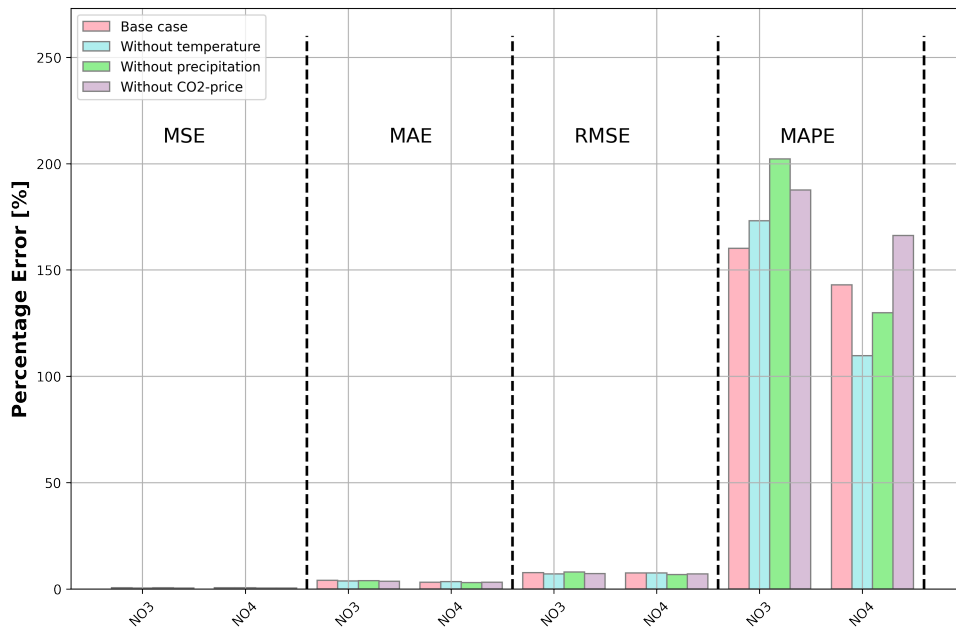
Figure 6.13: Removal of certain input parameters in NO3 and NO4 utilising the base case of Model A.
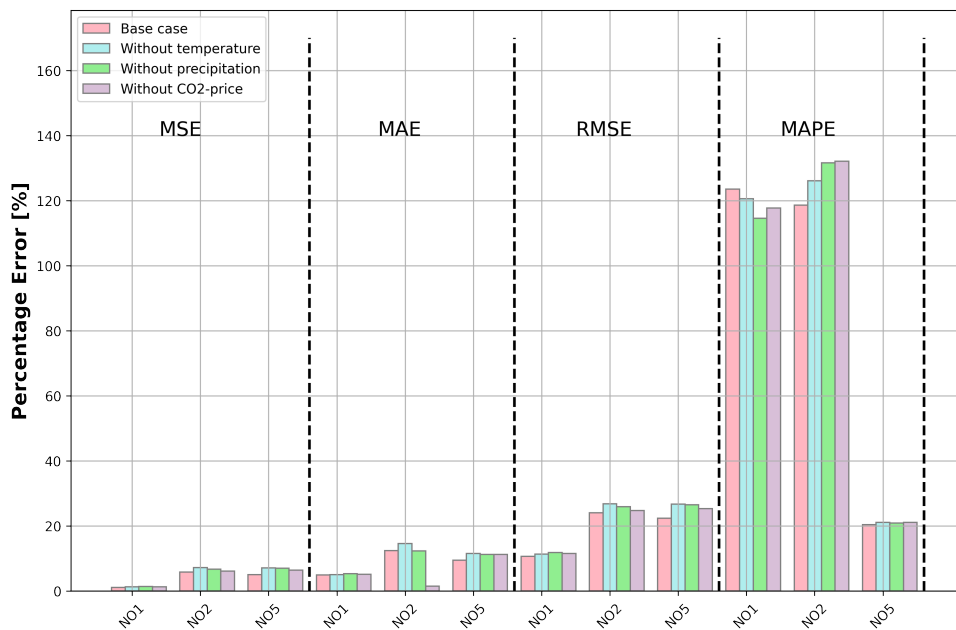
Figure 6.14: Removal of certain input parameters in NO1, NO2 and NO5 utilising the base case of Model D.1.

6.2.5 ANN and LSTM behaviour

A certain forecasting pattern is detected between all the zones and the ML models, Model A and D. Hence, the following results of e.g. NO5 is provided as to illustrate the claim, seen in Figure 6.15. Results from the remaining zones may be found in Appendix C.
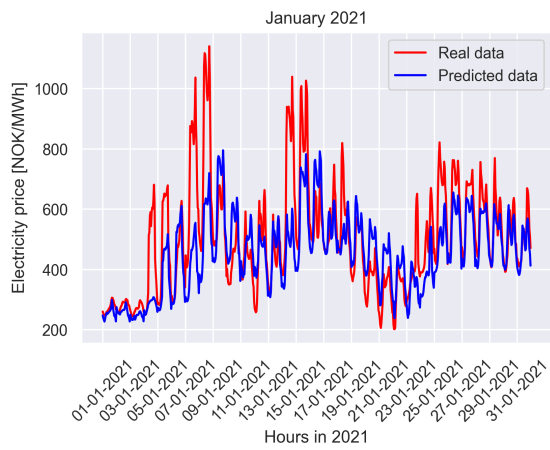
(a) January - Model A
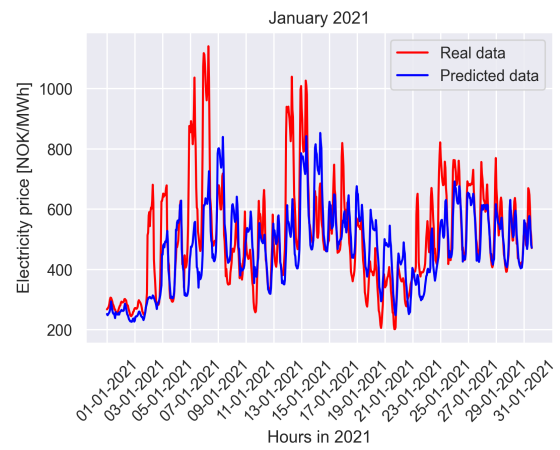
(b) January - Model D
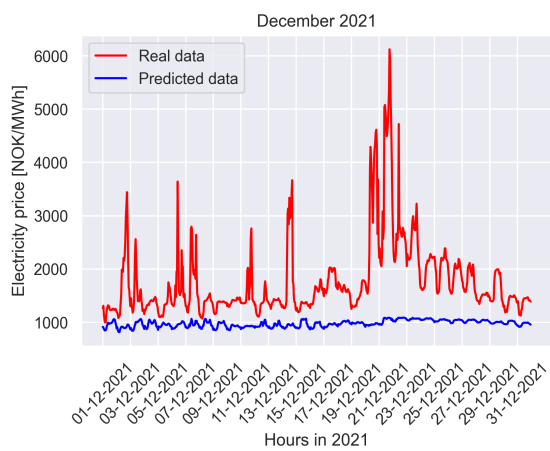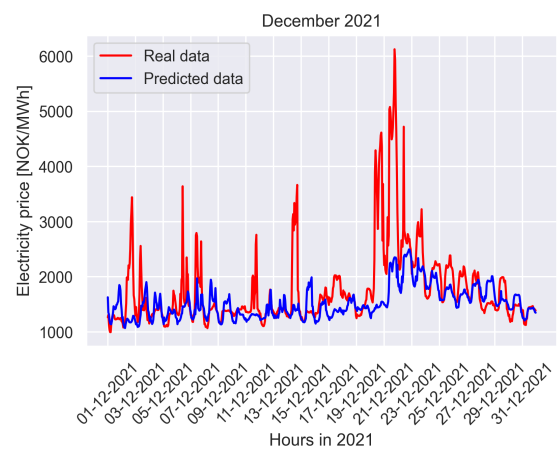
(c) December - Model A

(d) December - Model D

Figure 6.15: The actual and predicted electricity prices of 2021 in NO5 in January and December utilising Model A and Model D.

Chapter 7

Discussion

Most of the received MAPEs from all results presented in Chapter 6 and Appendix C were reaching a level of values circumscribing 100-200%, most likely due to the many outliers that were present in the forecasting. As stated in a paper [77], if the actual electricity price is immense and the predicted value is small, the resulting MAPE will be of approximately 100%. As the values were too high to be interpreted, MAPE has been less involved in the discussion and less contributing to decision-making of the best-performing models and cases. Regardless, a thorough analysis is to be conducted further based on the received findings from Chapter 6.

7.1 Hyperparameter Tuning

The batch size, timesteps and activation functions were manually determined by varying the parameters for a certain range, as described in Section 6.1. Exploiting hyperparameter tuning optimization tools that checks all combination of values of these parameters would have most likely yielded enhanced results. In that case, a hyperparameter tuning may have been performed in varying the type of utilising optimizer and its learning rate, revealing outcomes that are not handled in this thesis. However, due to the demanding time consumption, this option was disregarded, and thus, one should bear in mind that this has an influence on the hyperparameter tuning results of this thesis.

The lowest MSE, MAE and RMSE values were obtained with the use of tanh as activation function between each layer in ANN as observed in Figure 6.1. The MAPE, however, did not seem to be affected much by the hyperparameter tuning. A clear batch size in ANN as well as batch size, timesteps and activation functions in the LSTM model, seen in Figure 6.2 and Figure 6.3, cannot be determined as the best solution due to the varying results in each bidding area. Appendix C provides the exact hyperparameter tuning that produced the overall lowest evaluation metrics for each model in each zone of Norway.

7.2 Manual and Unsupervised Clustering

In the investigation of the working mechanism of the manual and unsupervised clustering methods, the outcome of utilizing the unsupervised clustering in fact exposes a general overlap of containing what may be defined as peak, normal and off-peak values of each input parameter. There were no strong coupling between the clusters, e.g. three clusters encompassing data regarding respectively workdays, Saturdays and Sundays such as the manual clustering. However, a connection seems to be present looking at how the data

regarding the day type is segregated, and a good example is the NO1 day type clustering depicted in Figure 7.1.
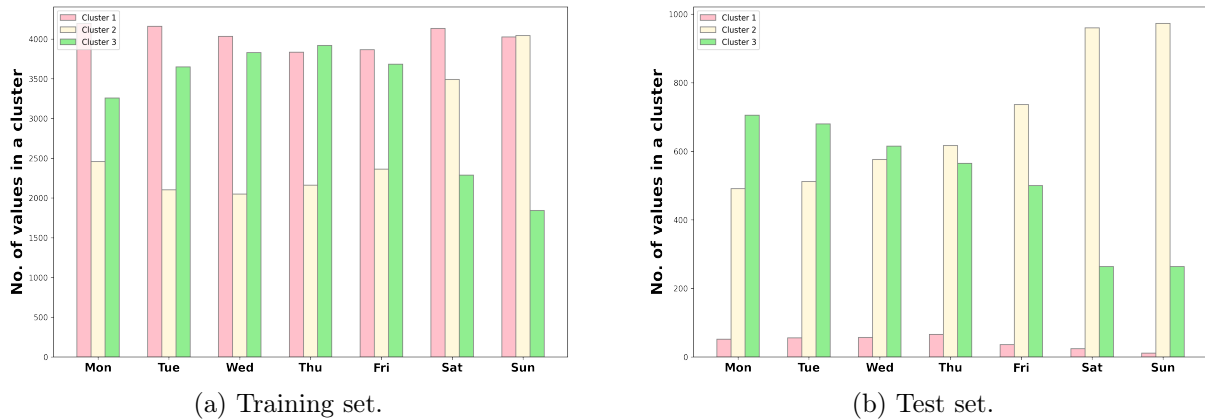

(a) Training set.

(b) Test set.

Figure 7.1: Clustering of the day-parameter in NO1.

Cluster 2 is embodying more weekend-related data, while cluster 3 is composed of an increased amount of data associated with working days in both cases of training and test sets. The first cluster seems to be containing a general amount of all day types in both data sets. Similar sequence is observed in most of the bidding zones for many of the clusters as presented in Appendix B.

As unsupervised clustering takes the entire training set of the various input parameters into consideration when grouping the data, in contradiction to the manual clustering, it is thus expected to perform better. Results from e.g. Figure 6.9 reveal that unsupervised clustering is outperformed by manual clustering in regards of the MAPE in all zones, but varying for the remaining zones concerning the rest of the evaluation metrics.

7.3   The Performance of ANN and LSTM

There are noteworthy highlights of the different forecasting trends in the AI-models that were observed when predicting the area prices. LSTM seemed to be giving the affect of reacting slower to sudden changes in the electricity prices, based on the the obtained results in NO5, depicted in Figure 6.15. Similar behaviour is seen in the other zones as well, and these results may be found in Appendix C.

More precise, there is to be found a slow reaction of the magnifying electricity price in NO5 occurring around December 19-23th. Another remark is the enormous difference between the almost flat-curved ANN prediction of the electricity price in December compared to the more oscillating LSTM forecasting. The ANN model is unable to react to the tremendously elevating spike occurring in December, while an uplift is detected when using an LSTM, yet, the predicted electricity price is far from close to the actual electricity price.

Regardless, ANN and LSTM are two methods sharing similar elements as they both are categorized as DL-models, and therefore making less of a difference in forecasting especially the months spanning from January to June, e.g. in Figure 6.15a and Figure 6.15b in January in NO5. An interesting contribution to this thesis would have been additionally executing day-ahead electricity price forecasting with models found outside the scope of DL-models, such as gradient boosting algorithms, or other hybrid solutions as to analyse how largely this may impact the results.

7.4 Zonal Differences

The general overview of the performance of the models, A-D, in each zone is presented in Section 6.2.1. Albeit each zone produces its unique predicted findings differentiating from each other, a connectivity between zones NO3-NO4 and NO1-NO2-NO5 is observed based on the given results, which may seem to be linked to the usage of the ML methodology. To substantiate this, the results are summarized in Table 7.1 accordingly to the best-performing model of each evaluation metric.

Table 7.1: A summary of the findings presented in Section 6.2.1.

	MSE	MAE	RMSE	MAPE
NO1	Model D	Model D	Model D	Model B
NO2	Model D	Model D	Model D	Model D
NO3	Model C	Model A	Model C	Model D
NO4	Model C	Model A	Model C	Model C
NO5	Model D	Model D	Model D	Model D

A recurrence is seen in Table 7.1 among groups of zones NO1-NO2-NO5 and NO3-NO4 in which is the persistence in the LSTM model D producing the most ideal forecasting for the zonal batch, NO1-NO2-NO5, which stands in contrast to the other zonal group, NO3-NO4, accomplishing the best evaluation metrics values with models A and C, both ANN-based methodologies.

There is also a relationship found internally in the two clusters of bidding zones due to the range of the evaluation metrics results. Figure 7.2 is therefore formed as to effectively recapitulate the shape of the percentage error spans, all based on the results from Section 6.2.1.
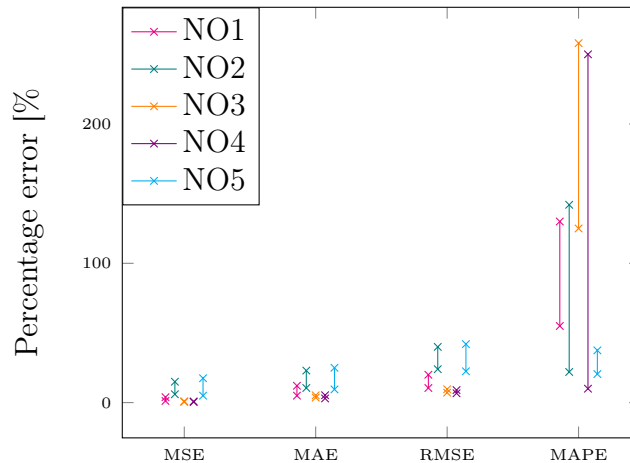
Figure 7.2: An alternative summary of the results in Section 6.2.1

The MAPE ranges seem to be partly disconnected. However, as for the remaining areas, NO2 and NO5 have approximately equal percentage error spans, and are more elevated from the relatively similar ranges of NO3 and NO4 when it comes to MSE, MAE and RMSE. The percentage error scope of NO1, however, is located in the grey zone, touching the end of the NO3-NO4 range and the beginning of the NO2-NO5 domain concerning the same evaluation metrics.

Basing on these observations, further discussion conducted in this section will be segregated into the stable zones, consisting of areas NO3 and NO4, and the unstable zones, embodying NO1, NO2 and NO5. This is due to common trends and patterns recognised in the overall results, such as the choice of the ML forecasting method and the evaluation metrics ranges. The names "stable" and "unstable" are signifying the zonal category of correspondingly relatively low (NO3, NO4) and magnified (NO1, NO2, NO5) values of evaluation metrics.

7.4.1 Stable zones

With historical data provided by Nord Pool, the stable zones capturing NO3 and NO4 is proven to share similar electricity price development as elaborated in Figure 5.2. The area prices of the stable zones in 2021 are located thereabouts the past data with similar trend patterns and no apparent irregularities most of the year, due to the overproduction in hydropower present in 2021 in NO3 and NO4. The electricity prices in the stable zones in 2021 are also composed of more enlarged peaks and troughs, having in mind that an oscillating pattern is seen in former years, but with compressed area prices with amplitudes closer to the equilibrium point.

However, attention goes to the abnormal activity in parts of November and December of 2021 in the stable zones with area prices peaking to almost seven times the regular price range of approximately 500 NOK/MWh seen in previous years. One theory for this phenomenon may be attached to the occurrence of low precipitation in the spring and summer in both of the stable zones, as seen in Figure 7.3.
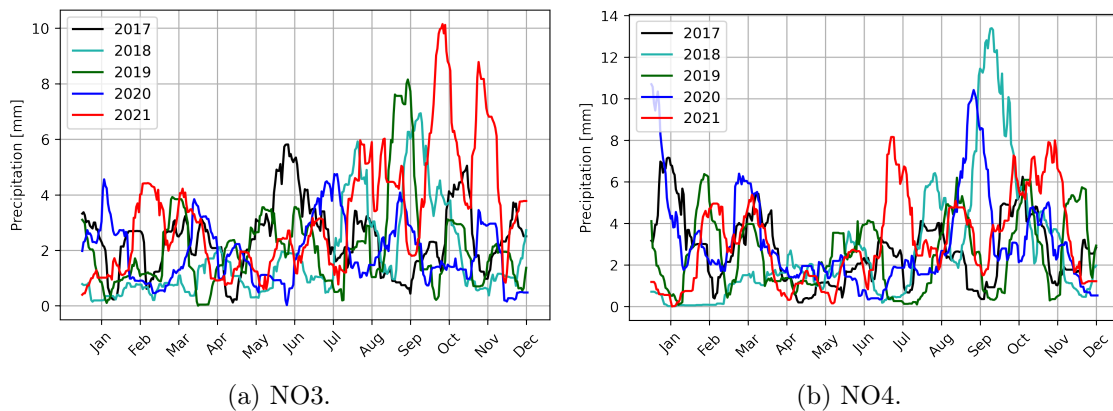

(a) NO3.   (b) NO4.

Figure 7.3: The precipitation in the stable zones. Moving average is applied with window size = 100.

This leads to the lack of water in the reservoirs of the hydropower, the dominating energy source of Norway. This is critical for a country that normally encounters high demand in the winter season due to the low temperature. Going towards the winter of 2021 with a reduced water amount in the reservoirs against the magnified demand lead to the producers' wish of withholding of the water and rather supply consumers power through interconnected cables from Norwegian and abroad bidding zones that in the case of 2021 were inflicted by high electricity prices. It should be noted that there is in fact a rise of precipitation from October and throughout 2021 in both of the stable zones. However, suppliers most likely preferred retaining the water in this case as well for securing future supply in critical situations where production in neighbouring zones could be dramatically declined for reasons.

Therefore, it is expected that a typical forecasting model should be able to perform well on the year 2021 on the stable bidding zones, excluding parts of November, December and certain peaking electricity prices through the year as these do not resemble previous pricing trends.

Comparison of the Models

According to Figure 6.9, the stable zones are clearly forecasting at its best through any ANN-based model with acceptable forecasting errors of MSE, MAE and RMSE below 5%. This may be interpreted as a prediction output that has reduced amount of outliers and is a generally performing forecasting model. However, the MAPE results indicate the Model D.1 to produce the most accurate predictions. As discussed in Section 4.5, the MAPE may be a confusing target to follow in regards of forecasting the electricity price. The usage of the regular ANN method in combination with either manual or unsupervised clustering is either resulting in a marginally increased percentage error, or equivalent results to the original model A.

Internally among the stable zones, NO4 scores lower percentage errors compared to NO3. This may be connected to the power flows across the stable zones. Section 5.2 presents all relevant power flows regarding NO3 and NO4, among others, in the time span 2017-2021. Most of the flow is revealed to be heading from NO4 to NO3 on the cable connection between the stable zones. NO4-SE1 and NO4-SE2 share almost the same trends of more power flow directing towards Sweden most of the time of the year, with almost no power flowing to NO4 in the summer. NO3 is also detected to have mostly outgoing power flows seen on cables SE2-NO3 and NO1-NO3. The NO3-NO5 cable, however, vary largely from year to year, but the largest exception occur on the power flow between NO3 and NO4 which as stated earlier, was directed towards NO3. In other words, NO4 has more power flow going outwards, especially in the summer, making it less dependent on neighbouring electricity production and more reliable on its own generation compared to NO3.

For the predicting year 2021, an anomaly occurs, detecting almost no flow from NO5 to NO3 from April to December, making NO3 less conditional on the power production in NO5 for specifically year 2021. Thus, for the forecasting year in particular, the area price in NO3 seems to be less influenced by the power flow input parameters from connections SE2-NO3, NO1-NO3 and NO3-NO5, while more dependent on the power supply from NO4 when predicting the electricity price. The amplified dependency of NO3 on the power production in NO4 may be the possible cause for the more precise forecasting in NO4. Another reason may be connected to the binary definition of the power flow input to the model, recalling from Section 4.1 describing the data collection of the methodology. If the original power flow values had been injected, a more precise power flow between nodes, NO3 and NO4, had been depicted, thus increasing the forecasting accuracy in NO3.

Improving the ML model

No visible improvements are seen of the percentage errors regarding the predicted area price in NO3 by adjusting the model accordingly to cases 1-6, as presented in Figure 6.11. Similar observations are detected in Figure 6.12 regarding NO4 with the minor exception of Model A - case 2, the addition of a hidden layer with two neurons reduced, whereas the RMSE value is slightly decreased.

Adding a dropout layer to the input layer, that is case 5, is not well-received at all in most of the models A-C for both of the stable zones. In normal cases of running ML

models, an extension is added, namely the dropout layer with the purpose of contributing to refrain overfitting through excluding a particular amount of data randomly chosen for each epoch. This is, however, in the case of forecasting the electricity price, contradicting with its purpose. A possible cause for the situation may be the highly fluctuated electricity price spanning an immense range, that in itself produce a randomality in the input data. Adding a dropout layer either on the input or the hidden layer on top of the randomized electricity price input seems to rather disturb the prediction model than assisting it.

The MAPE is also included in the results and is found to be out of the scale in both of the stable zones. Therefore, the results on behalf of this particular metrics may be assumed to be non-interpretable in this case. Setting aside minor exception, none of the modifications improved the forecasting accuracy in the stable zones, most likely due to overfitting.

Removal of Data

To ease the analyze of the significance in involving the temperature, precipitation and CO_2-price data, the presented results in Figure 6.13 is transformed into a briefly summary in Table 7.2. Although, several papers raised the importance of including the CO_2-price as one of the input parameters for electricity price forecasting as emphasized in the introduction, removing the CO_2-price data in fact increases most of the evaluation metrics in both of the stable zones, as observed in Table 7.2. This may be connected to the Norwegian electricity price normally with low relevance to the CO_2-price as most of the Norwegian generation stems from hydropower production whereas other factors such as the temperature and precipitation are more involved.

Table 7.2: A brief presentation of the results in Figure 6.13.

		Base case	(-) Temperature	(-) Precipitation	(-) CO_2-price
NO3	MSE	-	⇓	⇑	⇓
	MAE	-	⇓	⇓	⇓
	RMSE	-	⇓	⇑	⇓
	MAPE	-	⇑	⇑	⇑
NO4	MSE	-	⇓	⇓	⇓
	MAE	-	⇑	⇓	⇓
	RMSE	-	⇓	⇓	⇓
	MAPE	-	⇓	⇓	⇑

However, it also shows that excluding the temperature data leads to improving most of the evaluation metrics. The precipitation data, on the other hand, acts as a contributing factor to the forecasting of the electricity price in NO3 and rather a disturbance of predicting the area price in NO4. One substantiating argument for such results may be the greater variation internally in NO3 and NO4 in the average temperature, as depicted in Figure 7.4, such that the ML models operating with the temperature from one single place in a zone cannot be counted as representative for a whole stable zone. If temperature data of several cities in a certain zone were included, the results may have looked differently.
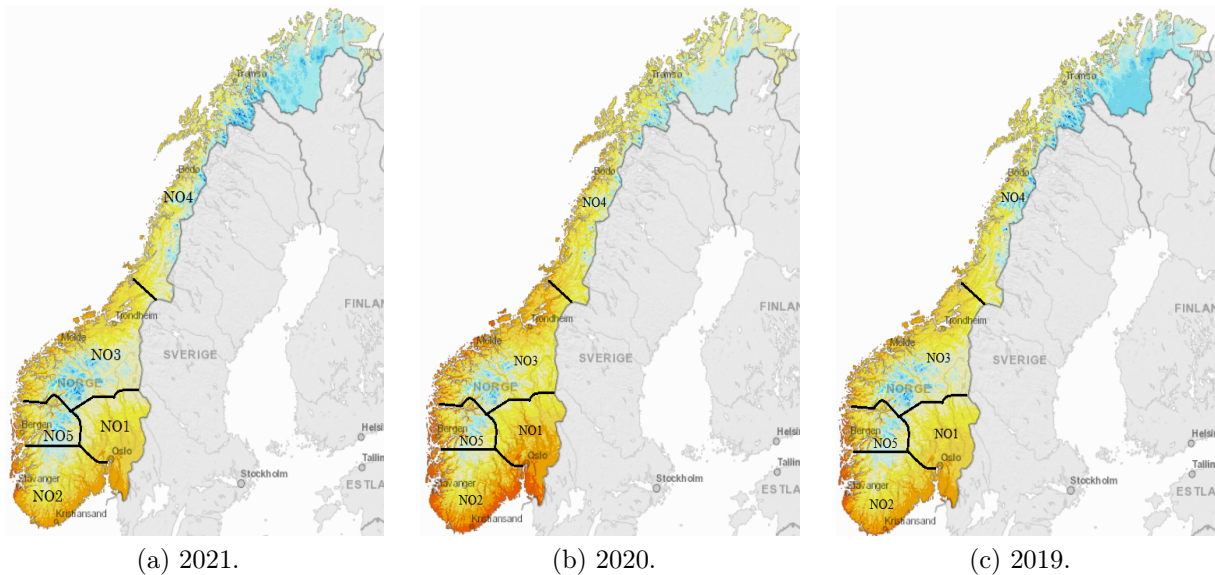
(a) 2021. (b) 2020. (c) 2019.

Figure 7.4: The yearly average temperature in Norway [12].

As for the precipitation, observing Figure 7.5, the coast of NO3 seems to be exposed to a greater amount of precipitation in comparison to the coast of NO4. Another remark would be the precipitation in 2021 in NO3 as shown earlier in Figure 7.3 which is far more in the last quarter of the year than in NO4, leading to the amplified dependency of the precipitation data regarding area price prediction in NO3 for particularly 2021.

(a) 2021. (b) 2020. (c) 2019.
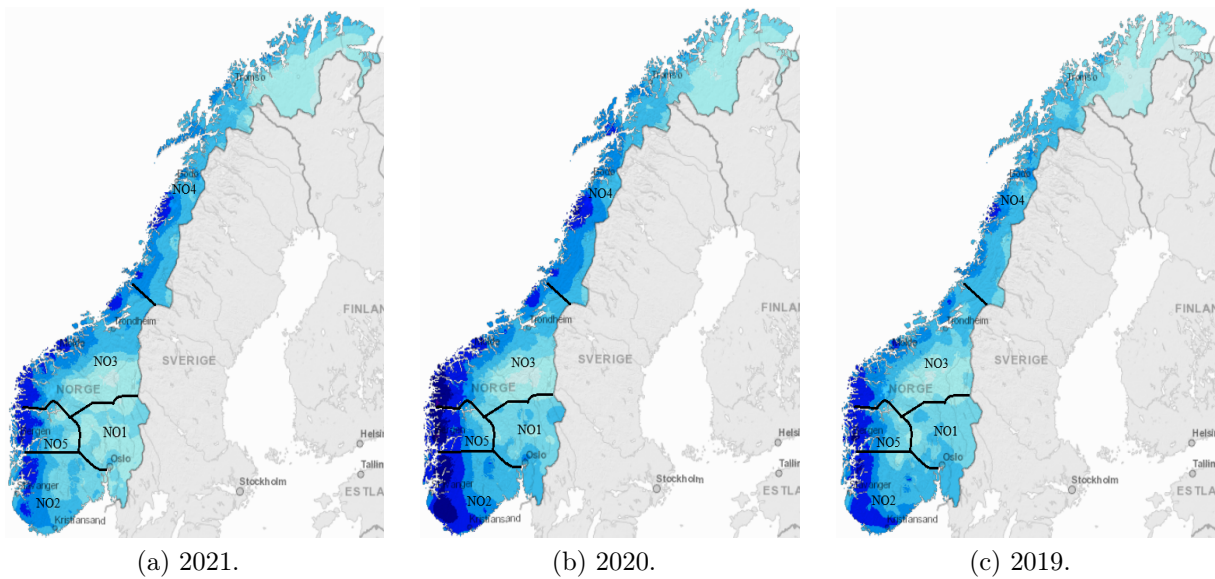
Figure 7.5: The yearly average precipitation in Norway [12].

7.4.2 Unstable zones

Previously in Figure 5.1 with the presented historical electricity prices, it was underlined that NO1, NO2 and NO5 was sharing similar features. The electricity prices from January to approximately August in 2021 in these zones also resemble past years in the sense of being in the normally expected price range. A dramatic lift in the electricity price is observed from around August till December, with the greatest peak found in the last month of 2021. A similar pattern is seen among the area prices of the stable zones, however,

while those were reaching towards 3500 NOK/MWh, the remaining zones elevated to prices close to 6000 NOK/MWh. That is roughly twelve times the regularly experienced price range. As for the stable zones, NO1, NO2 and NO5 are inflicted with more extreme peaks and troughs in 2021 than previous years, indicating a remarkably more volatile electricity price observed in 2021 in general. The cause for such circumstances is first of all coupled with the low precipitation in 2021, also found in the unstable zones as seen in Section 5.3. Unlike the stable zones, the precipitation remained comparatively low at the end of 2021 in all the unstable zones, making it an even greater challenge of relaying on the hydropower production in these bidding areas. The overproduction from the stable zones may have been exploited to compensate for the absence of production in the unstable zones, however, transmission congestion limited this solution. Therefore, NO2 was highly dependent on its border-extended interconnections to especially the Netherlands and Germany which in 2021 encountered record-high electricity prices due to the magnified gas, fuel and CO_2-prices, influencing the electricity price in NO2 and further to NO1 and NO5 as these areas are dependent on the power supply from NO2.

Hence, a greater challenge is expected when forecasting the area prices of NO1, NO2 and NO5 than for the stable zones due to the increased volatility in 2021, the sudden arise in the electricity price commencing earlier than for the stables zones, and the tremendously greater electricity price peak in December.

Comparison of the Models

According to Figure 6.9, LSTM Model D.1 is revealed to be performing better for the unstable zones. As opposed to the stable zones, the MSE, MAE and RMSE values of NO2 and NO5 are retaining higher levels of respectively 10-12%, 16-17% and 33-34% which is dramatically reduced to levels of 5-6%, 9-12% and 23-25% exploiting the Model D.1, making it more tolerable, yet, not as well-performing as the stable zones.

The results from NO1, on the other hand, deviates largely from the rest of the unstable zones. Despite being an area inflicted by the magnified electricity prices as NO2 and NO5, the evaluation metrics of MSE, MAE and RMSE are as low as approximately 1%, 5% and 10%, and only maximum 5% away from percentage errors of the stable zones. Such altering forecast results in NO1 may be caused by several factors. Norway, with most of its power production from hydropower, has the least amount of generators in NO1. This amount is in fact almost half the size compared to NO5 and remarkably less than half the quantity in NO2, despite comprising around half the population in Norway. NO1 is therefore highly contingent on power supply from neighboring zones, NO2, NO3, NO5, and SE3, and this dependency has been present for the past years. By analyzing the historical power flow presented in Section 5.2, it may be observed that flows in 2021 between NO1 and the border areas in point of fact follow a similar pattern to previous years with low digression. Using binary values to describe the power flows connected to NO1 is in other words an efficient simplification in this case. However, one should have in mind that this thesis is not proving it to perform better than certain other cases of defining power flows. The temperature and precipitation in 2021, however, are more stable in NO1 compared to NO2 and NO5 which have greater variations internally in the zones, as indicated in Figure 7.4 and Figure 7.5 with repeating pattern in 2020 and 2019 as well. Thus, a more reliable weather condition in NO1 may be a contributing factor in predicting a more accurate area price.

NO2 produce a repeatedly higher percentage error than NO5 in all cases given the best scenario; the Model D.1. This occurrence may be clarified through the newly introduced cable between NO2 and DE that as observed in the historical power flow plot in Figure 5.8,

only covers for 2021. In other words, there is a new factor introduced to the test set that may be unfamiliar for the ML model as no training has been performed with the inclusion of data from the NO2-DE cable before. The equivalent case is not present in NO5, thus, explicating the diminishing percentage error in NO5 in comparison to NO2.

Further combining LSTM with the hybrid solution of clustering either produced a marginal difference or aggravated the forecasting percentages in the unstable zones. The MAPE regarding these zones are challenging to interpret as each of the unstable zones follow a unique pattern for each model type. However, certain points may be highlighted. The lowest MAPE is achieved with the Model D.1 in NO2 and NO5, although the MAPE value is around 60% in NO2, an immensely inadequate percentage error in comparison to the 20% in NO5. NO1 differentiates again in the results by scoring the lowest MAPE with the employment of Model B rather than Model D.1, obtaining a value of around 60% similar to NO2.

Improving the ML model

Modifying the well-performing Model D.1 in terms of forecasting the unstable areas either unaltered or exacerbated the forecasting percentages. The incorporation of the dropout layer on the input layer is also here, as well as for the stable zones, arising the most aggravated results, and the cause may be substantiated with the same argument as presented in Section 7.4.1.

Removal of Data

When summarizing the results from Figure 6.14 to the Table 7.3, it evidently shows the contradictory outcome of the stable zones. Including the CO_2-price is in fact improving most of the percentage errors in the unstable zones, as emphasized in several papers. This may be substantiated with how the CO_2-price influenced the unstable area prices in 2021, as elaborated earlier. Not to mention that predicted unstable area prices seem to be sensitive to removal of weather conditional data as well. A deeper look into Figure 6.14 reveal a greater change in percentage errors when temperature or precipitation data is neglected in NO2 and NO5 rather than in NO1, indicating a stronger dependency between the weather data and areas NO2 and NO5, circumstances that may be supported by the internally increased deviation in weather conditions in these bidding zones as pointed out earlier, leading to higher sensitiveness. It is thus verified that there is a correlation between the electricity prices in the unstable zones and the temperature, precipitation and CO_2-price data. If gas and fuel price had additionally been included, which as highlighted in the introduction were claimed to have a connection to the electricity price, a further refinement in the results may have been detected.

However, looking from a broader perspective in Figure 6.14, there is mostly a marginal change in percentage errors of approximately 0.1-2% in general when either temperature, precipitation and CO_2-price data is neglected in the forecasting model. Despite the minor improvement, the few percentages of reduction may spare producers and consumers of large economic losses.

Table 7.3: A brief summary of the presented results in Figure 6.14.

		Base case	(-) Temperature	(-) Precipitation	(-) CO$_2$-price
NO1	MSE	-	⇑	⇑	⇑
	MAE	-	⇑	⇑	⇑
	RMSE	-	⇑	⇑	⇑
	MAPE	-	⇓	⇓	⇓
NO2	MSE	-	⇑	⇑	⇑
	MAE	-	⇑	⇓	⇓
	RMSE	-	⇑	⇑	⇑
	MAPE	-	⇑	⇑	⇑
NO5	MSE	-	⇑	⇑	⇑
	MAE	-	⇑	⇑	⇑
	RMSE	-	⇑	⇑	⇑
	MAPE	-	⇑	⇑	⇑

Chapter 8

Conclusion and Future Work

8.1   Conclusion

In this thesis, the Norwegian day-ahead electricity price of the five bidding zones, NO1-NO5, are predicted through the DL-based models, ANN and LSTM, with pre- and post processing techniques applied. Model types A-D and for the best-performing model, cases 1-6, are evaluated for investigating further possibility of improving the prediction. Certain input parameters are eliminated from the model injection as to observe how it affects the forecasting. The hybrid solution of combining the DL model with either manual or unsupervised clustering were explored. MSE, MAE, RMSE and MAPE were utilised to measure the performance of the forecasting models. However, the outcome turned out to be producing immensely high, and thus, un-interpretive MAPEs that proves the inability MAPE has for measuring forecasting error in regards of predicting the electricity price, and also confirms the claims of error measurement reviews. A clear recurring factor is the effectively minimized percentage errors with the usage of the tanh activation function in ANN, but otherwise, there were no strongly correlating observations in the hyperparameter tuning between the bidding areas.

The two different clustering methods exploited in this thesis showed to produced vitally different grouping structure in the input data. The unsupervised clustering which takes the full training set into consideration, in fact revealed to excel a certain resembling pattern to manual clustering when analysing the clustering of the day-parameter data. One cluster was capturing more weekdays, another including more weekends and the latter having a mixture of both. This proves the fact that there is a connection between the electricity prices and the day types, but following such strategy in a literal manner as in the manual clustering may not produce the best forecasting. Although it was expected to have unsupervised clustering outperforming the manual clustering method, as the primary method takes more input parameters into account, the results show a varying trend in the best-performing clustering method in the zones of Norway. Thus, a clear conclusion cannot be drawn on the best-performing clustering method, however, it may be stated that neither of them were out-performing the non-hybrid methodologies of ANN and LSTM.

As for the execution of the ANN and LSTM models, a generally reoccurring trend is the effect of lagging in the forecasting that is observed due to the low capability of reacting rapidly to unanticipated change in the growth of electricity price. This is especially seen at volatile points such as the record-high electricity prices that Norway was facing in December in 2021 in all of the zones. ANN is also perceived as a model that overall has low ability to respond to highly volatile electricity prices.

A strong coupling in the gathered findings were detected among the zonal groupings, NO1-NO2-NO5 and NO3-NO4, naming the unstable (more volatile) and the stable (less

volatile) zones. Each of the categorized zonal groups were sharing similar electricity price trends in 2021, there was a resemblance in the best-performing ML method internally in each zonal group, and to a certain extent, they also had similar spanning range of percentage errors when looking at the overall total simulations undergone for this thesis. The results revealed the fascinating outcome of ANN performing better among the stable zones, while LSTM was executing of a higher quality among the unstable zones. In other words, a memory-based model such as LSTM is the more recommended DL model in the cases of predicting highly fluctuating area prices compared to previous years' experiences, and otherwise, ANN should be utilised. Further improvement on the models by adding a hidden layer with variations of number of neurons, did lower the RMSE of NO4 using model A, however, more refinements were not visible. The introducing of the dropout layer did not lower the percentage errors of neither of the models for all zones, especially when the dropout feature was incorporated to the input layer. This thesis also reveals the non-dependency of temperature, precipitation and CO_2-price among the unstable zones which in fact is to be contradicting with statements from papers and studies, while the opposite is observed in the unstable zones, affirming these statements.

Electricity price forecasting has achieved much attention lately for the tremendously growing price detected in 2021. It has thus, emphasized the importance in having well-performing forecasting models which indeed has been noticeable as a vital need among the market participants. Therefore, this thesis was decided to encompass the electricity price forecasting of the bidding zones in Norway, which in turn has led to the discovery of connectivity among certain areas and the usage of ML method. Although the employed modifications in this report did not enhance the DL models, there is still quite a potential of improving the models through other methodologies that may be explored.

8.2 Future Work

Based on this thesis, the following work may be further conducted in the future. This is based in the reflections made in Chapter 7.

- **Use other error measurements rather than percentage errors:** As mentioned in the early stages of Chapter 7, MAPE was not a well-fitted evaluation measurement in the case of predicting the electricity price. Unreasonable values were received in the results and thus were the MAPEs purposeless when interpreting the findings. Next to the scale-dependent metrics, MSE, MAE and RMSE, relative-based measurements such as mean relative absolute error (MRAE) and geometric mean relative absolute error (GMRAE) may be utilised.

- **Utilise other hyperparameter optimization methodologies:** The hyperparameters were tuned manually. This is both time consuming, inefficient and imprecise in terms of the way the hyperparameter tuning was conducted in this thesis. The parameters were delimited in the process of tuning, such that there might have been a more minimizing value of the evaluation metrics with parameter values outside this scope. In order to discover all possible combinations of hyperparameter values, other popular tuning methods may be utilised, such as grid search, randomized search, bayesian optimization and the Keras Tuner optimization python package compatible with a Keras- and Tensorflow-based model development.

- **Investigate other ML models and hybrid solutions:** The proceeded ANN and LSTM model forecasting may be served as a benchmark for exploring other models such as the gradient boosting algorithm, XGBoost, and extreme learning

machines, ELM, and also hybrid solutions of LSTM-ANN, or ML models combined with particle swarm optimisation, genetic algorithm and discrete wavelet transform (DWT).

- **Change the optimizer and vary the learning rate:** In addition to the Adam optimizer, exist the SGD, RMSprop Adagrad algorithms that were mentioned in Chapter 4. An adjustable learning rate is associated with each optimizer which was not varied in this thesis. For further work, optimizers and their belonging learning rates may be modified as to detect improvements in the ML models.

- **Expand the weather conditional input data:** As elaborated in Chapter 7 certain bidding zones had more internally varying temperature and precipitation, affecting the forecasting accuracy in the particular areas. Including temperature and precipitation data from one city in each zone are thus not enough to illustrate the total weather conditional situation in the areas. One recommendation would be to extend this by including the required temperature and precipitation data from several places for each zone, as to see if this in fact has a positive effect on the forecasting accuracy.

- **Include other types of input parameters:** The Norwegian day-ahead electricity prices in 2021 have, in addition to the included input parameters in this thesis, also been dependent on e.g. gas and fuel prices, which should be included in future works if such data is available.

- **Redefine power flows:** Although a binary definition of the power flows were utilised in this thesis, neither here nor previous studies emphasize this being an enhancing alternative to keeping the original power flow values. A verification may be performed in order to confirm that such an alternative is improving the forecasting.

Bibliography

[1] M. T. C. Bang, F. Fock, "The existing nordic regulating power market," 2011.

[2] Wikipedia, "Energi i norge," https://no.m.wikipedia.org/wiki/Energi_i_Norge [Accessed 2021/12/10].

[3] I. Wangensteen, "Power system economics - the nordic electricity market," 2012.

[4] Wikipedia, "Economic surplus," https://en.wikipedia.org/wiki/Economic_surplus [Accessed 2021/12/10].

[5] H. V. Haghi and S. M. Tafreshi, "An overview and verification of electricity price forecasting models," 2007.

[6] R. Weron, "Electricity price forecasting: A review of the state-of-the-art with a look into the future," 2014.

[7] S. K. Aggarwal, L. M. Saini, and A. Kumar, "Electricity price forecasting in deregulated markets: A review and evaluation," 2009.

[8] I. P. Panapakidis and A. S. Dagoumas, "Day-ahead electricity price forecasting via the application of artificial neural network based models," 2016.

[9] M. M. T. Jyothi Varanasi, "Electricity price forecasting using lstm network and k-means clustering by considering the effect of wind power generation," 2022.

[10] C.-J. H. Ping-Huan Kuo, "An electricity price forecasting model by hybrid structured deep neural networks," 2018.

[11] M. Fneish, "Keras_lstm_diagram," https://github.com/MohammadFneish7/Keras_LSTM_Diagram [Accessed 2022/05/19].

[12] M. NVE and S. Vegvesen, "Temakart," https://senorge.no/map [Accessed 2022/06/17].

[13] G. Vamathevan, "A proposal of a machine learning-based day-ahead area price forecasting model of the nordic market, specialization project," *Unpublished*, 2021.

[14] N. Pool, "Trading," https://www.nordpoolgroup.com/en/trading/ [Accessed 2022/06/09].

[15] UN, "The paris agreement," https://www.un.org/en/climatechange/paris-agreement [Accessed 2022/06/09].

[16] E. Commission, "European climate law," https://ec.europa.eu/clima/eu-action/european-green-deal/european-climate-law_nl [Accessed 2022/06/09].

[17] I. E. Agency, "Electricity market report - january 2022," 2022.

[18] B. D. S. Jesus Lago, Grzegorz Marcjasz and R. Weron, "Forecasting day-ahead electricity prices: A review of state-of-the-art algorithms, best practices and an open-access benchmark," 2021.

[19] I. O. Umut Ugurlu and O. Tas, "Electricity price forecasting using recurrent neural networks," 2018.

[20] Y. Z. Zihan Chang and W. Chen, "Electricity price prediction based on hybrid model of adam optimized lstm neural network and wavelet transform," 2019.

[21] P.-H. Kuo and C.-J. Huang, "An electricity price forecasting model by hybrid structured deep neural networks," 2018.

[22] M. F. Azam and M. S. Younis, "Multi-horizon electricity load and price forecasting using an interpretable multi-head self-attention and eemd-based framework," 2021.

[23] J. Varanasi and M. M. Tripathi, "Electricity price forecasting using lstm network and k-means clustering by considering the effect of wind power generation," 2022.

[24] M. G. M. M. M. Ghayekhloo, R. Azimi and E. Shekari, "A combination approach based on a novel data clustering method and bayesian recurrent neural network for day-ahead price forecasting of electricity markets," 2019.

[25] A. P. Marin Cerjan and M. Delimar, "Hira model for short-term electricity price forecasting," 2019.

[26] Nordpool, "Day-ahead market," https://www.nordpoolgroup.com/the-power-market/Day-ahead-market/ [Accessed 2021/10/17].

[27] N. Pool, "Capacities," https://www.nordpoolgroup.com/trading/Day-ahead-trading/capacities/ [Accessed 2021/12/17].

[28] ——, "Nordic system price - methodology for calculation," 2020.

[29] Nordpool, "Single hourly order," https://www.nordpoolgroup.com/trading/Day-ahead-trading/Order-types/Hourly-bid/ [Accessed 2021/10/24].

[30] N. Pool, "Block order," https://www.nordpoolgroup.com/trading/Day-ahead-trading/Order-types/Block-bid/ [Accessed 2021/12/17].

[31] ——, "Ramping," https://www.nordpoolgroup.com/trading/Day-ahead-trading/Ramping/ [Accessed 2021/12/17].

[32] B. D. S. R. W. Jesus Lago, Grzegorz Marcjasz, "Forecasting day-ahead electricity prices: A review of state-of-the-art algorithms, best practices and an open-access benchmark," 2021.

[33] G. H. LianLian Jiang, "A review on short-term electricity price forecasting techniques for energy markets," https://ieeexplore.ieee.org/stamp/stamp.jsp?tp=&arnumber=8581312&tag=1 [Accessed 2021/11/09].

[34] S. Dash, "Smoothing techniques for time series data," https://medium.com/@srv96/smoothing-techniques-for-time-series-data-91cccfd008a2 [Accessed 2021/11/09].

[35] Y. Verma, "How to apply smoothing methods in time series analysis," https://analyticsindiamag.com/how-to-apply-smoothing-methods-in-time-series-analysis/ [Accessed 2021/11/09].

[36] A. Cruz, A. Muñoz, J. Zamora, and R. Espinola, "The effect of wind generation and weekday on spanish electricity spot price forecasting," 2011.

[37] S. Koopman, M. Ooms, and M. Carnero, "Periodic seasonal reg-arfima-garch models for daily electricity spot prices," 2007.

[38] R. J. Hyndman and G. Athanasopoulos, "Forecasting: principles and practice," 2018.

[39] K. D. Lawrence, R. K. Klimberg, and S. M. Lawrence, "Fundamentals of forecasting using excel," 2009.

[40] R. Weron and A. Misiorek, "Forecasting spot electricity prices with time series models," 2005.

[41] A. Conejo, M. Plazas, R. Espínola, and A. Molina, "Day-ahead electricity price forecasting using the wavelet transform and arima models," 2005.

[42] N. Haldrup and M. Nielsen, "A regime switching long memory model for electricity prices," 2006.

[43] R. Garcia, J. Contreras, M. van Akkeren, and J. Garcia, "A garch forecasting model to predict day-ahead electricity prices," 2005.

[44] Z. Tan, J. Zhang, J. Wang, and J. Xu, "Day-ahead electricity price forecasting using wavelet transform combined with arima and garch models," 2010.

[45] C. Huurman, F. Ravazzolo, and C. Zhou, "The power of weather," 2012.

[46] C. Bordin, H. I. Skjelbred, J. Kong, and Z. Yang, "Machine learning for hydropower scheduling: State of the art and future research directions," 2020.

[47] H.-T. Pao, "Forecasting electricity market pricing using artificial neural networks," 2007.

[48] J.-J. Guo and P. B. Luh, "Improving market clearing price prediction by using a committee machine of neural networks," 2004.

[49] U. Cali, M. Kuzlu, M. Pipattanasomporn, J. Kempf, and L. Bai, "Digitalization of power markets and systems using energy informatics," 2021.

[50] L. Wang and X. Fu, "Data mining with computational intelligence," 2005.

[51] N. Chaâbane, "A novel auto-regressive fractionally integrated moving average-least-squares support vector machine model for electricity spot prices prediction," 2014.

[52] J. Che and J. Wang, "Short-term electricity prices forecasting based on support vector regression and auto-regressive integrated moving average modeling," 2010.

[53] T. Christensen, S. Hurn, and K. Lindsay, "It never rains but it pours: modeling the persistence of spikes in electricity prices," 2009.

[54] V. Vahidinasab, S. Jadid, and A. Kazemi, "Day-ahead price forecasting in restructured power systems using artificial neural networks," 2008.

[55] M. M. H.-M. T. Y. W. Siyu Zhou, Lin Zhou, "An optimized heterogeneous structure lstm network for electricity price forecasting," 2019.

[56] F. K. Gholamreza Memarzadeh, "Short-term electricity load and price forecasting by a new optimal lstm-nn based prediction algorithm," 2021.

[57] S. P. S. Venkateswarlu Gundu, "Pso–lstm for short term forecast of heterogeneous time series electricity price signals," 2020.

[58] W. C. Zihan Chang, Yang Zhang, "Electricity price prediction based on hybrid model of adam optimized lstm neural network and wavelet transform," 2019.

[59] Y. Z. Zihan Chang and W. Chen, "Effective adam-optimized lstm neural network for electricity price forecasting," 2018.

[60] L. L. Jiang and G. Hu, "Day-ahead price forecasting for electricity market using long-short term memory recurrent neural network," 2018.

[61] M. M. H.-M. T. Siyu Zhou, Lin Zhou and Y. Wan, "An optimized heterogeneous structure lstm network for electricity price forecasting," 2019.

[62] G. Z. C. Z. S. C. X. Y. Anbo Menga, Peng Wang and H. Yin, "Electricity price forecasting with high penetration of renewable energy using attention-based lstm network trained by crisscross optimization," 2019.

[63] G. Memarzadeh and F. Keynia, "Short-term electricity load and price forecasting by a new optimal lstm-nn based prediction algorithm," 2021.

[64] Statnett, "Tall og data fra kraftsystemet," https://www.statnett.no/for-aktorer-i-kraftbransjen/tall-og-data-fra-kraftsystemet/ [Accessed 2022/05/20].

[65] ——, "Prøvedrift på nsl starter den 1. oktober," https://www.statnett.no/for-aktorer-i-kraftbransjen/nyhetsarkiv/provedrift-pa-nsl-starter-den-1.-oktober/ [Accessed 2022/05/20].

[66] EEX, "Eu ets auctions," https://www.eex.com/en/markets/environmental-markets/eu-ets-auctions [Accessed 2022/05/20].

[67] M. Cerjan, A. Petricic, and M. Delimar, "Hira model for short-term electricity price forecasting," 2019.

[68] M. R. S. S. S. Mehrnoosh Torabi, Sattar Hashemi and A. Mosavi, "A hybrid clustering and classification techniquefor forecasting short-term energy consumption," 2018.

[69] E. C. W. B. Hujun Yin, Peter Tino and X. Yao, "Intelligent data engineering and automated learning - ideal 2007," 2007.

[70] J. Brownlee, "Difference between a batch and an epoch in a neural network," https://machinelearningmastery.com/difference-between-a-batch-and-an-epoch/ [Accessed 2022/05/21].

[71] Keras, "Optimizers," https://keras.io/api/optimizers/ [Accessed 2022/06/11].

[72] ——, "Losses," https://keras.io/api/losses/ [Accessed 2022/06/11].

[73] R. K. Yifan Peng, Anthony Rios and Z. Lu, "Chemical-protein relation extraction with ensembles of svm, cnn, and rnn models," 2018.

[74] R. C. J. H. A. G. C. F. R. P. Sercan O. Arik, Markus Kliegl and A. Coates, "Convolutional recurrent neural networks for small-footprint keyword spotting," 2017.

[75] A. Davydenko and R. Fildes, "Forecast error measures: Critical review and practical recommendations," 2016.

[76] J. T. Chao Chen and J. M. Garibaldi, "A new accuracy measure based on bounded relative error for time series forecasting," 2017.

[77] M. Shihidehpour and Z. Li, "Technique for forecasting market pricing of electricity," 2003.

Appendix A

Other Input Data Plots

This appendix provide additional plots of the remaining input data that were not included in Chapter 5. Moving average has been applied to the demand, power flows and precipitation with a window size = 100 in order to clearly visualise the characteristics in the behaviour of the particular input parameter for the past years. The CO_2-price, which is common for all Norwegian bidding zones, is shown below in Figure A.1 for the years 2017-2021. There is a remarkable increase in the $CO2_2$-price observed in 2021.
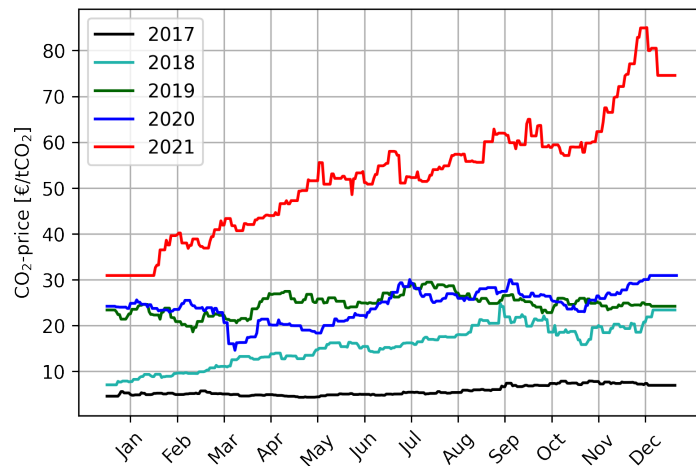
Figure A.1: The historical CO_2-prices from 2017-2021.

Continuing is the demand of each of the zones plotted in Figure A.2.
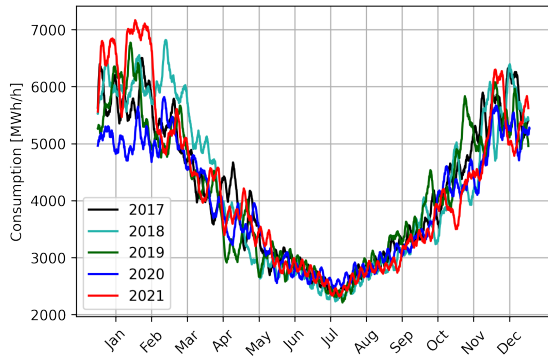
(a) NO1.
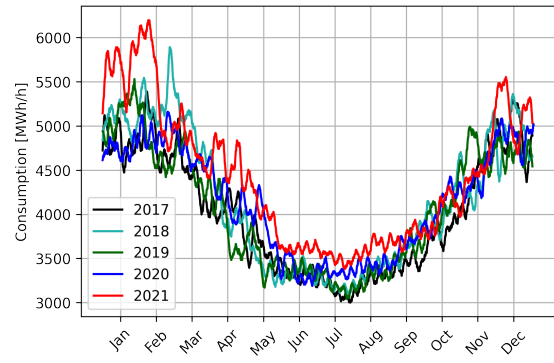
(b) NO2.
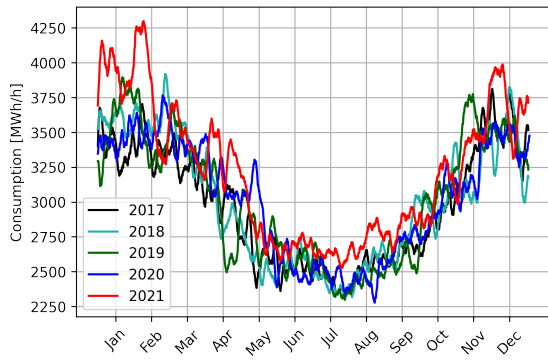
(c) NO3.
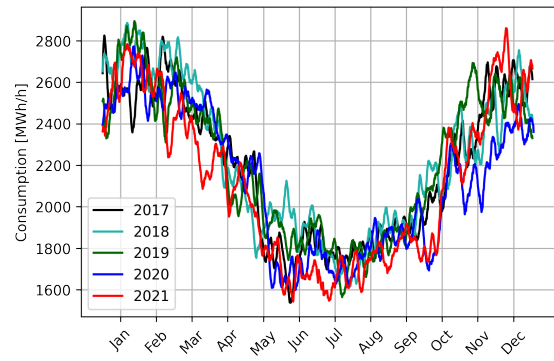
(d) NO4.
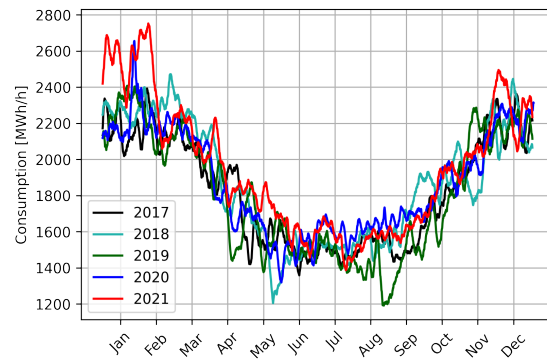
(e) NO5.

Figure A.2: The hourly historical demand from 2017-2021.

The remainder of the power flows, that is the NO2-DK1, NO5-NO2 and NO2-NL nodal connections are depicted in respectively Figure A.3, Figure A.4 and Figure A.5.
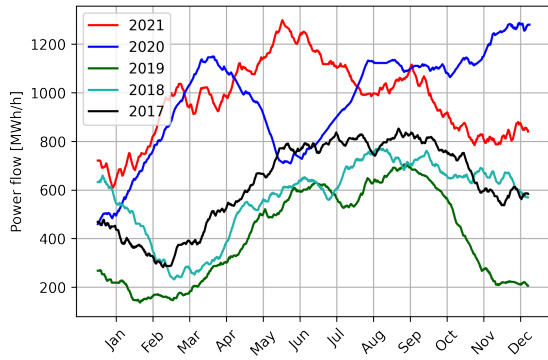
(a) NO2->DK1.
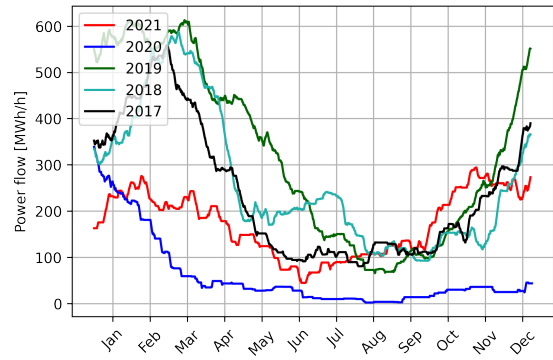
(b) DK1->NO2.

Figure A.3: Power flow between nodes NO2 and DK1 in each direction.
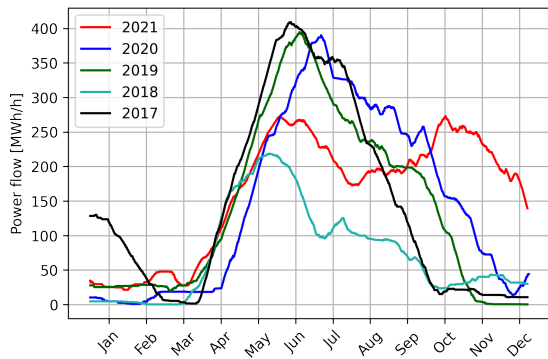
(a) NO5->NO2.
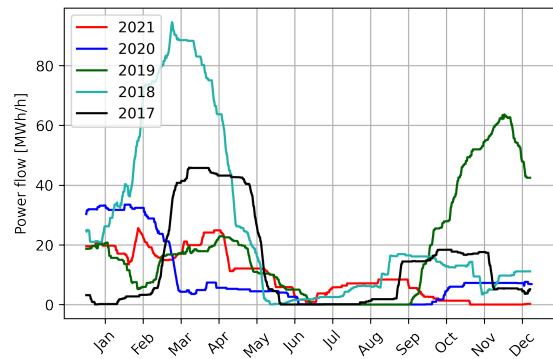
(b) NO2->NO5.

Figure A.4: Power flow between nodes NO5 and NO2 in each direction.
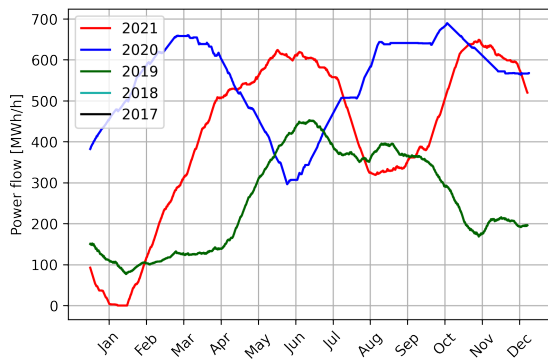
(a) NO2->NL.
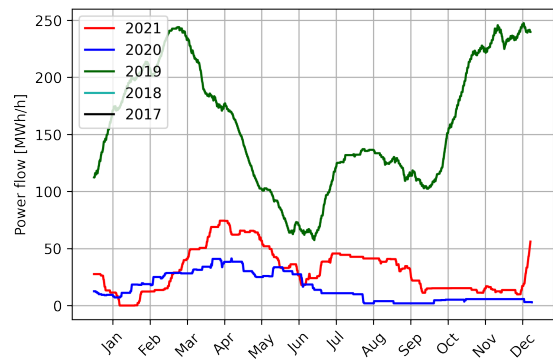
(b) NL->NO2.

Figure A.5: Power flow between nodes NO2 and NL in each direction.

Weather conditional input data is presented below in Figure A.6 depicting the past years of temperature in the unstable zones.
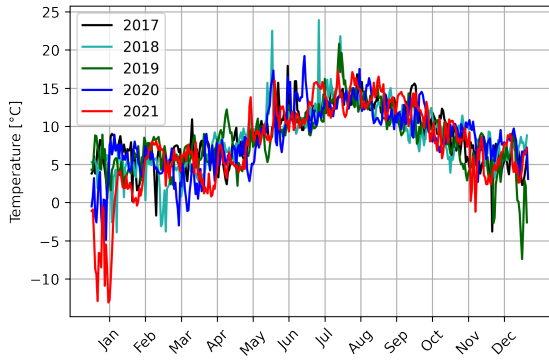
(a) NO1.
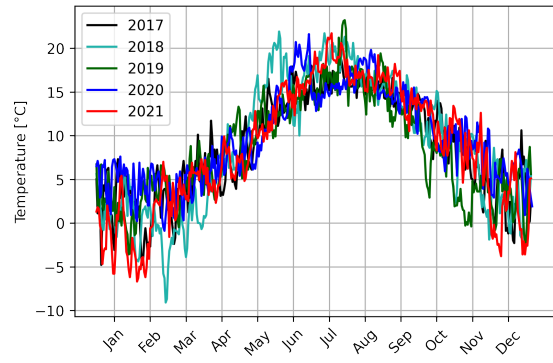
(b) NO2.
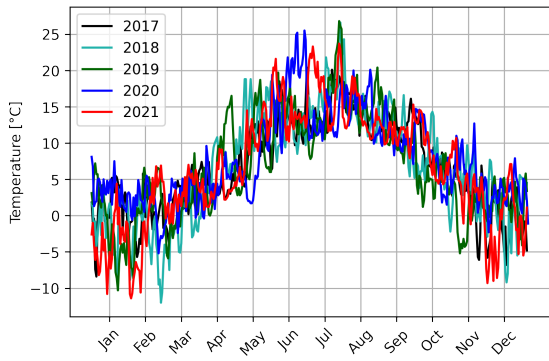
(c) NO3.
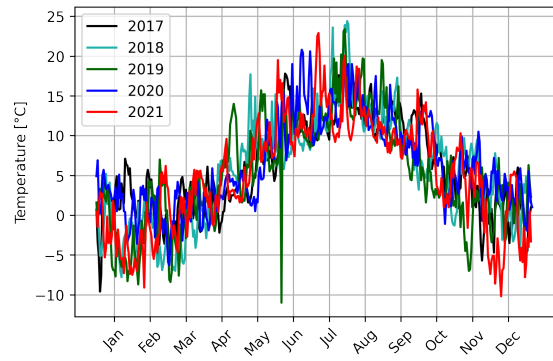
(d) NO4.
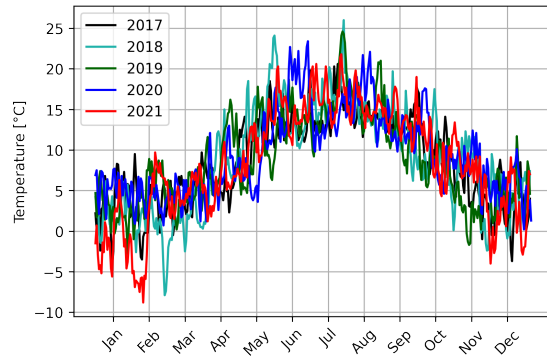
(e) NO5.

Figure A.6: The historical temperature data from 2017-2021.

Appendix B

Remaining Clustering Results

The clustering results of the training and test sets of the residual input parameters may be found in this appendix. The findings are structured in sections according to the input parameter types. Many of the plots are based on parameters: P, N and O denoting peak, normal and off-peak values in which the approximate ranges are defined based on the input data from 2017-2021.

B.1 Electricity prices

This section presents all electricity price-related input parameters clustering, that is, the electricity price of one day, two days, one week and approximately one month from the forecasting hour. The clustering of NO1, NO2 and NO5 are shown in respectively Figure B.1, Figure B.2 and Figure B.3. These figures are based on the following sharing ranges due to the similarities in electricity prices:

- O = [0,200 $\rangle$

- N = [200,900 $\rangle$

- P = [900, ∞ $\rangle$

(a) Training set.
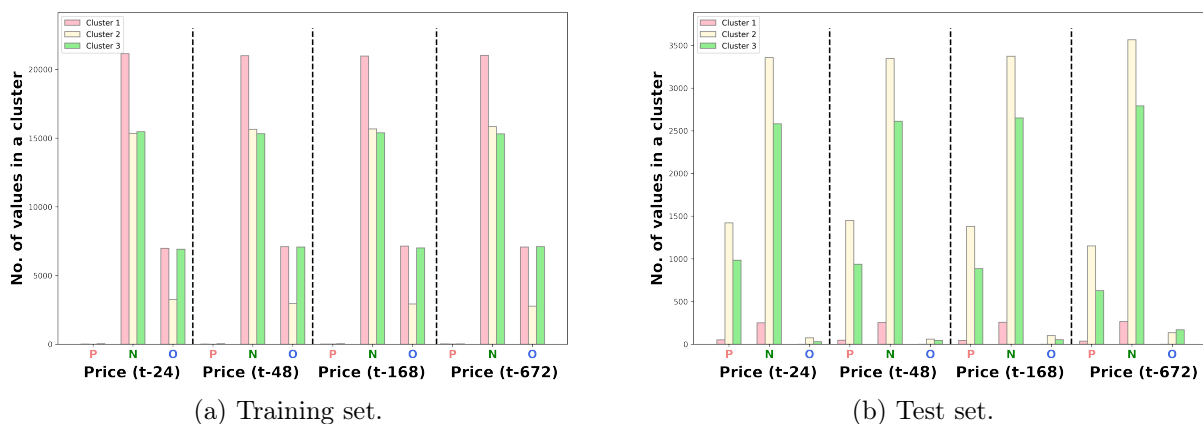
(b) Test set.

Figure B.1: Clustering of the electricity price parameters in NO1.
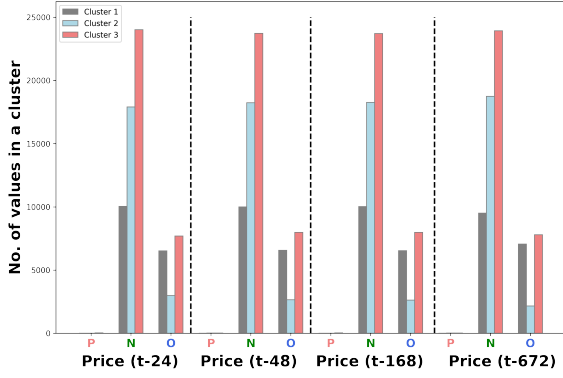
(a) Training set.
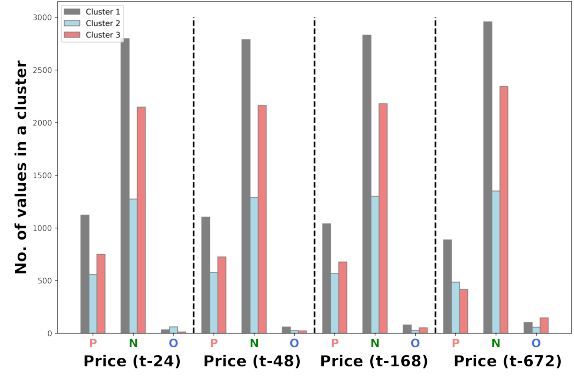
(b) Test set.

Figure B.2: Clustering of the electricity price parameters in NO2.
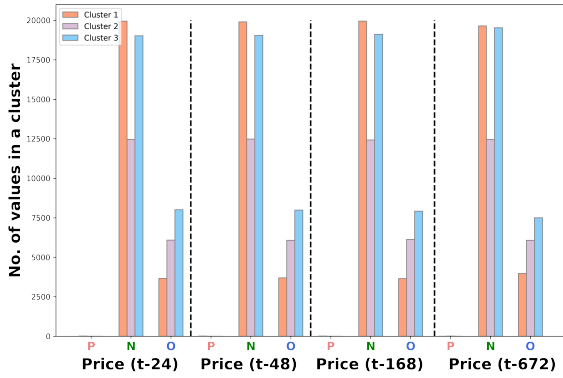
(a) Training set.
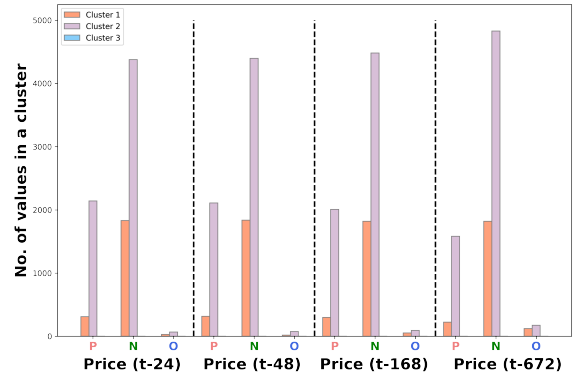
(b) Test set.

Figure B.3: Clustering of the electricity price parameters in NO5.

The residual bidding areas utilise the following ranges, and clustering results of NO3 and NO4 may be found in Figure B.4 and Figure B.5:

- O = [0,300 ⟩

- N = [300,600 ⟩

- P = [600, ∞ ⟩
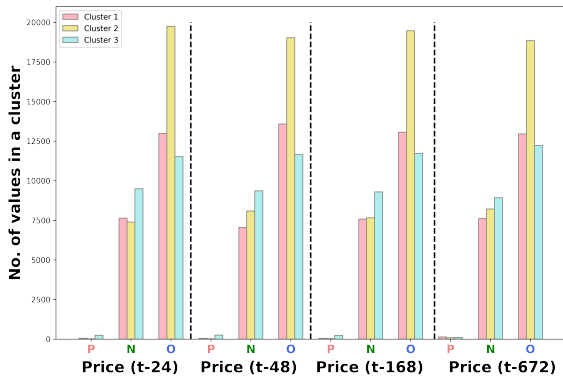
(a) Training set.
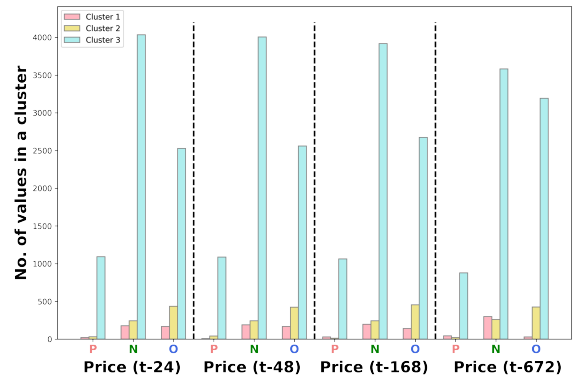
(b) Test set.

Figure B.4: Clustering of the electricity price parameters in NO3.

(a) Training set.   (b) Test set.
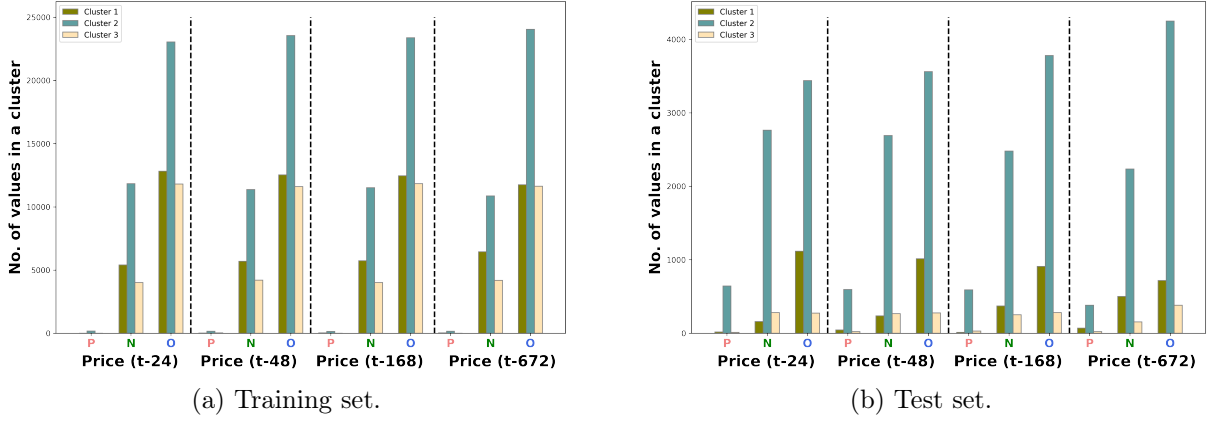
Figure B.5: Clustering of the electricity price parameters in NO4.

B.2   Demand

The demand, however, is varying from area to area in Norway. Thus, separate ranges must be defined for each zone. The clustering results of the four demand parameters injected to the DL models are included. NO1, illustrated in Figure B.6 is using the following spanning values:

- O = [0,3000 ⟩

- N = [3000, 5000 ⟩

- P = [5000, ∞ ⟩

(a) Training set.   (b) Test set.
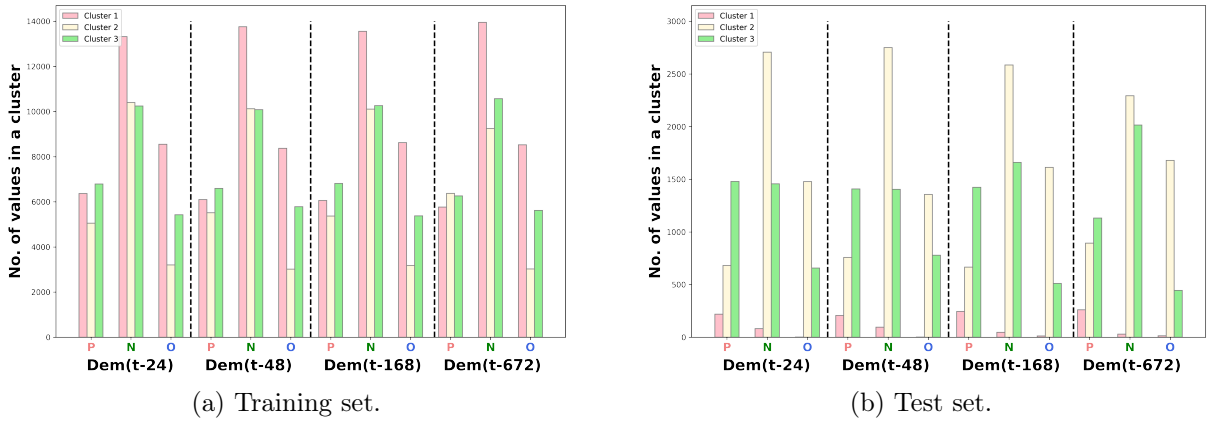
Figure B.6: Clustering of the four demand parameters in NO1.

The ranges for NO2 are slightly modified as presented below, exploited in Figure B.7:

- O = [0,3900 ⟩

- N = [3900, 5000 ⟩

- P = [5000, ∞ ⟩
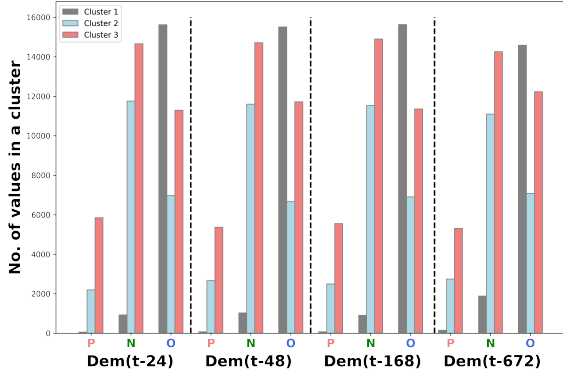
(a) Training set.
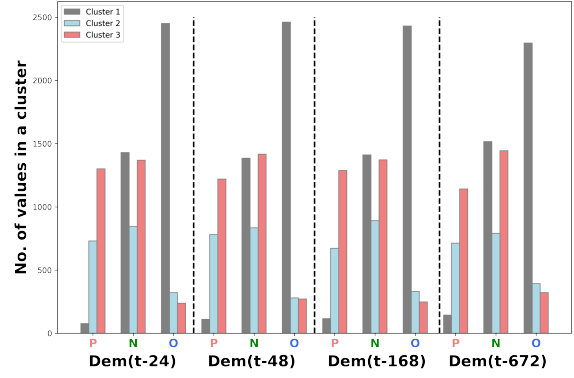
(b) Test set.

Figure B.7: Clustering of the four demand parameters in NO2.

The demand in NO3 is detected to be lower than for the above-mentioned areas. Hence, O, N and P that are utilised in Figure B.8 must be lowered as:

- O = [0,2800 ⟩

- N = [2800, 3500 ⟩

- P = [3500, ∞ ⟩
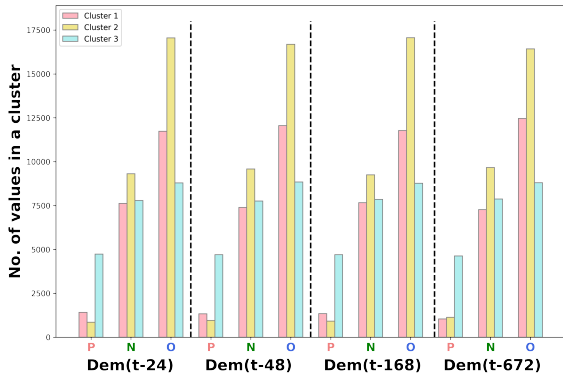
(a) Training set.
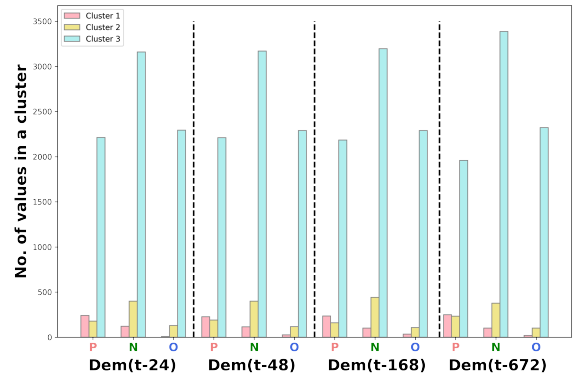
(b) Test set.

Figure B.8: Clustering of the four demand parameters in NO3.

The trend of low demand continues in NO4, such that quite similar ranges of values are used for analysing the three clusters of NO4 as presented in Figure B.9:

- O = [0,2000 ⟩

- N = [2000, 2500 ⟩

- P = [2500, ∞ ⟩

(a) Training set.

(b) Test set.
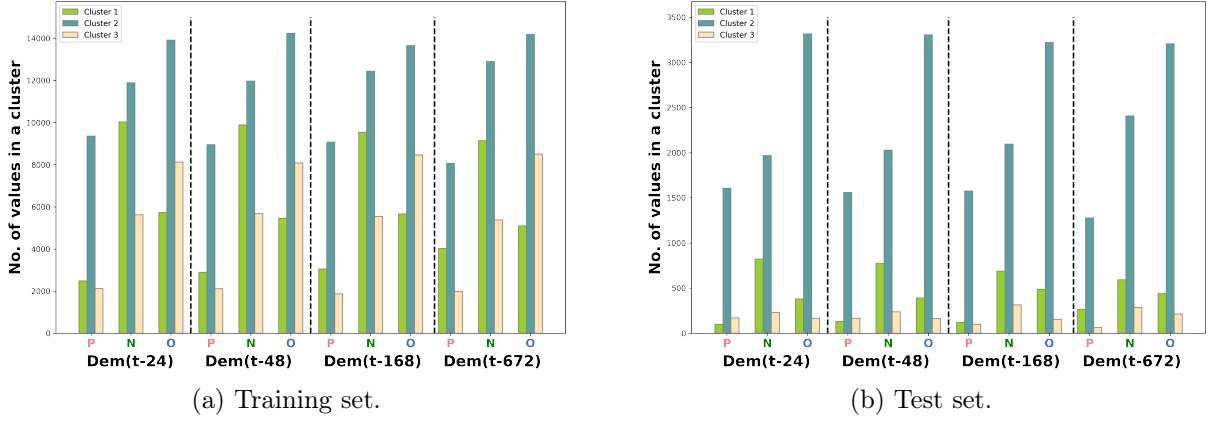
Figure B.9: Clustering of the four demand parameters in NO4.

Lastly, the clustering results of NO5 as illustrated in Figure B.10 are based on the ranges:

- $O = [0,1800\rangle$

- $N = [1800, 2400\rangle$

- $P = [2400, \infty\rangle$

(a) Training set.

(b) Test set.
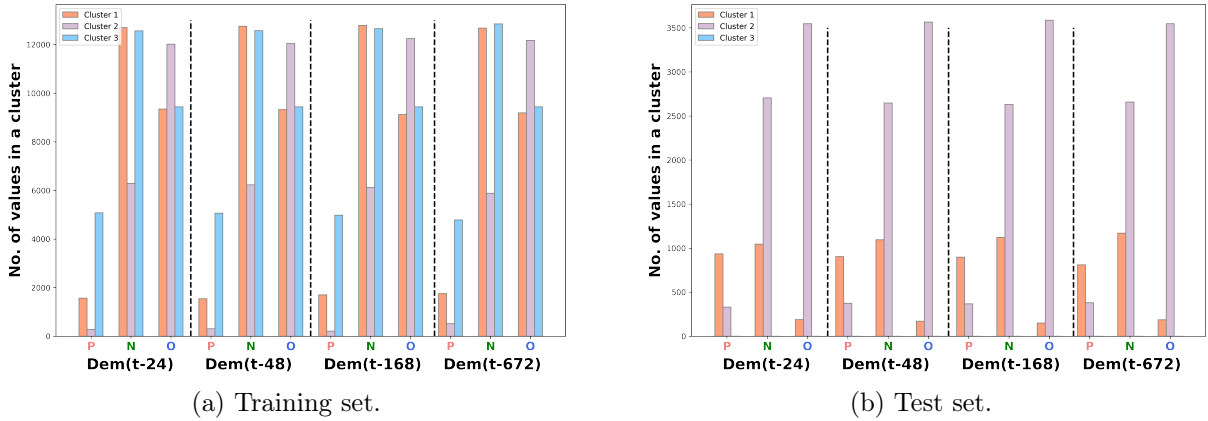
Figure B.10: Clustering of the four demand parameters in NO5.

B.3   Days

In order to understand the clustering of the days, the data is segregated accordingly to the day types = {Monday, ..., Sunday}. Clustering of NO1, NO2, NO3 and NO4 are presented in respectively Figure B.11, Figure B.12, Figure B.13 and Figure B.14.
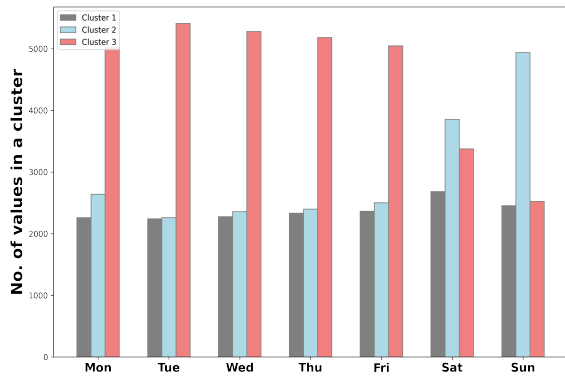
(a) Training set.
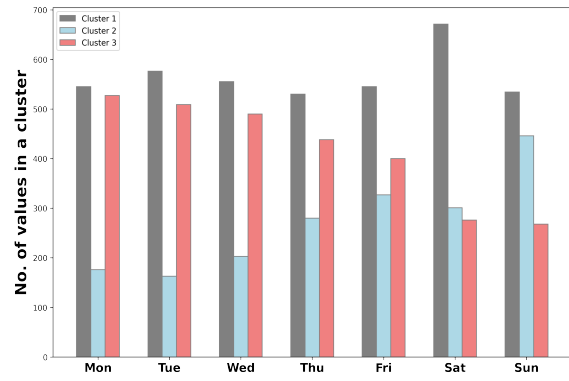
(b) Test set.

Figure B.11: Clustering of the day-parameter in NO2.
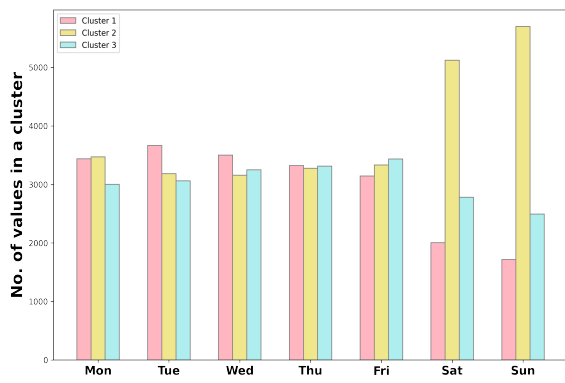
(a) Training set.
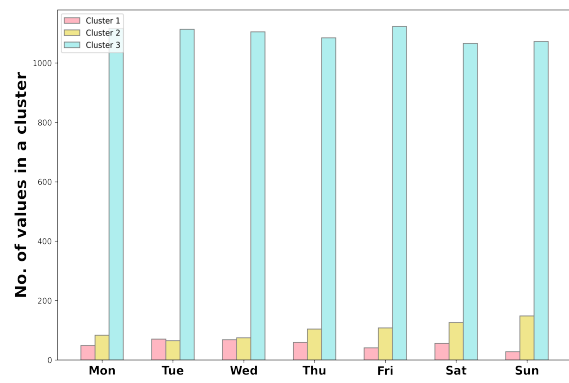
(b) Test set.

Figure B.12: Clustering of the day-parameter in NO3.
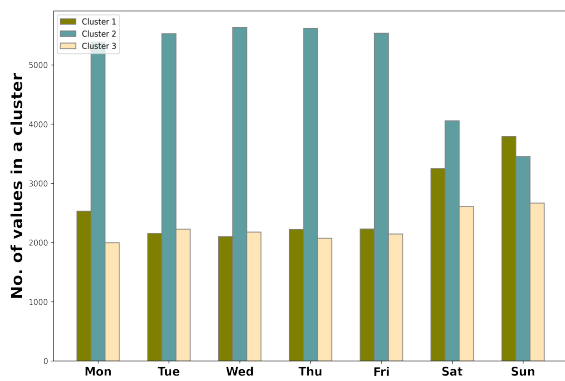
(a) Training set.
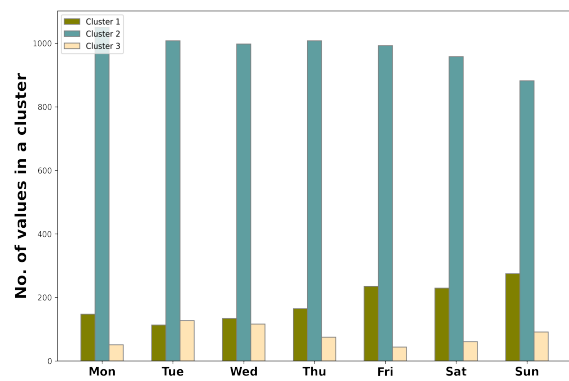
(b) Test set.

Figure B.13: Clustering of the day-parameter in NO4.

(a) Training set.

(b) Test set.
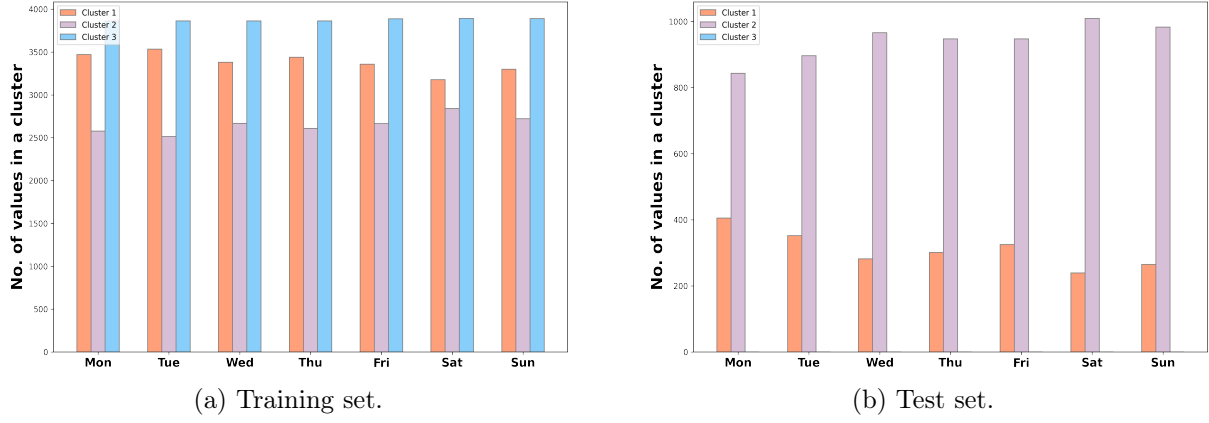
Figure B.14: Clustering of the day-parameter in NO5.

B.4 Hours

The clustering of the hours are based on the presented Table B.1.

Table B.1: Peak, normal and off-peak hours overview. Table from the specialization project [13].

Cluster no.	Type of day	Peak (P)	Normal (N)	Off-peak (O)
1	Workdays	8-22	7, 23, 24	1-6
2	Saturdays	10-22	8, 9, 23, 24	1-7
3	Sundays	10-23	1, 9, 24	2-8

On behalf of these delimitations, the clustering outcome of NO1, NO2, NO3, NO4 and NO5 are illustrated in Figure B.15.

(a) NO1.

(b) NO2.

(c) NO3.

(d) NO4.

(e) NO5.
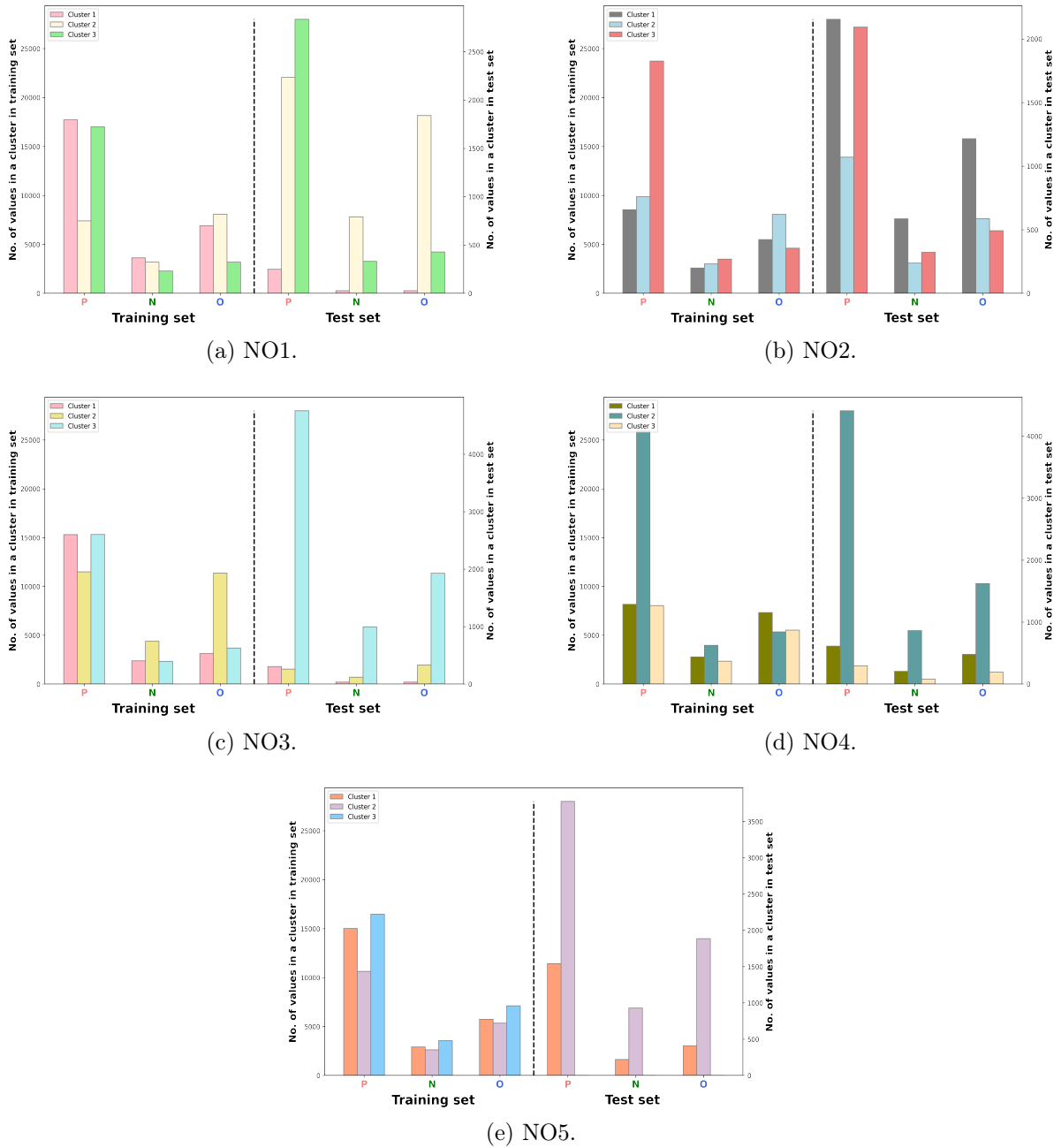
Figure B.15: Clustering of the hour-parameter in the five bidding zones of Norway.

B.5 Temperature

As the temperature is varying immensely in Norway, separate ranges for peak, normal and off-peak values must defined for each zone. The spanning values are presented below and the clustering results are shown in Figure B.16.

NO1:

- $O = \langle \infty, 3 \rangle$

- $N = [3, 10 \rangle$

- $P = [10, \infty \rangle$

NO2:

- O = $\langle \infty, 3 \rangle$

- N = $[3, 13 \rangle$

- P = $[13, \infty \rangle$

NO3:

- O = $\langle \infty, 3 \rangle$

- N = $[3, 11 \rangle$

- P = $[11, \infty \rangle$

NO4:

- O = $\langle \infty, 2 \rangle$

- N = $[2, 10 \rangle$

- P = $[10, \infty \rangle$

NO5:

- O = $\langle \infty, 7 \rangle$

- N = $[7, 13 \rangle$

- P = $[13, \infty \rangle$

(a) NO1.

(b) NO2.

(c) NO3.

(d) NO4.

(e) NO5.
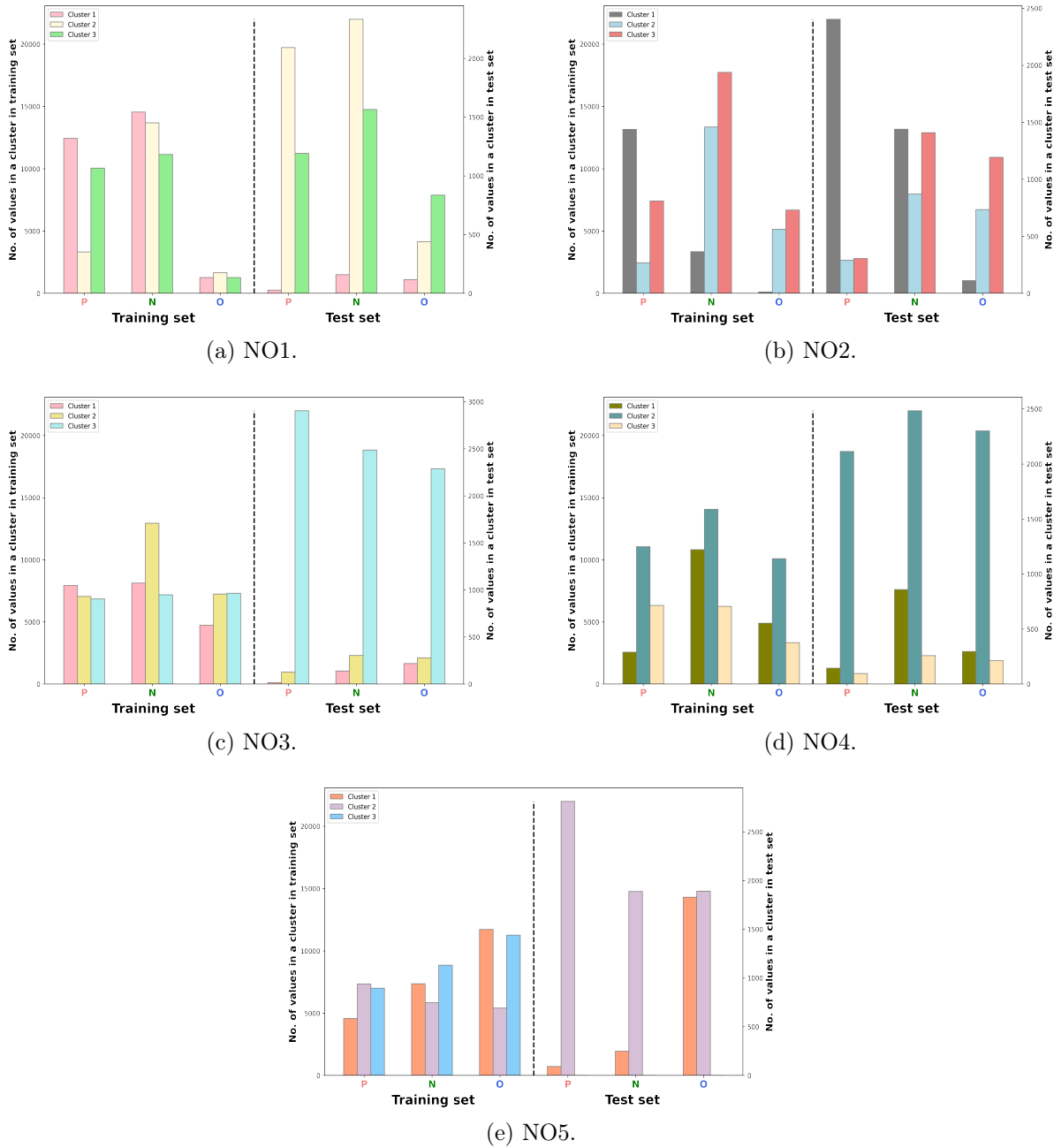
Figure B.16: Clustering of the temperature data in NO1-NO5.

B.6 Precipitation

The precipitation clustering results are also analysed by defining P, N and O as below, with the results depicted in Figure B.17.

NO1:

- $O = [0, 5\rangle$

- $N = [5, 18\rangle$

- $P = [18, \infty\rangle$

NO2:

- $O = [0, 5\rangle$

- N = [5, 11 ⟩

- P = [11, ∞ ⟩

NO3:

- O = [0, 3 ⟩

- N = [3, 8 ⟩

- P = [8, ∞ ⟩

NO4:

- O = [0, 4 ⟩

- N = [4, 10 ⟩

- P = [10, ∞ ⟩

NO5:

- O = [0, 9 ⟩

- N = [9, 20 ⟩

- P = [20, ∞ ⟩

(a) NO1.

(b) NO2.

(c) NO3.

(d) NO4.

(e) NO5.
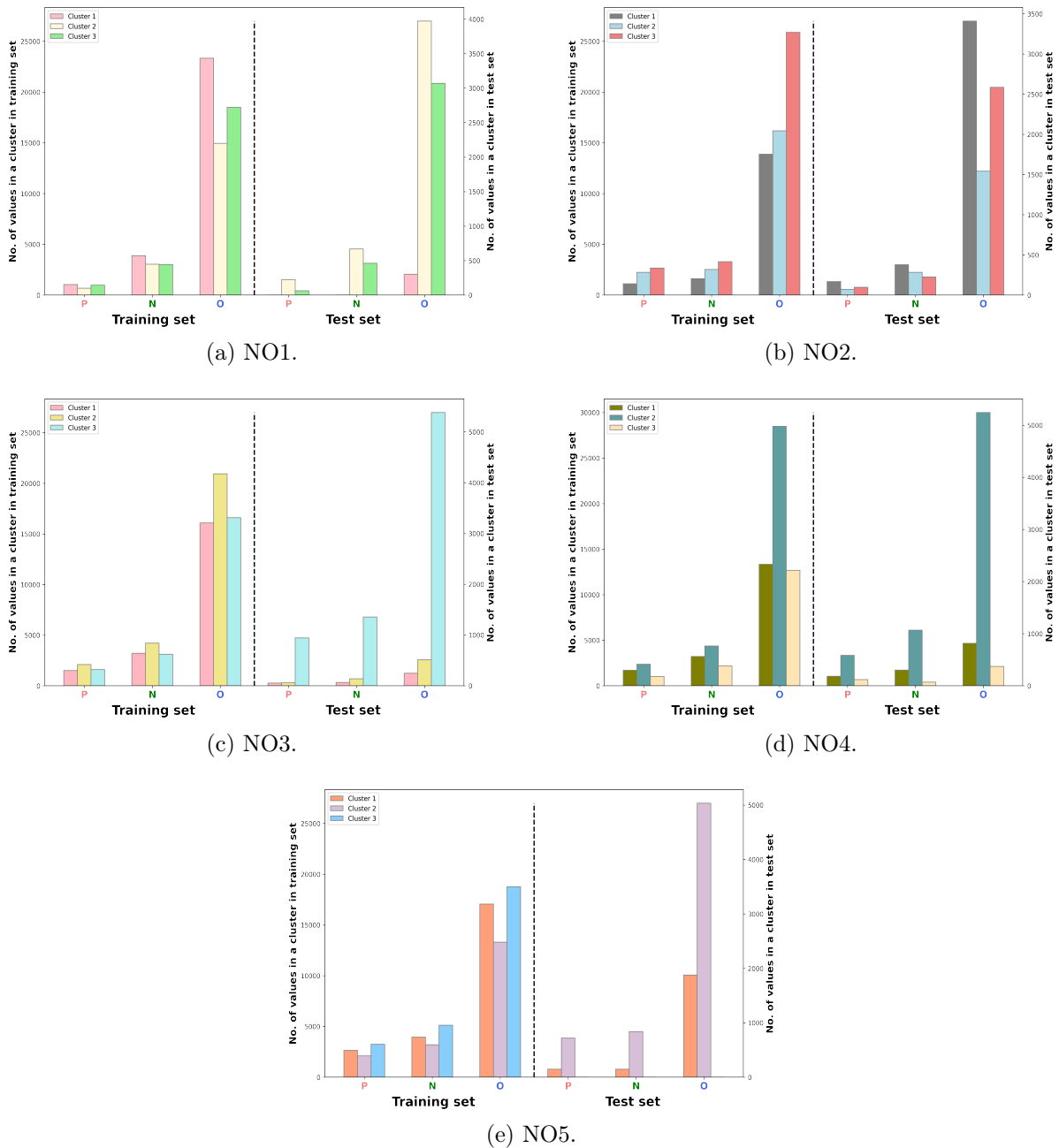
Figure B.17: Clustering of the precipitation data in the five bidding zones of Norway.

B.7 CO$_2$-price

The identical CO$_2$-price data is employed on all bidding zones as the same EU CO$_2$-prices apply to all areas of Norway. However, since the training of unsupervised clustering is exerted on each individual zone without including information about other zonal data, the clustering of the CO$_2$-data in each zone is varying, as seen in Figure B.18.
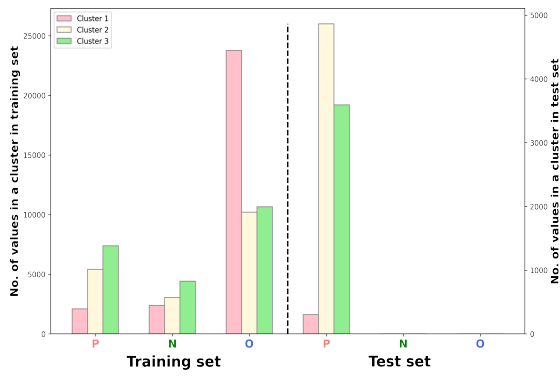
(a) NO1.
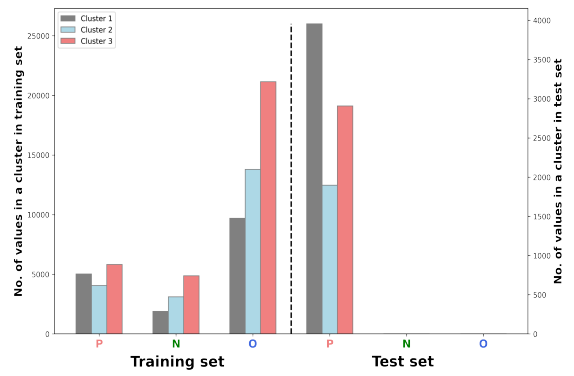
(b) NO2.
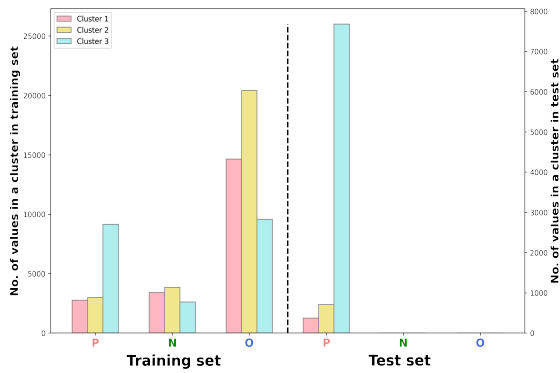
(c) NO3.
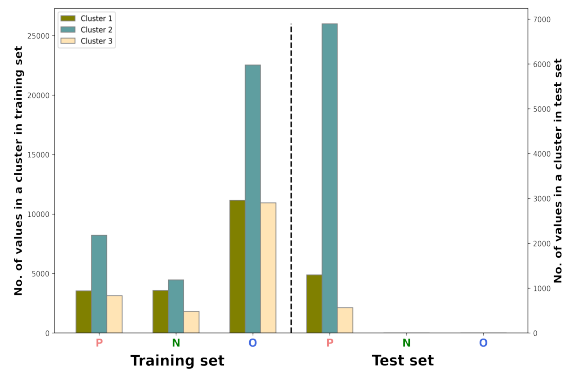
(d) NO4.
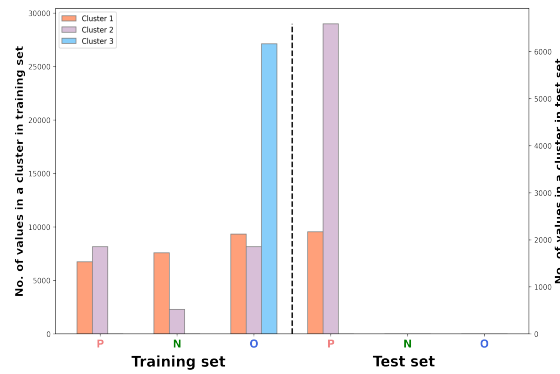
(e) NO5.

Figure B.18: Clustering of the CO_2-price data in NO1-NO5.

The peak, normal and off-peak values are defined as:

- $O = [0, 10 \rangle$

- $N = [10, 22 \rangle$

- $P = [22, \infty \rangle$

Appendix C

Further Results

C.1 Hyperparameter Tuning

As explained in Section 6.1, two optimization processes were conducted for the LSTM model. Batch size (BS) and timesteps (TS) were first to be varied (Part 1). The second procedure (Part 2) involved utilising the optimal batch and timesteps found in the previous step, in order to detect the activation functions yielding the lowest percentage errors. The latter process is presented in Table C.1 with the red-colored values underlining the lowest percentage error internally in the specific zone.

Table C.1: LSTM hyperparameter tuning - Part 2

Zone	Act. func.	Rec. Act.	Epochs	BS	TS	MSE	MAE	RMSE	MAPE
NO1	Tanh	Sigmoid	14	10	5	1.585%	5.762%	12.59%	114.805%
	Tanh	Tanh	12	10	5	2.759%	8.258%	16.610%	98.443%
	Sigmoid	Sigmoid	10	10	5	1.233%	5.181%	11.103%	119.925%
	Sigmoid	Tanh	11	10	5	1.554%	5.758%	12.466%	110.599%
NO2	Tanh	Sigmoid	11	15	5	5.780%	12.468%	24.042%	118.619%
	Tanh	Tanh	7	15	5	8.813%	16.367%	29.687%	112.894%
	Sigmoid	Sigmoid	11	15	5	6.288%	10.885%	25.076%	111.822%
	Sigmoid	Tanh	9	15	5	7.665%	13.190%	27.685%	108.261%
NO3	Tanh	Sigmoid	8	15	15	0.596%	4.008%	7.723%	164.600%
	Tanh	Tanh	15	5	5	0.763%	4.622%	8.736%	255.512%
	Sigmoid	Sigmoid	10	5	5	0.557%	3.850%	7.461%	170.530%
	Sigmoid	Tanh	7	5	5	0.573%	3.991%	7.567%	166.345%
NO4	Tanh	Sigmoid	9	10	15	0.468%	3.369%	6.839%	149.678%
	Tanh	Tanh	7	10	15	0.692%	4.386%	8.317%	157.683%
	Sigmoid	Sigmoid	11	10	15	0.469%	3.183%	6.851%	153.324%
	Sigmoid	Tanh	6	10	15	0.511%	3.322%	7.151%	160.050%
NO5	Tanh	Sigmoid	7	10	10	6.194%	10.636%	24.887%	21.315%
	Tanh	Tanh	7	10	10	8.155%	13.364%	28.558%	23.097%
	Sigmoid	Sigmoid	11	10	10	5.016%	9.513%	22.395%	20.422%
	Sigmoid	Tanh	7	10	10	9.086%	13.994%	30.143%	23.594%

The evaluation metrics of the base cases are shown in Table C.2 with the Model D.1 results being the best cases of each zone from Table C.1.

Table C.2: The base cases regarding each model and each zone in Norway.

Zone	Model	Act. func. (ANN)	Act. func. (LSTM)	Rec. act.	Epochs	BS	TS	MSE	MAE	RMSE	MAPE
NO1	A	Tanh	-	-	10	10	-	1.378%	5.111%	11.740%	117.751%
	B	Tanh	-	-	86	10	-	1.330%	5.158%	11.533%	113.217%
	C	Tanh	-	-	47	15	-	1.404%	5.400%	11.850%	108.253%
	D.1	-	Sigmoid	Sigmoid	10	10	5	1.233%	5.181%	11.103%	119.925%
NO2	A	Tanh	-	-	13	15	-	10.814%	16.352%	32.885%	122.784%
	B	Sigmoid	-	-	119	15	-	11.047%	16.829%	33.237%	108.755%
	C	Tanh	-	-	57	15	-	10.653%	17.049%	32.639%	119.312%
	D.1	-	Tanh	Sigmoid	11	15	5	5.780%	12.468%	24.042%	118.619%
NO3	A	Tanh	-	-	14	15	-	0.511%	3.560%	7.150%	193.051%
	B	Tanh	-	-	30	10	-	0.534%	3.758%	7.310%	183.007%
	C	Tanh	-	-	28	10	-	0.582%	4.067%	7.629%	160.221%
	D.1	-	Tanh	Sigmoid	8	15	15	0.596%	4.008%	7.723%	164.600%
NO4	A	Tanh	-	-	18	15	-	0.506%	3.162%	7.111%	140.944%
	B	Tanh	-	-	52	15	-	0.475%	3.237%	6.890%	157.535%
	C	Tanh	-	-	46	10	-	0.492%	3.173%	7.015%	93.065%
	D.1	-	Sigmoid	Sigmoid	11	10	15	0.469%	3.183%	6.851%	153.324%
NO5	A	Tanh	-	-	9	15	-	10.969%	16.023%	33.120%	24.614%
	B	Tanh	-	-	29	5	-	11.809%	16.712%	34.364%	24.724%
	C	Tanh	-	-	24	10	-	11.590%	16.375%	34.045%	24.626%
	D.1	-	Sigmoid	Sigmoid	11	10	10	5.016%	9.513%	22.395%	20.422%

C.2   Forecasting

The remaining forecasting results are provided in this section. This encompasses additional model modification and ML model comparison findings.

C.2.1   A Closer Insight on Model Modifications

The remaining model modification plots are presented below. As ANN performed better among the stable zones, the LSTM results of model adjustments were disregarded in the thesis results, but may be found in Figure C.1 on the basis of the identical cases 1-6.

(a) NO3   (b) NO4
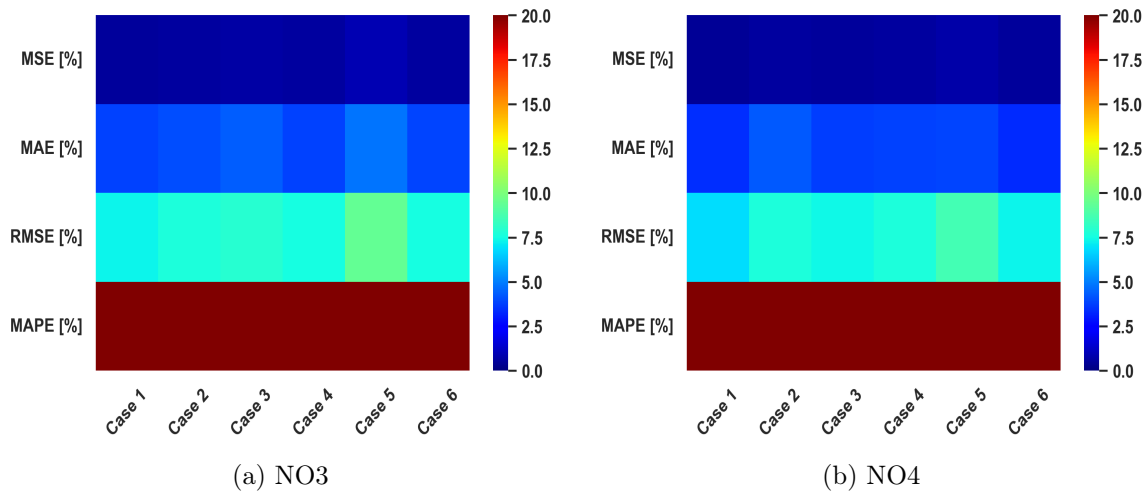
Figure C.1: Model modification results of cases 1-6 of the stable zones using Model D.1.

The unstable zones however, produced an improved forecasting accuracy through the LSTM model. Therefore, results regarding model A, B and C were neglected from the results in Chapter 6, but is to be found below. The evaluation metrics outcome of cases 1-6 in NO1, NO2 and NO5 are depicted in correspondingly Figure C.2, Figure C.3 and Figure C.4.
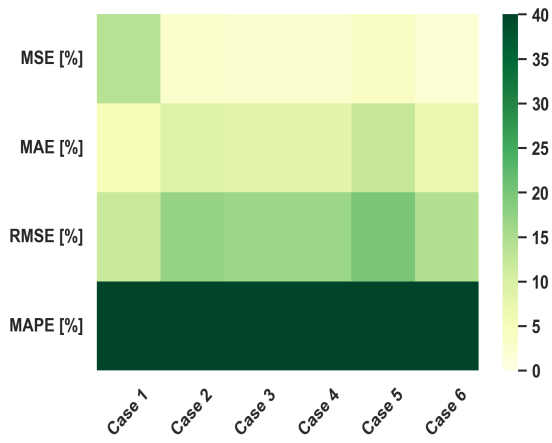
(a) Model A
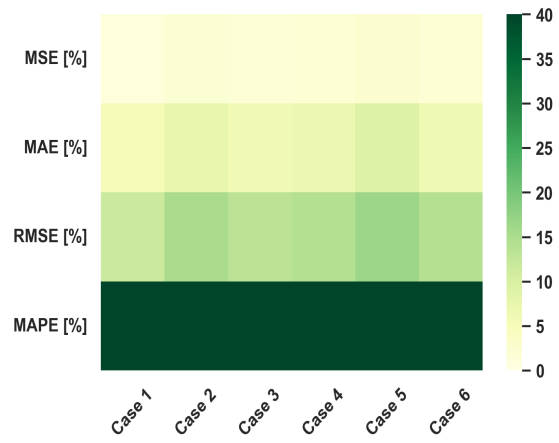
(b) Model B
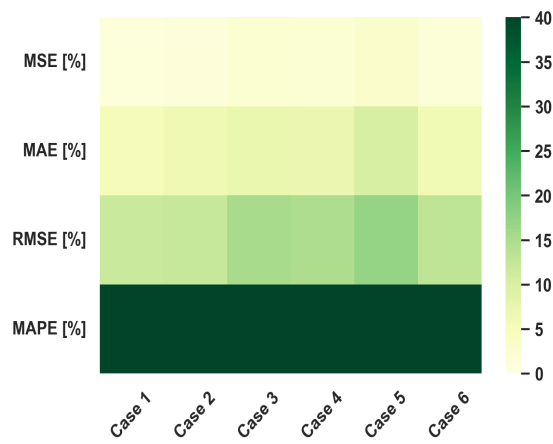
(c) Model C

Figure C.2: Model modification results of cases 1-6 of NO1 using Model A-C.
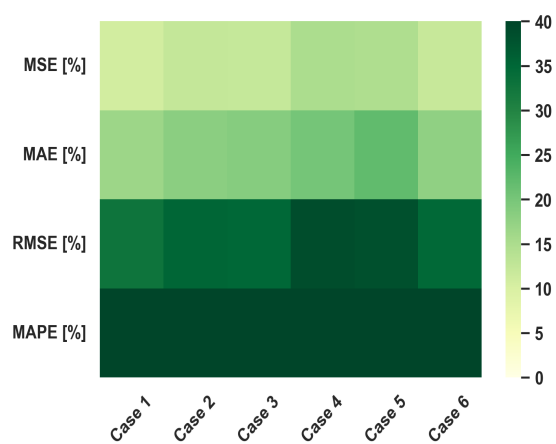
(a) Model A
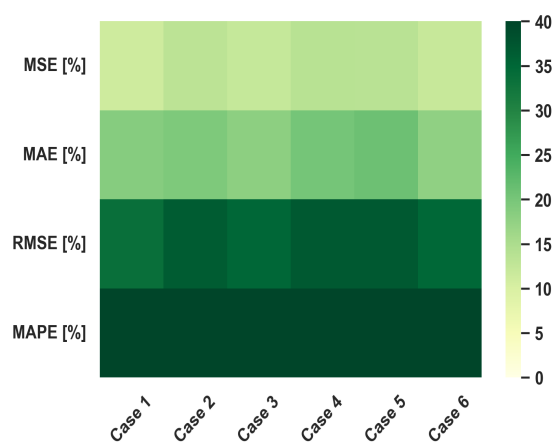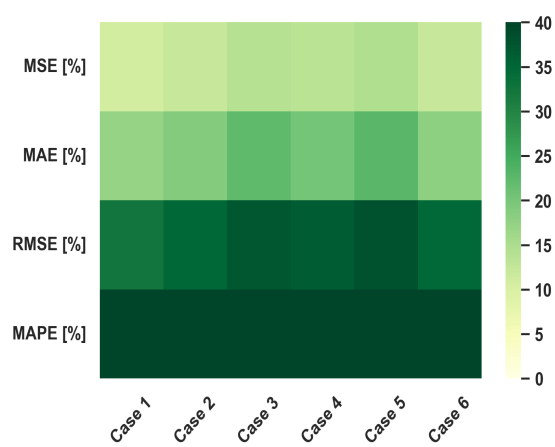
(b) Model B

(c) Model C

Figure C.3: Model modification results of cases 1-6 of NO2 using Model A-C.
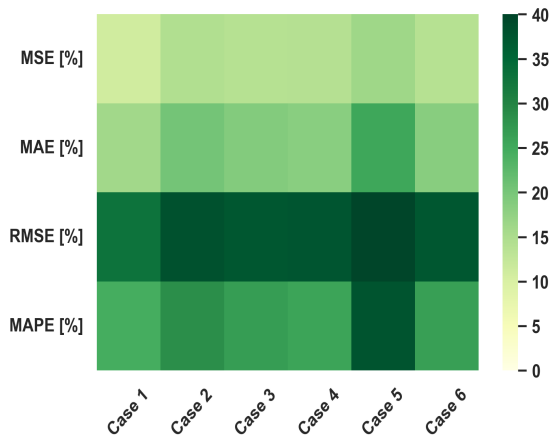
(a) Model A
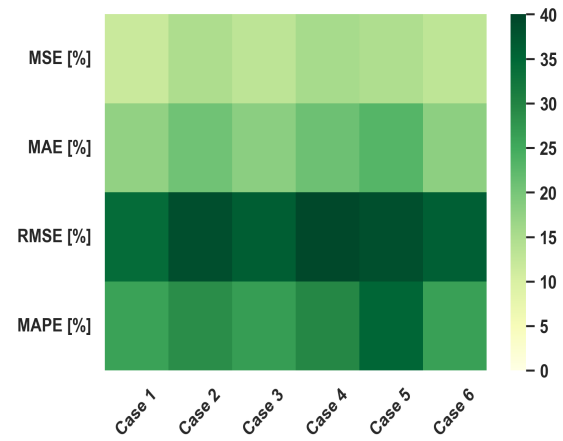
(b) Model B
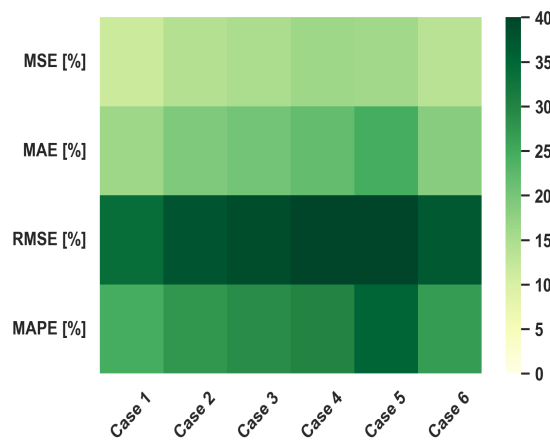
(c) Model C

Figure C.4: Model modification results of cases 1-6 of NO5 using Model A-C.

C.3 Comparison of ANN and LSTM

The forecasted and actual values of the electricity prices in January and December may be found for the bidding zones NO1, NO2, NO3 and NO4 in respectively Figure C.5, Figure C.6, Figure C.7 and Figure C.8. The aim was for comparing the performance of ANN and LSTM, hence, only Model A and Model D are included in the figures below.
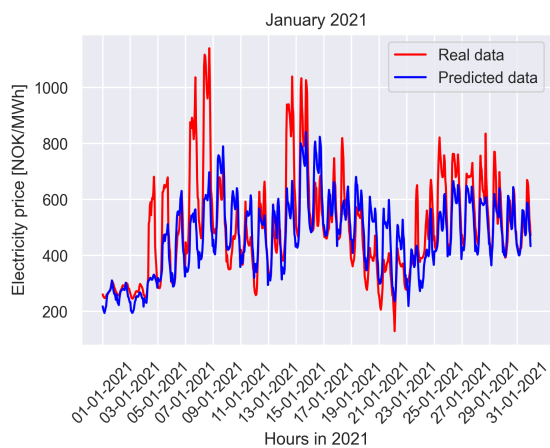
(a) January - Model A
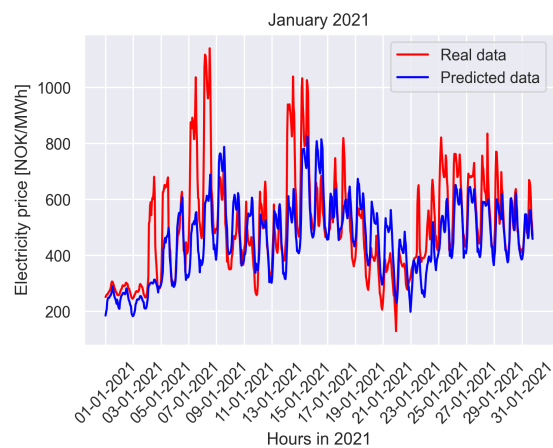
(b) January - Model D
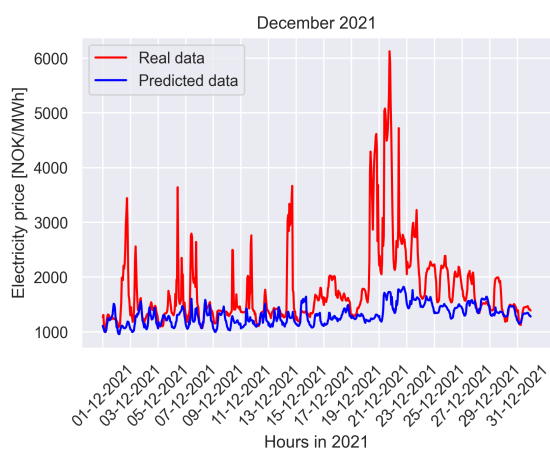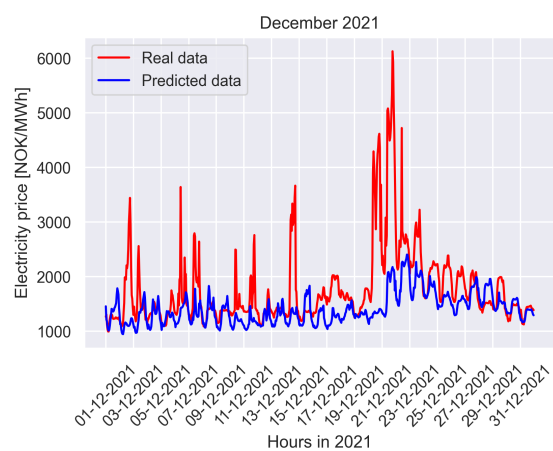
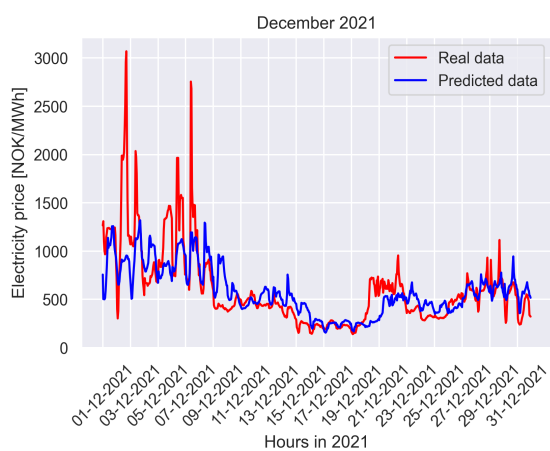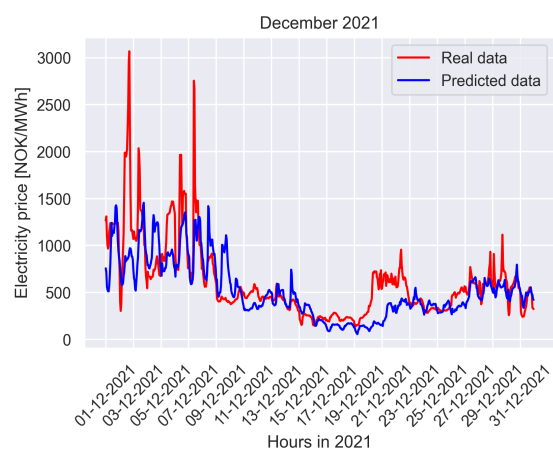(c) December - Model A

(d) December - Model D

Figure C.5: The actual and predicted electricity prices of 2021 in NO1 in January and December utilising Model A and Model D.
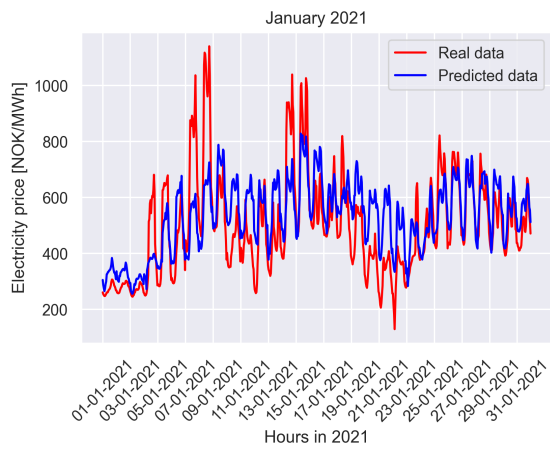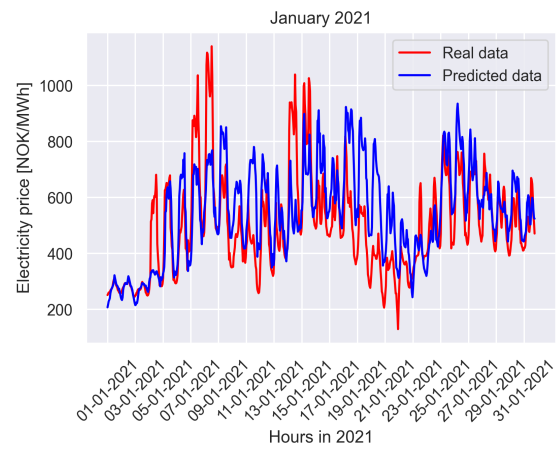
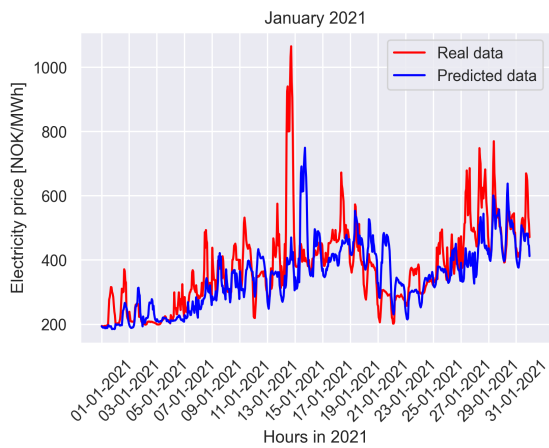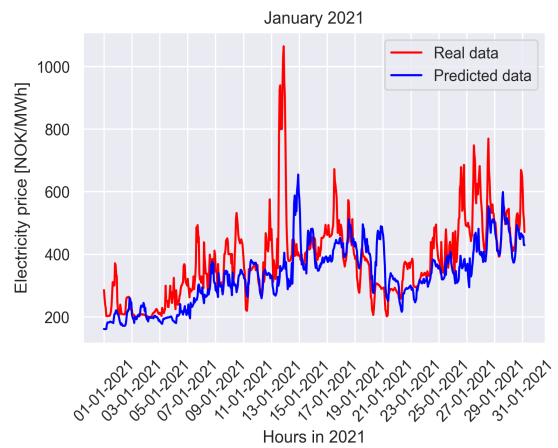(a) January - Model A
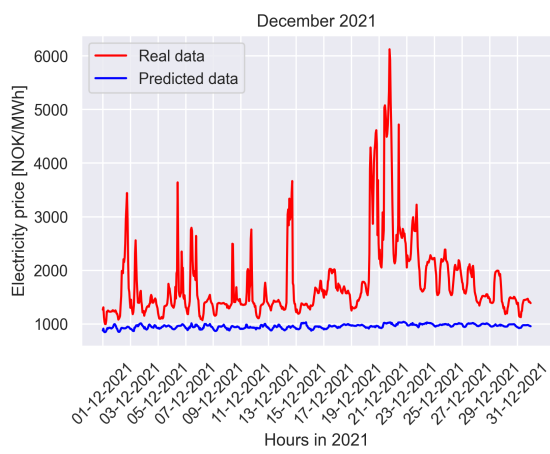
(b) January - Model D
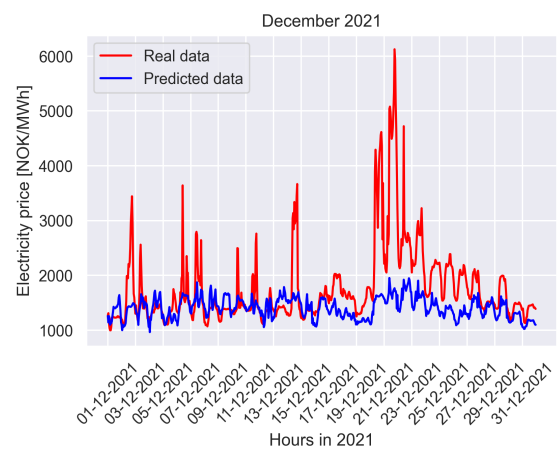
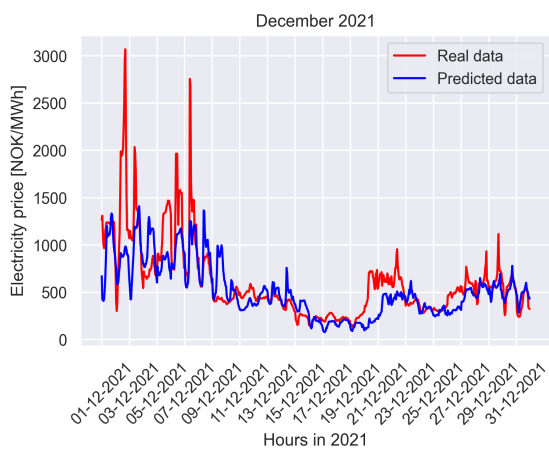(c) December - Model A

(d) December - Model D

Figure C.6: The actual and predicted electricity prices of 2021 in NO2 in January and December utilising Model A and Model D.
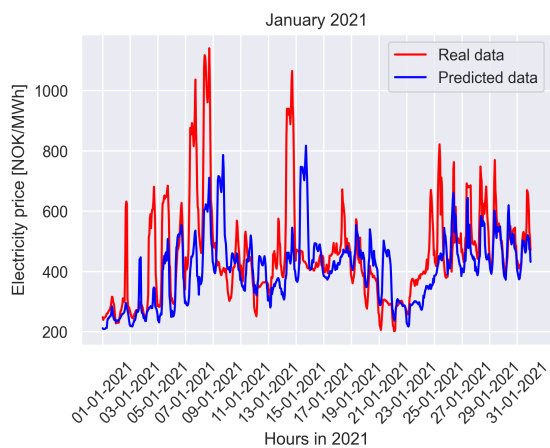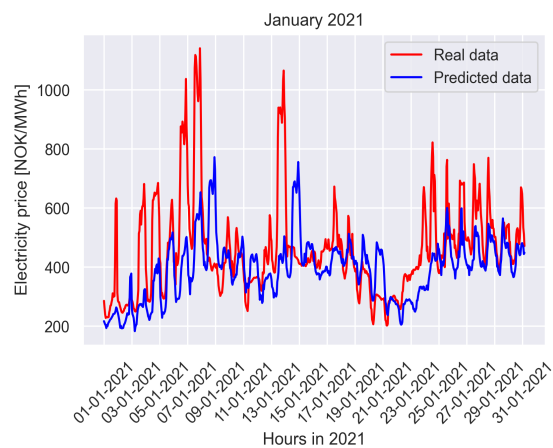
(a) January - Model A
(b) January - Model D
(c) December - Model A
(d) December - Model D

Figure C.7: The actual and predicted electricity prices of 2021 in NO3 in January and December utilising Model A and Model D.
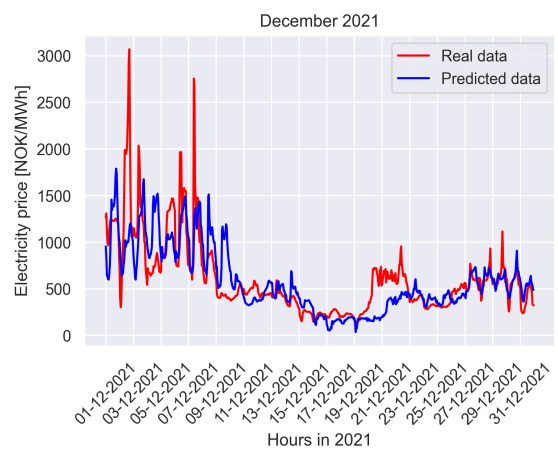
(a) January - Model A

(b) January - Model D

(c) December - Model A

(d) December - Model D

Figure C.8: The actual and predicted electricity prices of 2021 in NO4 in January and December utilising Model A and Model D.